

LOUGHBOROUGH
UNIVERSITY OF TECHNOLOGY
LIBRARY

AUTHOR/FILING TITLE

GALVIN, S.

ACCESSION/COPY NO.

036000244

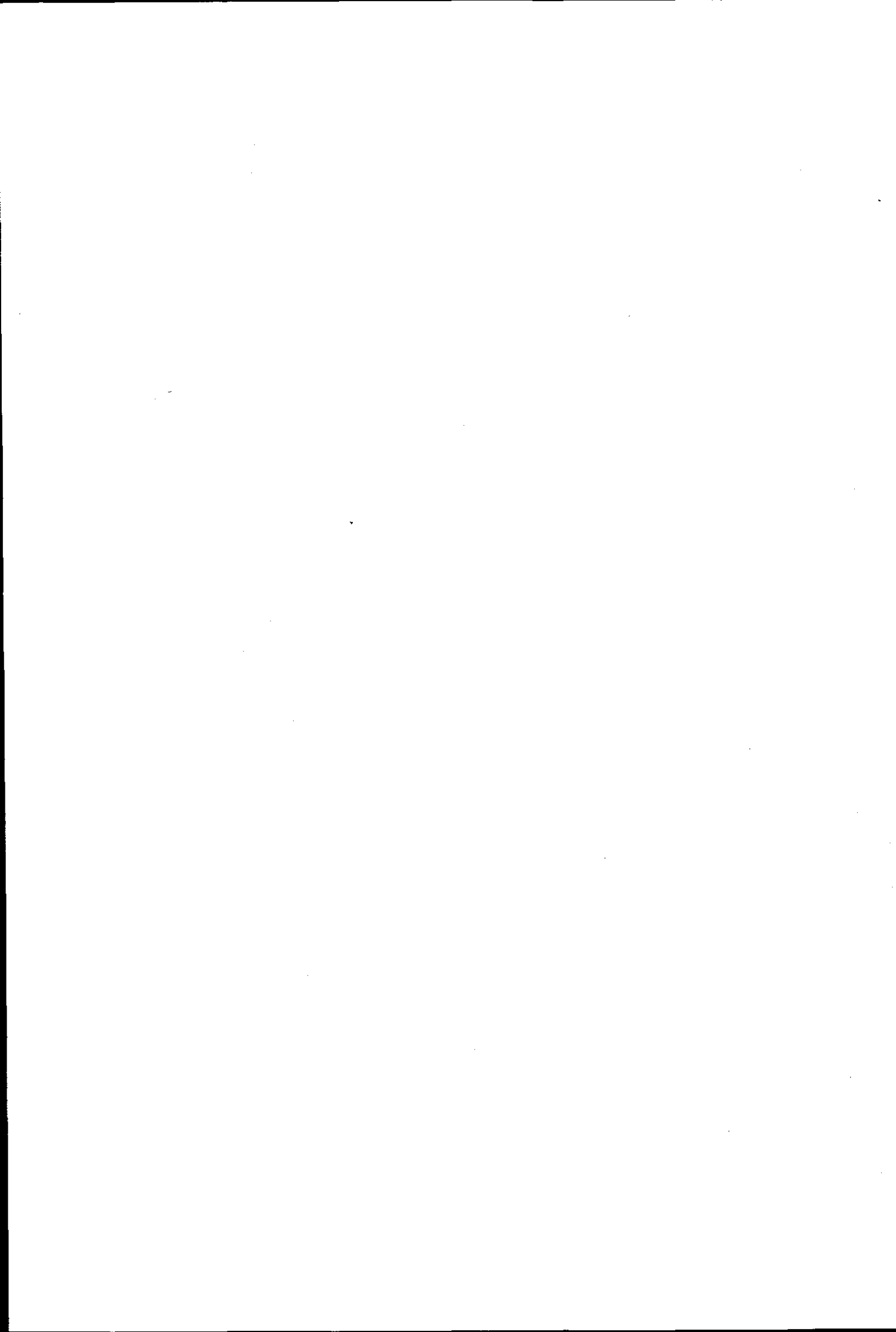
VOL. NO.

CLASS MARK

LOAN COPY

036000244 7





THE FLOW MEDIA CONTAINING COIL PUMP

by

S.Galvin B.Sc.

A Master's Thesis

Submitted in partial fulfilment of the requirements for
the award of Master of Philosophy of the Loughborough
University of Technology.

December 1988.

Supervisor: G. H. Mortimer, D.I.C., C.Eng., M.I.C.E.
Department of Civil Engineering

© S. GALVIN B.Sc. 1988

Loughborough University
of Technology Library

Date Mar 92

Author

Doc
ID: 036000244

69919087

SUMMARY

This project extends and develops the research on the coil pump which has been completed over the last six years at Loughborough University. It concentrates on the power consumption of the pump and how the inclusion of flow media affects its performance.

The hydraulic properties of flow media were first experimented upon. The resulting relationship was used later to explain their behaviour inside the pump.

A small bore coil pump with an enlarged inlet was experimented upon, to investigate its properties for the purpose of increasing its discharge.

A larger coil pump, including large diameter coils was experimented upon to investigate its power consumption and the flow media resistance properties.

A computer simulation of the coil pump was developed to help in the analysis and predication of the experimental data. The relationships resulting from the research were incorporated to improve the simulation.

keywords: Pumps, pumping, waterwheels, coil pump, manometric pump, hydrostatic pump, spiral pump.

ACKNOWLEDGEMENTS

I am most grateful to the following:

Mr. G.H. Mortimer for his guidance and supervision throughout the project.

Mr. L. Benskin for his high standard of workmanship in construction of all test apparatus.

My Mother and Father for helping to type this thesis.

PROJECT AUTHORISATION

Title: THE FLOW MEDIA CONTAINING COIL PUMP

Supervisor: G. H. Mortimer

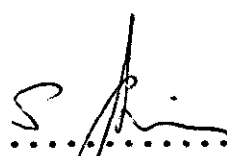
Moderator:

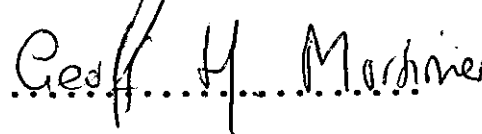
Aims: To investigate the power consumptions and efficiencies of the coil pump and the effect on these of the inclusion of flow media inside the coils.

Description: The experimental results are used to predict the power absorbed by the coil pump, and to validate the theories developed here.

Equipment: A low cost rotating coil pump already existing in the hydraulics department of the laboratory.

Outside Bodies: Severn Trent Water Authority.

Signature of Student: 

Signature of Supervisor: 

CONTENTS

	<u>Page</u>
TITLE PAGE	i
CERTIFICATION OF AUTHORSHIP	ii
SUMMARY	iii
ACKNOWLEDGEMENTS	iv
PROJECT AUTHORISATION	v
CONTENTS	vi
LIST OF FIGURES	xiv
REFERENCES	xviii
NOMENCLATURE	xxi

<u>Chapter 1</u>	INTRODUCTION	
1.1	BRIEF DESCRIPTION	(1-1)
1.2	EARLY WORK	(1-3)
1.2.1	Work by Wirtz	(1-3)
1.2.2	Work by Ohlemutz	(1-3)
1.3	PREVIOUS WORK AT LOUGHBOROUGH ..	(1-5)
1.3.1	Work by Bamforth	(1-5)
1.3.2	Work by Winstanley	(1-6)
1.3.3	Work by Robinson	(1-6)
1.3.4	Work by Annable	(1-8)
1.3.5	Work by Mortimer	(1-11)
1.4.	WORK AT SALFORD	(1-12)
1.4.1	Work by Stuckey and Wilson	(1-12)
1.4.2	Work by Wilson	(1-12)
1.5	WORK ON A WASTE WATER TREATMENT COIL PUMP	(1-15)

Chapter 2

FLOW MEDIA RESISTANCE EXPERIMENT

2.1	EQUIPMENT	(2-8)
2.2	CHECKING ORIFICE METER CALIBRATION	(2-12)
2.2.1	Procedure	(2-12)
2.2.2	Results	(2-12)
2.2.3	Error Analysis	(2-13)
2.2.4	Conclusion	(2-17)
2.2.5	Discussion	(2-17)
2.3	CHECKING ACCURACY OF HEADLOSS	
	TAPPINGS	(2-20)
2.3.1	Procedure	(2-20)
2.3.2	Results	(2-20)
2.3.3	Conclusion	(2-20)
2.3.4	Discussion	(2-21)
2.4	CALCULATING DARCY FRICTION FACTOR .	(2-24)
2.4.1	Results	(2-24)
2.4.2	Conclusions	(2-27)
2.4.3	Discussion	(2-27)
2.5	HEADLOSS RELATIONSHIP EXPERIMENT ..	(2-28)
2.5.1	Procedure	(2-28)
2.5.2	Results	(2-29)
2.5.2.1	Approach to Results Processing	(2-29)
2.5.2.2	Numerical Results	(2-31)
2.5.3	Conclusions	(2-33)
2.5.4	Discussion	(2-33)

Chapter 3.	INCREASED DISCHARGE EXPERIMENT	

3.1	EQUIPMENT	(3-3)
3.1.1	The Tank	(3-3)
3.1.2	The Drum	(3-6)
3.1.3	The Bucket and the Helix	(3-6)
3.2	PROCEDURE	(3-7)
3.3	RESULTS	(3-8)
3.4	CONCLUSION	(3-11)
3.5	DISCUSSION	(3-12)
Chapter 4.	MAIN POWER EXPERIMENT	

4.1	EQUIPMENT	(4-1)
4.1.1	The Tank	(4-6)
4.1.2	The Coil Pump	(4-9)
4.1.3	The Head Generator	(4-13)
4.1.4	The Data Logging Equipment	(4-14)
4.1.4.1	Power Input	(4-16)
4.1.4.2	Pressure Output	(4-16)
4.1.4.3	Angular Velocity of the Pump	(4-17)
4.1.4.4	The BBC Microcomputer	(4-18)
4.2	PROCEDURE	(4-20)
4.2.1	Procedure for Each Experiment	(4-22)
4.2.2	Parameter Organisation in the Experiment	(4-24)
4.3	RESULTS	(4-26)
4.3.1	Processing the Results	(4-27)

4.4	CONCLUSION	(4-32)
4.5	DISCUSSION	(4-33)
4.5.1	The Approach to regressing the Data	(4-33)
4.5.2	Observations Made During Experimentation	(4-35)
4.5.3	Summary	(4-37)

Chapter 5. PUMP THEORY

5.1	GENERAL HELIX THEORIES	(5-1)
5.1.1	The Pressure Build-up Inside the Helix	(5-1)
5.1.2	Air Plug Contraction	(5-4)
5.1.3	General Resistance to Flow	(5-6)
5.1.4	Flow Media Resistace	(5-6)
5.1.5	Water Plug Level Development	(5-11)
5.2	THE HELIX AT BELOW 50% D.O.I.	(5-14)
5.2.1	Low Headlift Pumping	(5-14)
5.2.2	Bubbling Medium Headlift Pumping .	(5-18)
5.2.3	High Headlift Pumping	(5-24)
5.3	THE HELIX AT OR ABOVE 50% D.O.I. .	(5-29)
5.3.1	Low Headlift Pumping	(5-29)
5.3.2	Spilling Medium Headlift Pumping .	(5-29)
5.3.3	High Headlift Pumping	(5-32)
5.4	MAXIMUM HEADLIFT PUMPING	(5-34)
5.5	FLOW MEDIA HELIX PUMPING	(5-36)

5.6	THE DELIVERY PIPE	(5-40)
5.7	THE PUMP DISCHARGE	(5-41)
5.7.1	Introduction	(5-41)
5.7.2	Increasing the Discharge	(5-43)
5.7.2.1	Introduction	(5-43)
5.7.2.2	Liquid Plug Volume Increase Calculation	(5-44)
5.7.2.3	Calculating the Discharge Through the Hole	(5-45)
5.7.2.4	Calculating the Increased Discharge	(5-47)
5.7.2.5	Calculating the Increased D.O.I. .	(5-48)
5.7.2.6	Discussing the Accuracy of this Theorem	(5-50)
5.8	THE HEAD GENERATOR	(5-52)
5.8.1	Introduction	(5-52)
5.8.2	Loss of Head Prevention	(5-53)
5.8.3	Prevention of Air Escaping	(5-55)

Chapter 6. THE COMPUTER SIMULATION

6.1	ASSUMPTIONS AND APPROXIMATIONS OF THE SIMULATION	(6-1)
6.1.1	Single Snapshot per Revolution ...	(6-2)
6.1.2	The Spilling Interface	(6-3)
6.1.3	The First and Last Coils	(6-3)
6.1.4	The Level Oscillations	(6-4)

6.2	THE HIGH-LEVEL FLOW OF PROGRAM LOGIC	(6-5)
6.3	FUNCTIONAL DESCRIPTION OF THE PROCEDURES	(6-8)
6.3.1	Control Procedure	(6-8)
6.3.2	The Input Procedure	(6-11)
6.3.3	The Initialisation Procedure	(6-11)
6.3.4	Non-Bubbling, Non-Spilling Procedure	(6-14)
6.3.5	Bubbling, Non-Spilling Procedure	(6-17)
6.3.6	Non-Bubbling, Spilling Procedure	(6-20)
6.3.7	Bubbling, Spilling Procedure	(6-25)
6.4	DISPLAYING OUTPUTS OF PROGRAMS ..	(6-32)
6.4.1	Tabular Output	(6-32)
6.4.2	Graphical Outputs	(6-33)
6.5	VALIDATING THE GRAPHICAL PROFILES GENERATED	(6-36)
6.5.1	The First Validating Experiment .	(6-36)
6.5.2	The Second Validating Experiment	(6-37)
6.5.3	Conclusion	(6-38)

Chapter 7

THESIS REVIEW

7.1	PREVIOUS RESEARCH	(7-1)
7.2	THE FLOW MEDIA RESISTANCE EXPERIMENT	(7-4)

7.3	INCREASING THE DISCHARGE EXPERIMENT	(7-5)
7.4	THE MAIN POWER EXPERIMENT	(7-6)
7.5	THE THEORY	(7-8)
7.6	THE SIMULATION	(7-10)
7.7	SUGGESTED FUTURE DIRECTIONS OF RESEARCH	(7-11)
7.7.1	Flow Media Properties	(7-11)
7.7.2	Sediment Deposit	(7-13)
7.7.3	The "Blow-Back" Phenomena	(7-13)
7.7.4	Increasing the Discharge of a Coil Pump	(7-14)
7.7.5	Different Types of Spirals	(7-15)
7.7.6	High Headlift Coil Pumping	(7-15)
7.7.7	The First and Last Water Plugs ..	(7-16)
7.7.8	Investigate the Interface Between Different Coils	(7-17)
7.7.9	Investigating Power Efficiencies .	(7-17)
7.7.10	Investigating Air Plug Power Loss	(7-18)
7.7.11	Investigating the Compressibility of Air Plugs	(7-18)
7.8	SUGGESTED FUTURE DIRECTIONS OF THE SIMULATIONS	(7-19)
7.8.1	Multi-Snapshot Programs	(7-19)
7.8.2	Finite Element Analysis	(7-19)
7.8.3	Use as a Designers Tool	(7-20)

7.8.4	Graphics Capabilities	(7-20)
7.8.4.1	Two Dimensional Profile Output ..	(7-21)
7.8.4.2	Three Dimensional Profile Outputs	(7-25)
7.8.4.3	Contour Map Output	(7-27)
7.8.4.4	Finite Element Analysis Output ..	(7-27)
7.9	EPILOGUE	(7-28)

Appendices

A.	FLOW MEDIA RESISTANCE EXPERIMENT RESULTS	(A-1)
B.	REGRESSION THEORY	(B-1)
C.	INCREASED DISCHARGE EXPERIMENT RESULTS .	(C-1)
D.	MAIN POWER EXPERIMENT RESULTS	(D-1)
E.	BBC MICROCOMPUTER PROGRAMS	(E-1)
F.	COMPUTER SIMULATION PROGRAM LISTING	(F-1)

Table of Figures

1.1	DIAGRAMS OF EARLY COIL PUMPS	(1-2)
1.2	DIAGRAM OF A TYPICAL LABORATORY COIL PUMP .	(1-7)
1.3	DIAGRAM OF A LIFTING PUMP	(1-10)
1.4	A WASTE WATER TREATMENT UNIT	(1-14)
2.1	THE FLOW MEDIA RESISTANCE EXPERIMENT	(2-3)
2.2	ORIFICE METER PHOTOGRAPH	(2-4)
2.3	CONTROL VALVES PHOTOGRAPH	(2-5)
2.4	FLOW MEDIA CONTAINING PIPE PHOTOGRAPH	(2-6)
2.5	MANOMETER TAPPINGS PHOTOGRAPH	(2-7)
2.6	EXPERIMENT OUTLET PHOTOGRAPH	(2-9)
2.7	ORIFICE METER CALIBRATION CHART PHOTOGRAPH	(2-11)
2.8	SCHEMATIC DIAGRAM OF THE MANOMETER TAPPINGS	(2-18)
2.9	MANOMETER CONFIGURATION TABLE	(2-19)
2.10	FLOW ANOMALIES AROUND THE FLOW MEDIA ELEMENTS	(2-34)
3.1	INCREASED DISCHARGE EXPERIMENT	(3-2)
3.2	COIL PUMP DRUM PHOTOGRAPH	(3-4)
3.3	COIL PUMP BUCKET AND HELIX PHOTOGRAPH	(3-5)
4.1	THE COIL PUMP POWER EXPERIMENT DIAGRAM	(4-2)

4.2	DRIVE CHAIN, CAM AND ETHER PHOTOGRAPH	(4-3)
4.3	HEAD GENERATOR AND SHAFT BEARING PHOTOGRAPH	(4-4)
4.4	VARIABLE HEIGHT OVERFLOW DEVICE AND VARIAC PHOTOGRAPH	(4-5)
4.5	HELIX PHOTOGRAPH	(4-7)
4.6	HELIX CONNECTOR PHOTOGRAPH	(4-8)
4.7	ROTARY VALVE AND PRESSURE TRANSDUCER PHOTOGRAPH	(4-10)
4.8	HEAD GENERATOR DIAGRAM	(4-11)
4.9	THE DATA LOGGING EQUIPMENT DIAGRAM	(4-12)
4.10	GRAPH OF PRESSURE AGAINST VOLTAGE FOR THE PRESSURE TRANSDUCER	(4-15)
4.11	EXPERIMENT ORGANISATION TABLE	(4-23)
5.1	A CASCADING MANOMETER	(5-2)
5.2	A COIL PUMP HEAD DIFFERENCE PROFILE	(5-3)
5.3	A ROTATED WATER PLUG	(5-8)
5.4	A ROTATED WATER PLUG ABOUT TO SPILL	(5-9)
5.5	A ROTATED WATER PLUG ABOUT TO BUBBLE	(5-10)
5.6	A LOW HEADLIFT PROFILE	(5-13)
5.7	A BUBBLING MEDIUM HEADLIFT PROFILE	(5-17)
5.8	THE RESTRICTING ROTATION ANGLE	(5-19)
5.9	A HIGH HEAD LIFT PROFILE	(5-21)
5.10	A BUBBLING FIRST WATER PLUG	(5-22)
5.11	A BUBBLING & SPILLING WATER PLUG	(5-23)
5.12	A SPILLING MEDIUM HEADLIFT PROFILE	(5-27)

5.13	A SPILLING AND BEING SPILT INTO WATER PLUG	(5-28)
5.14	MAXIMUM HEADLIFT PROFILE	(5-33)
5.15	VELOCITY OF A BUBBLING AND SPILLING WATER PLUG	(5-37)
5.16	DIAGRAM TO FIND THE BUCKET VOLUME	(5-42)
5.17	HEAD DIFFERENCE ACROSS THE PIPE HOLE	(5-49)
5.18	THE HELIX AND HEAD GENERATOR	(5-54)
6.1	CONTROL PROCEDURE FLOWCHART	(6-7)
6.2	THE INPUT PROCEDURE FLOWCHART	(6-9)
6.3	INITIALISATION PROCEDURE FLOWCHART	(6-10)
6.4	NON-BUBBLING, NON-SPILLING PROCEDURE	(6-13)
6.5	BUBBLING, NON-SPILLING PROCEDURE FLOWCHART	(6-16)
6.6	NON-BUBBLING, SPILLING FLOWCHART	(6-19)
6.7	BUBBLING, SPILLING PROCEDURE FLOWCHART ..	(6-24)
6.8	NON-BUBBLING, NON-SPILLING TABULAR OUTPUT	(6-28)
6.9	BUBBLING, NON-SPILLING TABULAR OUTPUT ...	(6-29)
6.10	NON-BUBBLING, SPILLING TABULAR OUTPUT ...	(6-30)
6.11	BUBBLING, SPILLING TABULAR OUTPUT	(6-31)
6.12	FIRST VALIDATING EXPERIMENT OUTPUT	(6-34)
6.13	SECOND VALIDATING EXPERIMENT OUTPUT	(6-35)
7.1	EXAMPLE OF AN ISOMETRIC SURFACE PROFILE .	(7-22)
7.2	EXAMPLE OF AN ISOMETRIC SURFACE PROFILE .	(7-23)
7.3	EXAMPLE OF AN ISOMETRIC SURFACE PROFILE .	(7-24)
7.4	EXAMPLE OF A CONTOUR MAP PROFILE	(7-26)

Results for Flow Media Plug

A.1 PLUG LENGTH = 0.660 m (A-2)
A.2 PLUG LENGTH = 1.385 m (A-3)
A.3 PLUG LENGTH = 1.975 m (A-4)
A.4 PLUG LENGTH = 2.955 m (A-5)
A.5 PLUG LENGTH = 3.880 m (A-6)
A.6 PLUG LENGTH = 5.000 m (A-7)

INCREASED DISCHARGE EXPT RESULTS (C-1)

Main Power Experiment Results

D.1 (D-1)
D.2 (D-8)
D.3 (D-15)
D.4 (D-22)

DATA LOGGING PROGRAM (E-1)

DOWNLOAD PROGRAM (E-2)

GRAPHICAL DISPLAY PROGRAM (E-3)

SIMULATION PROGRAM (F-1)

References

1. REES, A. et al.: The Cyclopedia of Science and Arts, Longman, Hurst, Rees, Orme and Brown, 1819 - 20
2. OHLEMUTZ, R: The Hydrostatic Pump. Unpublished 1975
3. BAMFORTH, A: A Low Cost Pump using a Rotating Helical Coil. Final Year Project, Loughborough University of Technology, April 1977
4. WINSTANLEY, C.B.F: Rotating Coil Pump. Final Year Project, Loughborough University of Technology, April 1977.
5. ROBINSON, P.A: A Rotating Coil Pump. Final Year Project, Loughborough University of Technology, April 1978.
6. ANNABLE, R.J: Rotating Coil Pump. Final Year Project, Loughborough University of Technology, April 1979.
7. ANNABLE, R.J: Analysis and Development of a Stream Powered Coil Pump. Post-Graduate Research Project. Loughborough University of Technology, January 1982.
8. STUCKEY, A.T. and WILSON, E.M: The Stream Powered Manometric Pump. Paper for 'Appropriate Technology in Civil Engineering' Conference, London 1980.
9. WILSON, C: Rotating Coil Pump. Final Year Project, Loughborough University of Technology, April 1981.
10. MASSEY, B.S: Mechanics of Fluids. Van Nostrand, Reinhold Company, London, p176, 1970.

11. MOODY, L.F: Friction Factors for Pipe Flow.
Trans. Am. Soc. Mech. Engineers, 1944.
12. FOX, J.A: An Introduction to Engineering Fluid
Mechanics. The MacMillan Press Ltd., London,
p198, 1974.
13. STEPHENSON, D: Rockfill in Hydraulic Engineering.
Elsevier Scientific Publishing Company.
Amsterdam, p19, 1979.
14. Snowdon, J: Basic Statistics. Butterworths.
London. p67, 1969.
15. MASSEY, B.S: Mechanics of Fluids. Van Nostrand.
Reinhold Company. London., 1970.
16. MORTIMER, G.H., ANNABLE.R.: The Coil Pump - Theory
and Practice, Journal of Hydraulic Research,
Vol. 22, 1984, No. 1.
17. MORTIMER, G.H.: An Estimation of the Performance of
the Coil Pump when Used for Treating Wastewater,
Internal Document, Loughborough University of
Technology, Unpublished, 1982.
18. STEPHENSON, G: Mathematical Methods for Science
Students. Longman Group Ltd., London. 1981.
19. MORTIMER, G.H. and GALVIN, S: The Coil Pump, an
unusual positive displacement pump. Paper for
'International Conference on Positive Displacement
Pumps', Chester, England, 1986.

20. MORGAN, P.R.A: New Water Pump: Spiral tube. Sci. News, Vol 13, No 1, Zimbabwe Rhodesia. p179 - 180, 1979.
21. SYFYDNSGRUPPEN: Stream Driven Spiral Pump. Manual, Denmark.
22. WEIR, A: The Stream Driven Hydrostatic Coil Pump for low lift irrigation, Internal Report. University Dar es Salaam. Tanzania.

Nomenclature

- A = mean cross sectional area of a pipe
- Ab = cross sectional area of the bucket extra to that of the inlet to the helix
- af = proportional coefficient of resistivity of the flow media, equal to 7.385 in the experiment in chapter 2
- Ah = cross-sectional area of a hole in a pipe wall
- As = wetted surface area of a coil pump
- bf = power coefficient of resistivity of the flow media, equal to 1.860 in the experiment described in chapter 2
- cc = correlation coefficient of a relationship being developed
- Cd = coefficient of discharge of an orifice
- D = diameter of the Drum
- Dx = the rotation of the xth water plug from its original position, which equals the summation of all the individual rotations of all the following water plugs due to the compressions of their air plugs
- d = internal diameter of the pipe
- dc = depth of holes in the vertical pipe in the Splash chamber below the centreline of the helix

DOI = depth of immersion the drum is sitting in
 (below the centreline of the drum)

DOIe = depth of immersion inside the helix

Dx = the rotation of the xth water plug from its
 original position

Ff = darcy Pipe Friction Factor

g = gravimetric constant (= 9.81 m / sec / sec)

Ha = atmospheric pressure head

hfx = resistance head of the flow media plug
 inside

Hh = head difference across a hole in the pipe
 wall

Hl = headloss across a flow media plug/manometer
 tapping

Hn = absolute pressure head at the outlet of a
 pump

Hr = total head generated by the helix

Hu = total head generated by all the bubbling
 only water plugs

Hv = total head generated by all bubbling and
 spilling water plugs

hrx = total flow media resistance head across the
 xth coil

hx = head difference across the xth water plug

hu = head difference generated by a bubbling only
 water plug

- h_v = head difference generated by a bubbling and spilling water plug
 h_w = head difference generated by a plug bubbling being spilt in to but not spilling itself
 H_x = absolute pressure head in the xth air plug
 i = the number of bubbling only water plugs
 l_{ax} = length of the xth air plug under pressure head H_x
 L_b = length of the bucket
 L_{eb} = length representing the reduction in volume of the liquid the bucket scoops up due to the orientation of the bucket relative to the surface of the liquid in the tank
 L_{rx} = reduction in the length of the xth air plug as the pressure rises from ' H_a ' to ' H_x '
 l_f = length of flow media plug in the flow media resistance experiment
 l_{fx} = length of the flow media plug in the xth coil
 l = length of the pipe in the Flow Media resistance Experiment
 l_{wx} = length of the xth liquid plug
 n = number of coils in a pump
 N_s = speed of rotation (r.p.m.)
 π = The ratio of a circle's circumference to its diameter,
 Q = mean discharge through the pump/experiment

Q_b = discharge of a helix with a bucket attached
 P = power absorbed by the coil pump
 Power fm = power absorbed by the flow media inside the
 coil pump
 P_{wsa} = power absorbed by the wetted surface area
 ρ = density of water
 = 1000 kg/m³
 R = radius of the drum
 R_b = radius of the bucket in the increased dis-
 charge experiment
 r = internal radius of the pipe
 T_h = time the liquid has to pass out of a hole in a
 pipe wall per revolution
 Vel = mean liquid velocity through an experiment
 Vel_x = mean velocity of the xth liquid plug through
 the helix
 V_h = mean velocity of the water through the hole
 in the pipe wall
 Vol_a = volume of last air plug
 Vol_b = volume of liquid scooped up by the bucket
 Vol_c = volume of splash chamber
 Vol_h = the volume of liquid passing out of a hole
 in a pipe wall per revolution
 Vol_x = volume of the xth water plug in the helix
 θ_{pe} = is half the angle subtended by the extended
 plug, at the centre of the drum

θ_x = half the angle the xth water plug subtends
at the centre of the helix

Φ_x = rotation of the preceding water plug
relative to the trailing edge of the xth air
plug

CHAPTER 1
-----THE HISTORY OF THE COIL PUMP
-----1.1 BRIEF DESCRIPTION

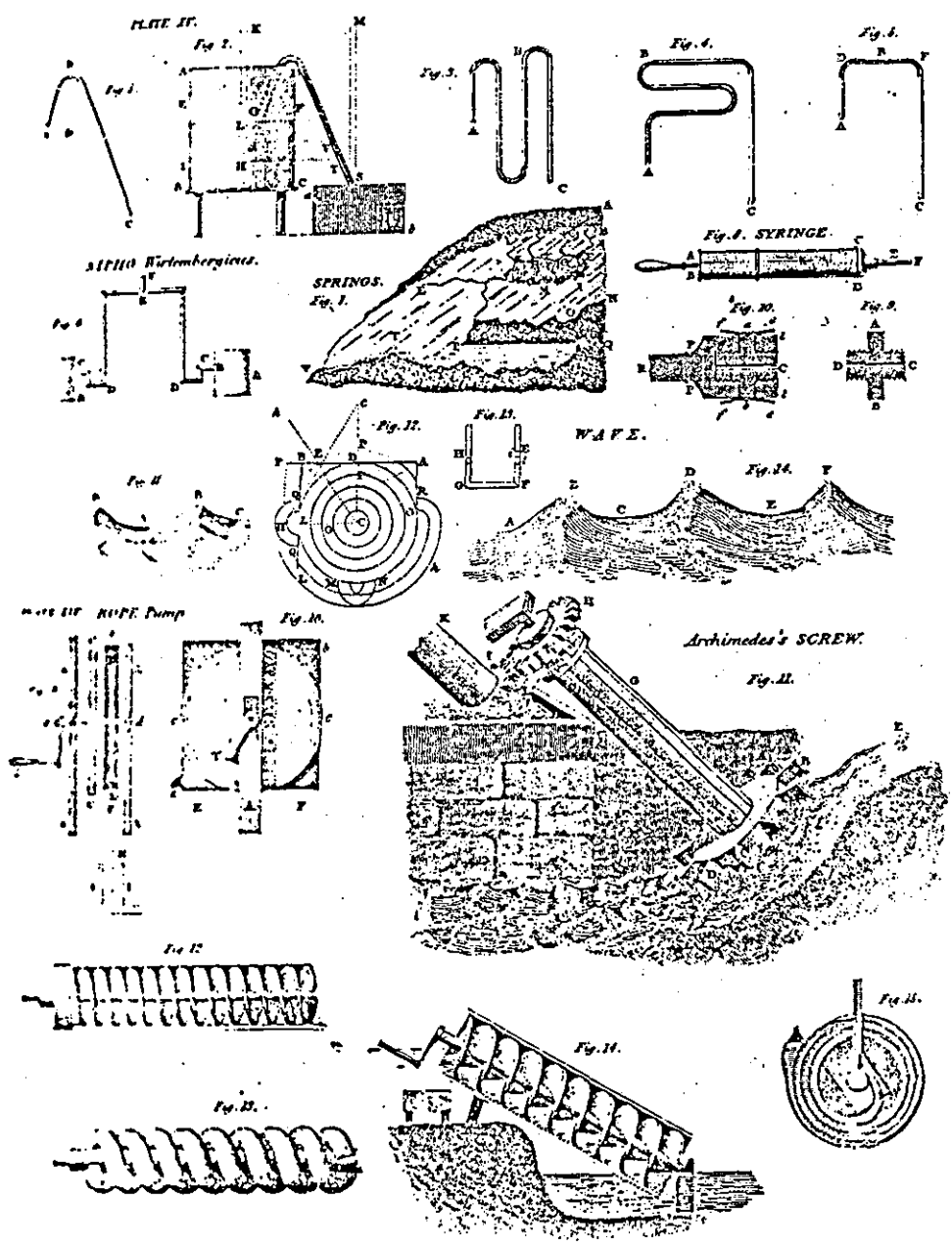
The Coil Pump is a simple device which stems from an old idea. It consists of a length of flexible piping wound into the form of a helix on a cylindrical drum. One end is left open to form the inlet of the pump while the other is connected to a vertical delivery pipe via a sealed rotary joint.

The drum is partially immersed in water with its longitudinal axis parallel to the water surface. The drum rotates around this axis causing the inlet to accept alternate plugs of air and water. The water plugs remain at the bottom of the coils as they pass towards the outlet. While ascending the delivery pipe the water plugs exert a back pressure on the helical coil. This pressure is resisted by the water plugs in the coils rotating away from the outlet, and thus setting up water level differences across each of them.

The sum of all the water level differences is equal to the back pressure exerted by the water plugs in the delivery pipe. This is all made possible by the fact that air is compressible.

HYDRAULICS.

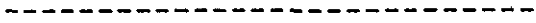
SIPHON.



Published at the Old Derby, etc., by Longman, Hurst, Rees, Orme & Brown, Paternoster Row.

Levy, Jr.

FIGURE 1.1, Diagrams of Early Coil Pumps



The aim of this research is to concentrate on extending the known theories found in previous investigations, and, in particular, to investigate the power requirements of the pump together with the complications involved when it is being used to treat waste water.

1.2 EARLY WORK

1.2.1 Work by Wirtz

The earliest reference to a coil pump can be found in the 'Cyclopedia of Arts and Sciences' (Ref.1). This shows two versions; one is a helix with a constant diameter and the other design is a spiral, in one plane with the radius of the helix reducing in size towards the outlet. These are shown in figure 1.1.

1.2.2 Work By Ohlemutz

The next reference (Ref.2) concentrates mainly on the spiral version of the pump. Rudolf Ohlemutz argued that the spiral version has a number of advantages over the coil version. He argued the spiral version is more economical in space as it utilises the space found inside the constant helix diameter coil pump version.

The spiral version he developed was very complicated in construction and could certainly not be made with unsophisticated materials. This questions its

suitability for applications in the Third World even though he envisaged its main values lie in irrigation and rural water supply.

The spiral version of the pump is based upon the same principles as the coil pump although in a complicated form, to take into account the varying radius of the helix. The version he developed included the relationship that the cross-sectional area of a coil at any point is inversely proportional to the distance from the axis. This helps to overcome the problem of the air and water plugs elongating as they travel towards the central axis, and so over-rotating to such an extent that the theory is corrupted.

Research by Morgan (Ref.20), Syfydngsgruppen (Ref.21), Weir (Ref.22) and others concentrated upon utilising the flow of a stream to rotate a coil pump. This is discussed in more detail in Section 1.3.4. which summarizes the research (Ref.7) completed by Annable into this subject.

1.3 PREVIOUS WORK DONE AT LOUGHBOROUGH UNIVERSITY

1.3.1 Work By Bamforth

Bamforth based his research on a 0.3 metre diameter pump (Ref.3). The relationships investigated were:

1. between speed of rotation and pressure for different depths of immersion, and for 5 and 10 coils
2. between discharge and speed of rotation,
3. between discharge and depth of immersion for different speeds of rotation.

The analytically useful relationship he derived is the equation to predict the theoretical discharge of a coil pump in any situation, it is:

$$Q = N_s * D * \pi * d^2 * \cos^{-1} (-2 * DOI/D) / 4$$

where Q = Discharge,

Ns = Speed of rotation,

D = Diameter of the Drum,

d = Internal Diameter of the coils,

DOI = Distance to the Water Level below the centreline of the shaft.

1.3.2 Work By Winstanley

Winstanley worked on a 0.5 metre diameter coil pump (Ref.4). His research can be summarised as follows:

1. A Video Camera was used to make a comparison between the water level differences while the pump was in motion, and at rest. He found the dynamic levels oscillated around the static ones.
2. He investigated the Bamforth's discharge relationship and gained a good correlation between the theory and experimental values.
3. An attempt was made to find a relationship between the efficiencies of the pump for given depths of immersion. Due to the random nature of the results obtained, it was not possible to draw any valid conclusions.

1.3.3 Work By Robinson

Robinson unsuccessfully attempted to determine the effect of the coil diameter on the efficiency of the pump, (Ref.5). He also measured the water level in each of the coils for various pumping heights. He concluded that the water plugs always adopted the same level for a given pumping height but did not say why.

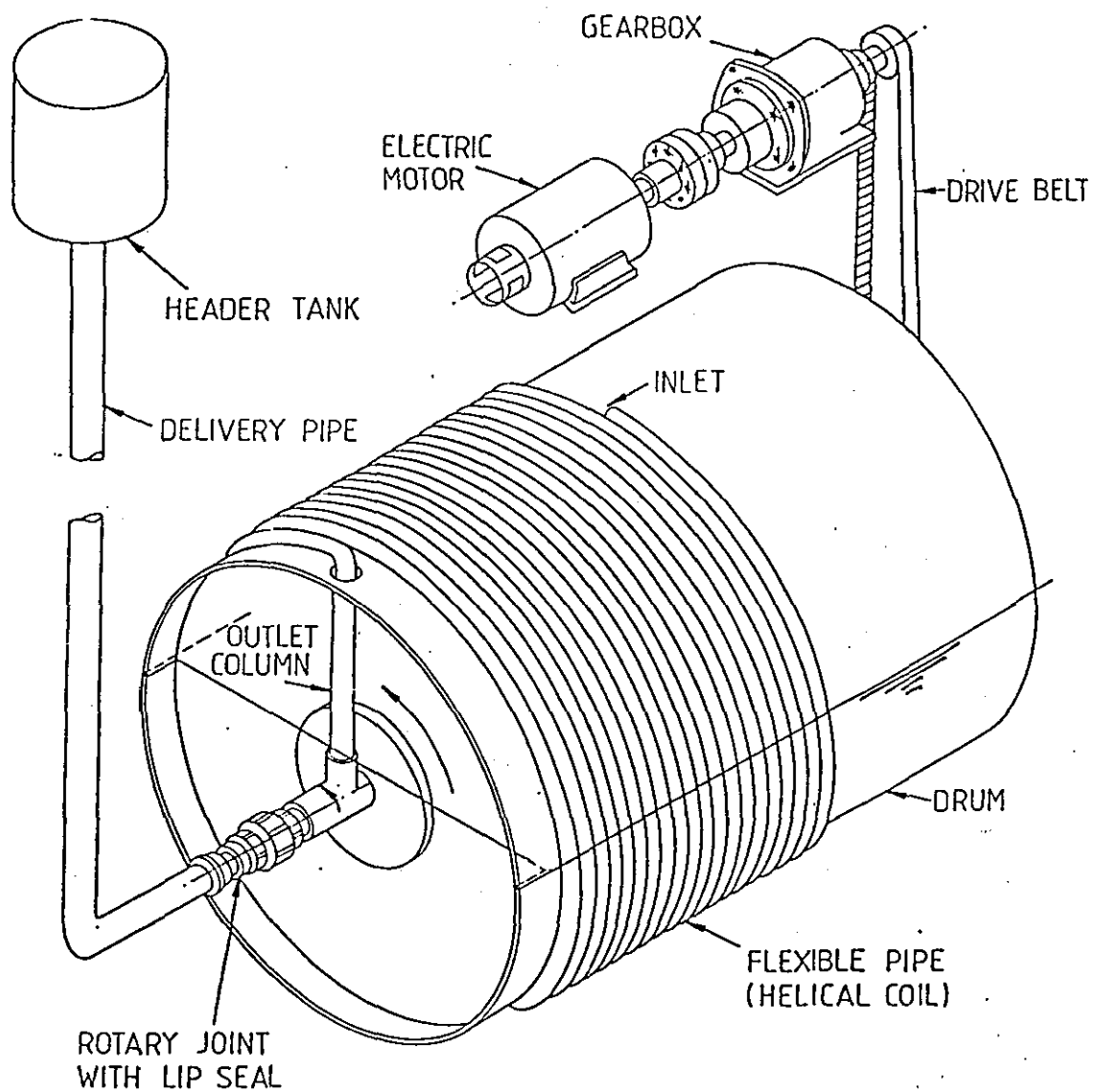


FIGURE 1.2, Diagram of a Typical Laboratory Coil Pump

1.3.4 Work By Annable

In his final year under-graduate project Annable reduced the number of coils on the drum from 20 to 2, in increments of 2, and investigated the effect this had on the water level differences in the coils for various pumping heights (Ref.6). He plotted the head differences in each coil and described and accounted for the characteristic profile of the results when drawn in graphical form. Namely, this profile has a low head difference in the inlet coil, rising to a maximum after a couple of coils, then reducing due to water spilling back from coil to coil.

A relationship was established between the head development and the pumping height, and although a questionable assumption was made in his analysis, that all the water plugs were the same length, his method of approach was correct.

His theory was used to suggest a method of designing a suitable sized pump to meet practicable requirements.

The pump (Figure 1.2) was studied further in post-graduate research (Ref.7). This consisted of a series of measurements of the water levels in the coils to see how they responded to changes in:

1. Speed of Rotation,
2. Depth of Immersion,

3. Internal Diameter of the Helical Coil,
4. Internal Diameter of the Delivery Pipe,
5. Diameter of the Drum,
6. Number of Coils.

A computer program was developed to simulate these situations and also the conditions of the delivery pipe, and it was also used to produce design charts for the pump.

He followed this with some tests on a water powered model in the nearby Blackbrook Stream. This was constructed from 25 millimetre diameter flexible pipe wrapped into 26 coils inside a 50 gallon oil drum. The bouyancy was provided by placing inflatable tyre inner-tubes inside the drum. Chevron shaped paddles were welded to the outside of the drum, together with a shroud. When immersed, these provided the impulse to rotate the coil pump. This apparatus managed to pump a discharge of 4 litres per minute to a height of 9.5 metres at a stream velocity of 0.8 metres per second.

His research lead to a paper being published (Ref. 16) describing the essential details of the pump together with the conclusions found.

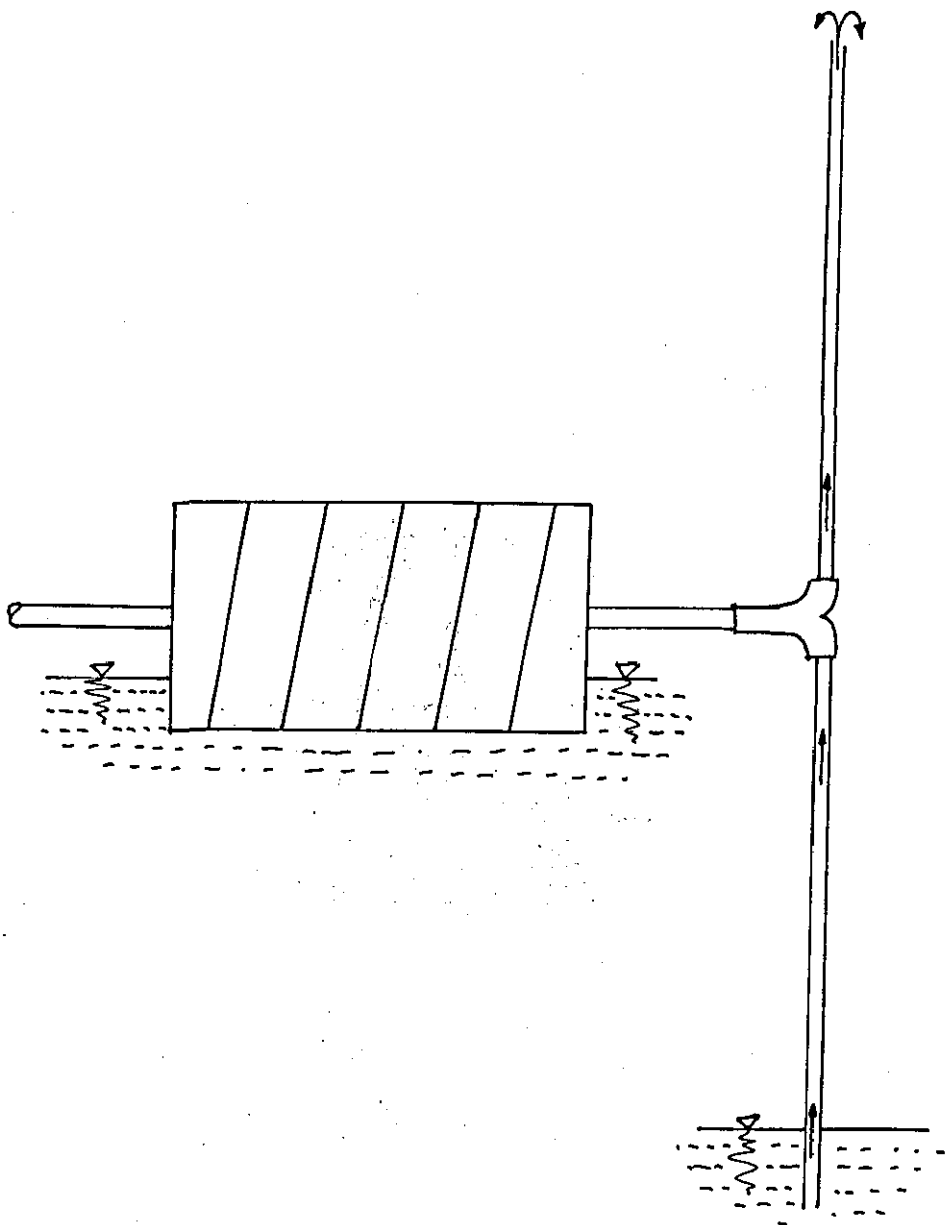


FIGURE 1.3, Diagram of a Lifting Pump

1.3.5 Work by Mortimer

Development work by Mr. G.H. Mortimer on the coil pump suggests that it is capable of lifting water up from a lower level to the level of the helix.

Consider a coil pump (Figure 1.3) mounted in a tank of water, with another tank of water at a lower level. A pipe is connected to the end of the helix normally considered to be the outlet, and the other end of the pipe is immersed into the lower tank.

To prime the helix with water, the coil pump must first pump a small amount of water to the lower level. When the helix and the delivery pipe are filled, the rotation of the pump can then be reversed and water can be pumped from the lower to the higher level.

This mode of operation might be given consideration when the installation of a coil pump at a low level is difficult, or at best inconvenient.

Further descriptions are unavailable as this variant is currently under research.

1.4 WORK AT SALFORD UNIVERSITY

1.4.1 Work by Stuckey and Wilson

In their paper A.T. Stuckey and E.M. Wilson described their work on a pump which they refer to as a manometer pump (Ref.8). Their work involved measuring the discharge at different speeds of rotation and different depths of immersion. They also related a lift ratio (lift at pumping collapse / maximum theoretical lift) to a form of Reynold's number. From this, it was found to be possible to predict the number of coils required for a particular pumping height.

They looked for ways of powering the pump using a stream and built a pump in which the axis was parallel to the stream flow and was powered by turbine blades inside the drum.

1.4.2 Work By Wilson

He continued the investigation of the coil pump (Ref.9) to try to provide a means of designing a suitably sized pump for any given situation.

His investigation could be separated into two main sections:

1. The measurement of heads built up in the individual coils to see if a predictable pattern could be established.
2. The measurement of the heads developed in both vertical and inclined delivery pipes, to determine the effects of rising air plugs on the pumping heights.

From the results of the investigation a computer program was written to be used to help in the design process. From this program the required number of coils could be established from the pumping head required and the diameter of helix of the coils.

He concluded by recommending that more work needed to be done verifying and modifying the theories, and investigating the different aspects of the pump. This included looking at combinations of the different ratios of parameters (such as drum diameter, numbers of coils, depths of immersion etc) for optimisation purposes.

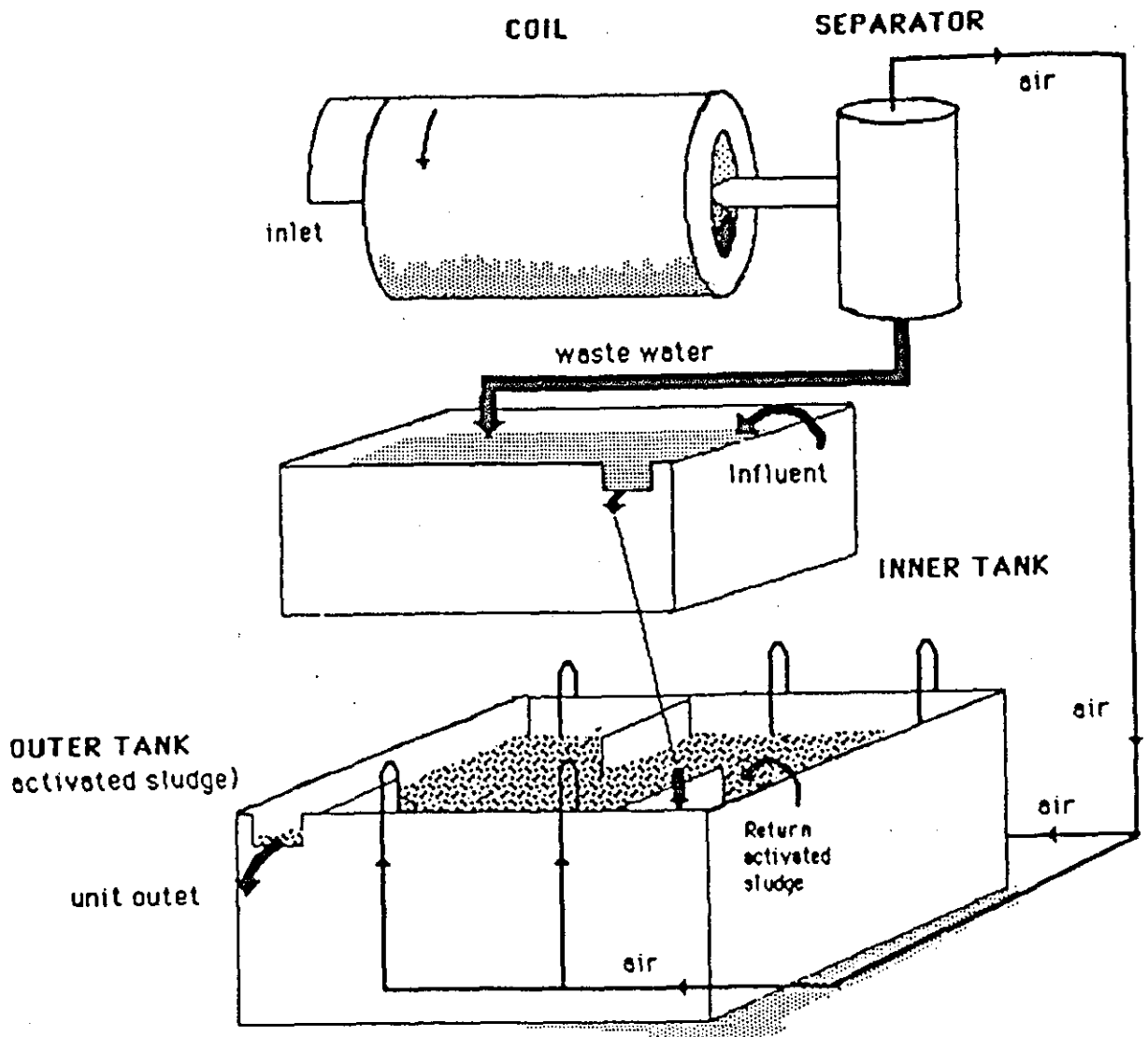


FIGURE 1.4, A Waste Water Treatment Unit

1.5 WORK ON A WASTE WATER TREATMENT COIL PUMP

Development work at Loughborough University by Mr. G.H. Mortimer on the coil pump (Figure 1.4) suggested that it is suitable for treating waste water (Ref. 17). The helix pumps both air and water, and any surface which comes in contact with the waste water will develop a biological film. At the helix outlet, the discharging pressurised waste water and air are used to enhance the treatment process. This is done by bubbling the air through the wastewater in the tank in which the coil pump resides. A proportion of the treated wastewater is also used to circulate back into the tank as activated sludge. This will help to initiate the biological process.

Consider a pump of 6 coils, with a diameter of 1.1 metres, 40 percent full of flow media (plastic filter media to enhance the internal surface area). If it rotates at 3 revolutions per minute, at a depth of immersion of approximately 60 percent, then at conservative estimate, this can provide facilities to cater for wastewater processing of 171 members of the population (Ref. 17).

On paper, this pump appears to have great potential because of its effectiveness and compactness. Further development work will prove whether this statement is correct.

CHAPTER 2

FLOW MEDIA RESISTANCE EXPERIMENT

Previous research in Loughborough suggests that the coil pump is suitable for waste water treatment (Ref 17). While it is operating, the surfaces which come in contact with the waste water develops a biological film. It is this film which treats the waste water as it is pumped. As the pump's capacity to treat, is proportional to the wetted surface area (amongst other parameters), to maximise the pump's performance the area has to be as large as possible. This has been achieved by increasing the coil diameter and incorporating a flow media inside the coils. The flow media has a surface area of 200 square metres per cubic metre of volume. It is made by taking μ PVC 30mm diameter corrugated pipes and cutting these into approximately 50mm lengths.

Incorporating flow media in the coils reduces the pumps performance by introducing a resistance to flow. It has to be investigated to predict the pump's behaviour and so the experiments in this chapter were performed to this end.

The experiments in this chapter were designed to find the headlosses across different lengths of flow media. A relationship could then be obtained linking the mean velocity of liquid flowing through the pipe with the length of the flow media plugs and the headloss

across them. This relationship could then be used to estimate the headlosses in the large pipe diameter coil pump.

Although this experiment attempts to represent the liquid flow through the helix, this can not be simulated perfectly, due to differences between the environments of this experiment and a typical pump. For example, differences due to the pipe being straight in this experiment as opposed to curved, in the helix of the coils. Another difference is the rough nature of the internal surface of the flexible pipe instead of the relatively smooth μ PVC pipe used in this experiment. The differences will undoubtedly change the environment in which the flow media will find itself. Bearing in mind that these are only minor points, this experiment may be considered to have achieved the design objective of giving a reasonable insight into the properties of the flow through the media.

A number of control experiments were performed before the main experiments commenced. They are fully set out under their own headings, together with explanations of why they were done, their procedures, results and discussions.

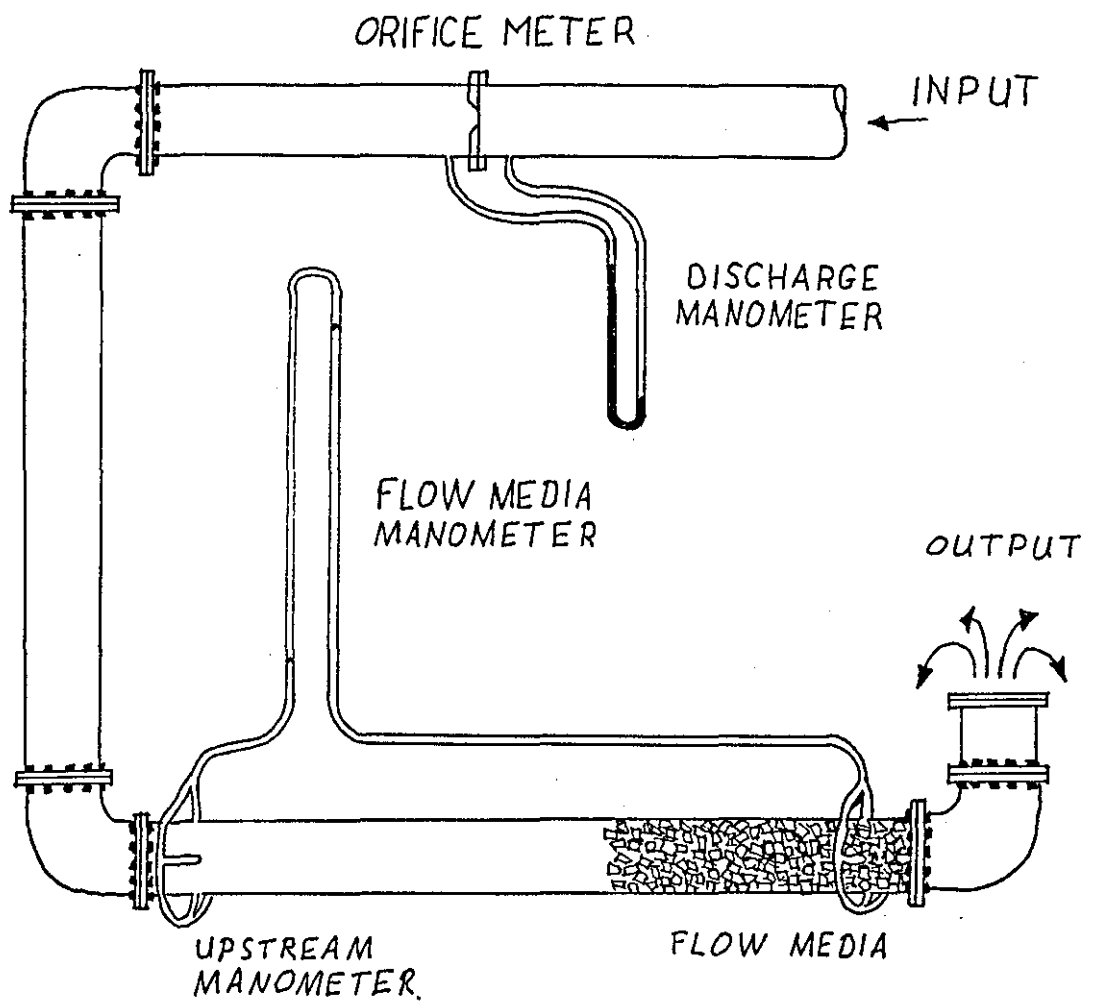


FIGURE 2.1, The Flow Media Resistance Experiment

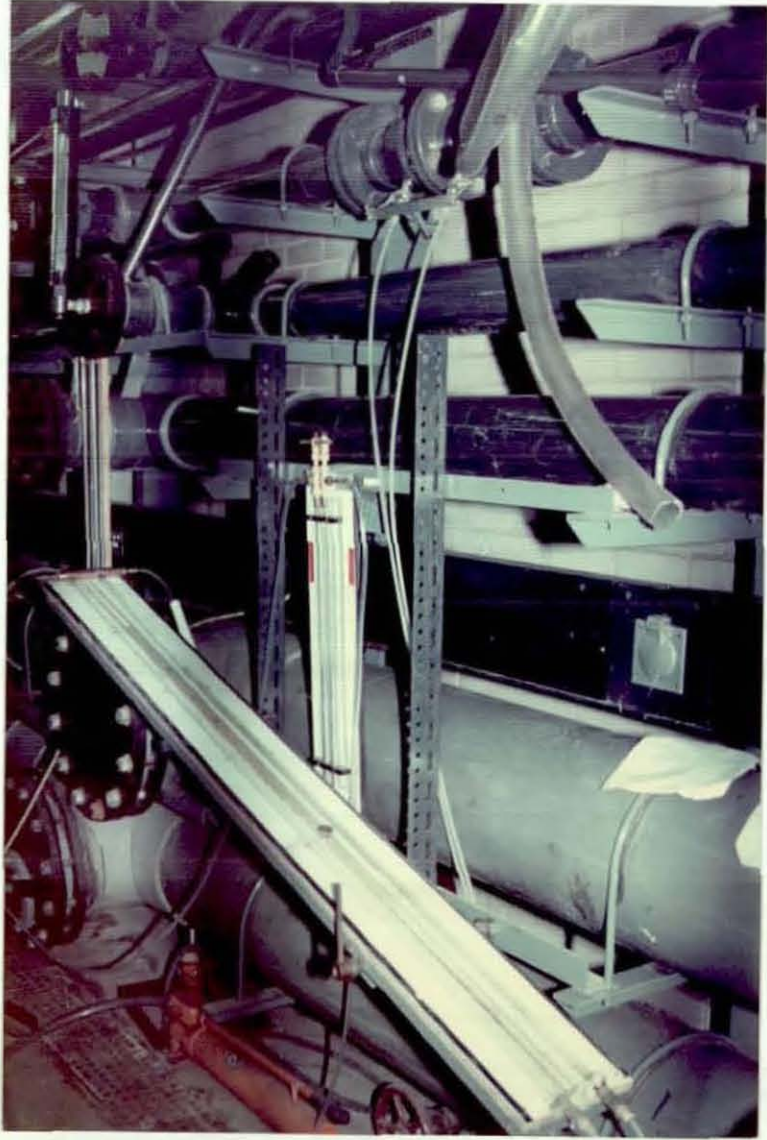


FIGURE 2.2, Orifice Meter Photograph

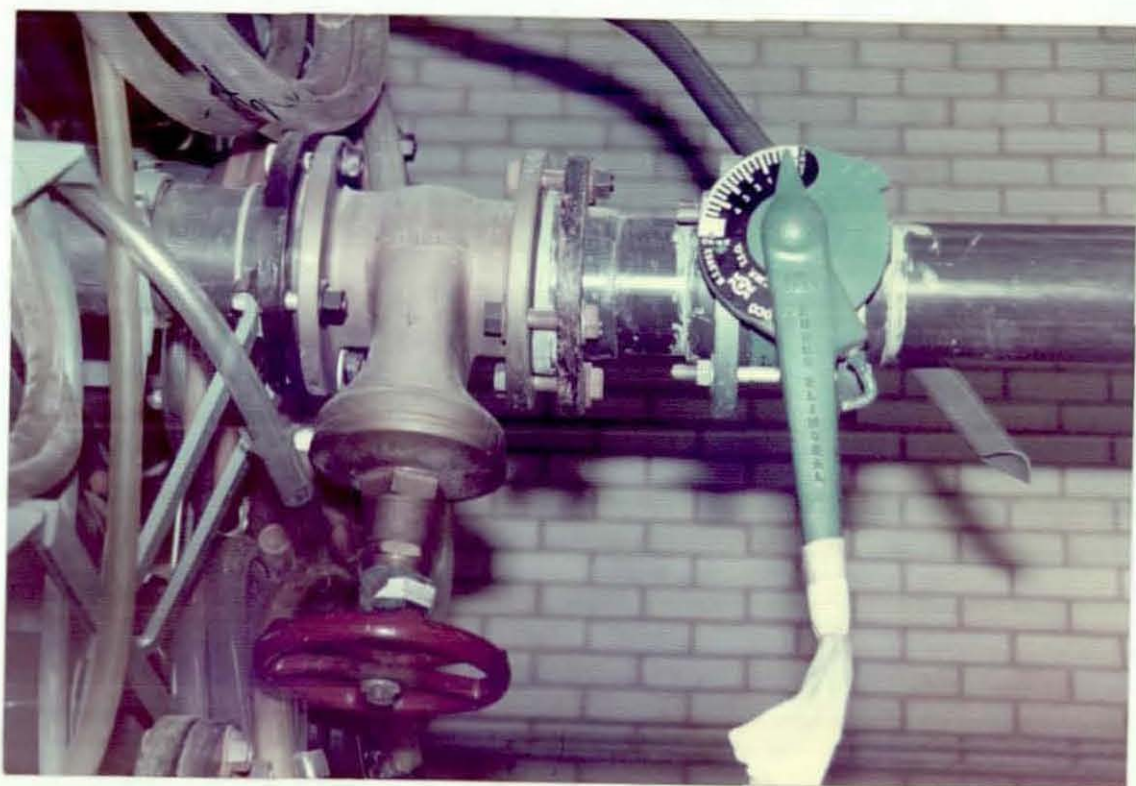


FIGURE 2.3, Control Valves Photograph



FIGURE 2.4, Flow Media Containing Pipe Photograph



FIGURE 2.5, Manometer Tappings Photograph

2.1 EQUIPMENT

Figure 2.1 shows the layout of the apparatus. The total head can be adjusted up to a maximum value of 15 metres using the main supply tank in the laboratory tower. Before the water reaches the experiment, the discharge was measured through a previously calibrated orifice meter (figure 2.2), but as a precaution, was checked as one of the control experiments.

Two valves upstream of the experiment (figure 2.3), controlled the discharge through the pipe. A butterfly valve was used as a main on/off switch and a gate valve sets the correct flow needed.

The pipe containing the flow media (figure 2.4) was 6 metres long and had an internal diameter of, $d = 153$ millimetres. This diameter was chosen to correspond with the diameter of the helix used in the main experiment described later in this thesis. Manometer tapings shown (figure 2.5) are included to measure the headloss across the length of the flow media in the pipe. The up-stream manometer tapings are 0.7 metres downstream of an up-stream bend. This was to enable the flow's velocity distribution to return to its optimum after turning through a 90 degrees bend.

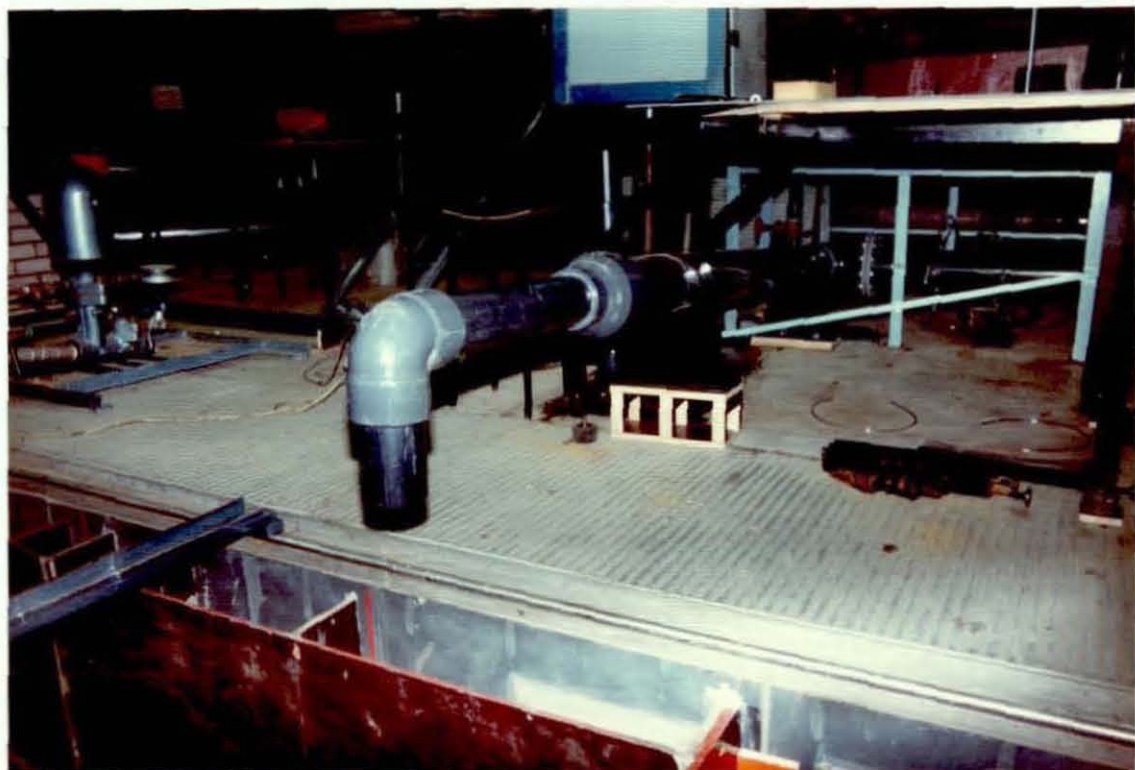


FIGURE 2.6, Experiment Outlet Photograph

A mesh has been placed at the down-stream end of the pipe to arrest the movement of the flow media. The downstream manometer tapings was situated 0.3 metres up-stream of the mesh to measure the mean pressure head at this point. This gives the differential manometer (figure 2.2) a distance of 5 metres to measure the headloss across, and so obtain the hydraulic gradient.

There are four tappings at each tapping location and these are connected together in parallel to give the mean pressure head at these locations. These extra tappings are included in the design as it is felt that the pressures could very easily be corrupted by the flow media. It also enables each of the tappings to be checked against the mean of the others.

The outlet of the experiment (figure 2.6), is above the flow media containing pipe to prevent air from travelling back into the rest of the experiment.

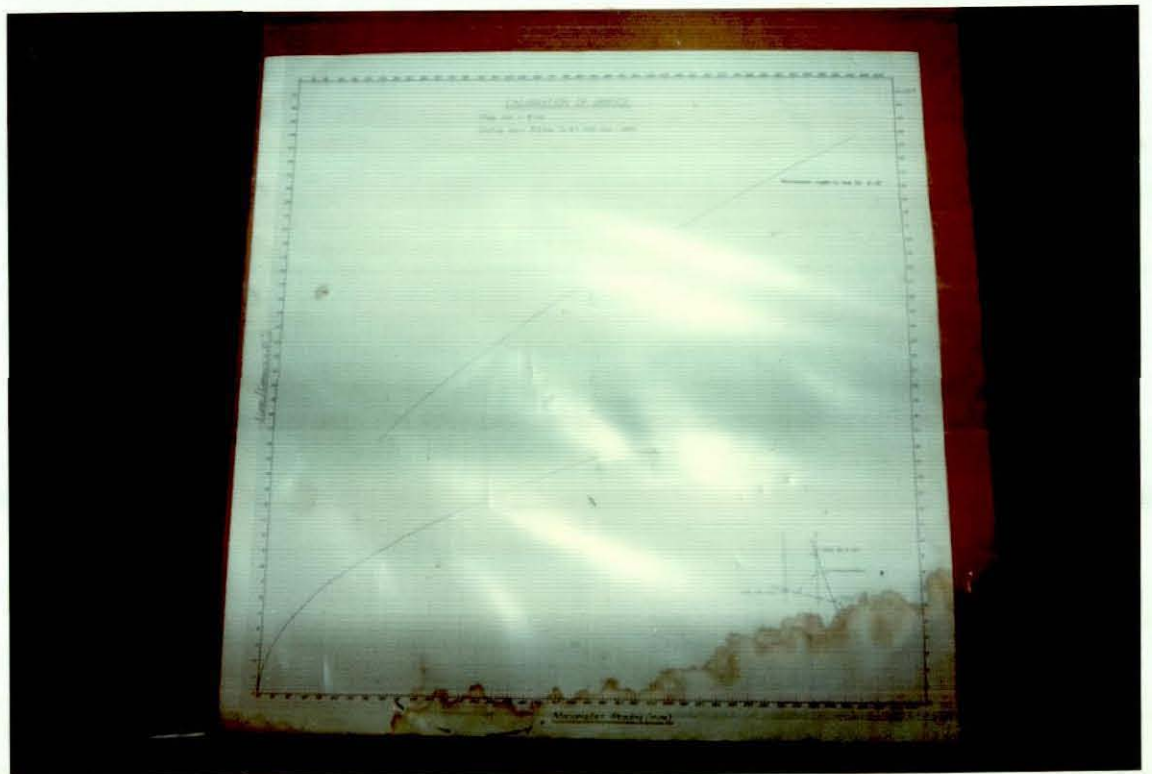


FIGURE 2.7, Orifice Meter Calibration Chart Photograph

2.2 CHECKING THE ORIFICE METER CALIBRATION

2.2.1 Procedure

Situated up-stream of the flow media, there was an orifice meter to measure the discharge through the experiment. This had been previously calibrated but as a precautionary measure *it had* to be checked.

Water eventually flows into a 10 tonne weigh tank, to compare the actual discharges with those measured through the orifice meter.

Discharges examined in the experiment were small (up to 30 litres per second) in comparison to the weigh tank size and therefore the time to collect the discharges was in the order of minutes. This resulted in taking a number of readings to limit errors due to gradually varying flow. It also helped to limit any inaccurate manometer readings or booking blunders.

2.2.2 Results

It was found that over a range of measurements, the actual flows recorded were on average, 1.5 percent higher than those processed from the orifice meter differential manometer and its calibration chart (figure 2.7). The maximum positive difference was 2.8 percent and the maximum negative difference was 0.8 percent.

N.B. Individual results taken are in Appendix A.

2.2.3 Error Analysis

To establish whether readings taken from the orifice meter calibration chart can be taken as actual discharges experienced by the apparatus it has to be proved that:

1. Readings taken from the orifice meter calibration chart are comparable to the actual discharges through the apparatus, and
2. The accuracy to which the readings can be resolved are within the bounds of the accuracies to which the actual discharges through the apparatus can be resolved.

The following error analysis determines the accuracy to which the actual discharge through the experiment can be measured.

Given that discharge can be expressed as:

$$q = \frac{v}{t}$$

Where v = volume, and

t = time

Then through partial differentiation, for an incompressible flow, a small change in discharge can be expressed as:

$$dq = \frac{q}{v} \cdot dv + \frac{q}{t} \cdot dt$$

Where dq = the small change in discharge,

dt = time during which the change in discharge occurs,

dv = the change in volume associated with the dt and dq ,

$\frac{dq}{dt}$ = the rate of change of discharge with respect to time,

$\frac{dq}{dv}$ = the rate of change of discharge with respect to volume,

Also, by differentiating discharge with respect to volume, it can be found that:

$$\frac{dq}{dv} = \frac{1}{t}$$

And by differentiating discharge with respect to time, it can be found that:

$$\frac{dq}{dt} = -\frac{v}{t}$$

Combining the above three equations it is possible to express the potential percentage error of an actual discharge as a function of the potential percentage errors in its associated measured volume and time duration:

$$\frac{dq}{q} \cdot 100 = \frac{1}{t} \cdot v \cdot \frac{t}{v} \cdot 100 - \frac{v}{t} \cdot t \cdot \frac{t}{v} \cdot 100$$

That is to say:

$$\begin{array}{l} \text{Percentage} \\ \text{error in } q \end{array} = \begin{array}{l} \text{Percentage} \\ \text{error in } v \end{array} - \begin{array}{l} \text{Percentage} \\ \text{error in } t \end{array}$$

Typical readings (and their possible inaccuracies) taken from this experiment are:

1. Weight of water collected in the weigh tank equals 2000 Kg (possible error equals 40 kg),
2. Time taken for water to be collected in the weigh tank equals 360 seconds (possible error equals 1 second),

Substituting these values into the above equation it can be found that:

$$\begin{array}{l} \text{Percentage} \\ \text{error in } q \end{array} = \frac{40}{2000} \cdot 100 - \frac{1}{360} \cdot 100$$

$$= 1.7 \text{ percent}$$

2.2.4 Conclusion

The differences between the actual and theoretical discharges found by the experimental results are within the bounds calculated by the above error analysis. This indicates that the orifice meter is still within calibration, taking into consideration the accuracies to which the experiment can be depended on.

2.2.5 Discussion

It was necessary for experimental completeness to eliminate any errors due to inaccurate data collection. It is to this end that this control experiment has been performed. It also gave the opportunity to become acquainted with the apparatus and so realise any problems before the commencement of the main experiment.

Over the range of flows envisaged in the following experiments, the meter reads approximately 1.5 percent lower than the actual flows through it. The error analysis shows the readings can only be calculated to an accuracy of 1.7 percent.

It confirms that the meter is within its calibration and so the experiment can proceed without any modification to the equipment.

Manometer Connections		Discharge	Headloss
Upstream	Downstream	(l/s)	(mm)
All	All	28.0	55.65
1	All	25.9	55.65
2	All	25.3	52.06
3	All	25.7	51.80
4	All	29.0	54.80
All	All	25.7	55.39
All	5	25.5	56.42
All	6	25.7	59.24
All	7	25.7	45.13
All	8	27.3	55.39
All	All	25.9	54.62

Figure 2.9, Manometer Configurations Table

2.3 CHECKING ACCURACY OF HEADLOSS TAPPINGS

2.3.1 Procedure

The tappings *were* constructed by drilling holes into the pipe wall. These could have imperfections (expanded upon in the associated discussion) and so these had to be checked. Tappings are designed to record the pressure at the pipe wall and therefore any imperfections will be detrimental to its performance. To check for aberrations, all the readings from one set of four tappings (Figure 2.8) are compared to the mean of the other set, and vice-versa. The flow past these points is varied and the head differences observed.

2.3.2 Results

Individual results taken are shown in figure 2.9.

2.3.3 Conclusion

The only significant aberration in this experiment occurs when the mean of the upstream manometer tappings is connected up to one side of the differential manometer and number 7 downstream tapping is connected to the other. The reading of approximately ten millimetres lower than the others, on first reflection presents a problem. However considering this, relative

to the main part of the experiment, with flow media head losses of up to two metres dwarfing these errors, then this small error may be considered to be insignificant. The detailed reasons needed to support this conclusion are considered in the discussion.

2.3.4 Discussion

It was felt to be worthwhile to check the construction of the eight manometer tapings, as inaccurate workmanship could have invalidated all the conclusions.

The tapping holes are constructed by drilling through the wall of the pipe and so the perimeter of these, at the intersection of the inside pipe surface, may have raised or uneven edges. Even though the skilled technicians who constructed the equipment did their best to clean these holes, there is a chance that imperfections remain. This is the reason for this control experiment.

A tapping is designed to record the pressure head of a liquid passing by the small orifice in the surface wall. For this to be performed accurately, it needs to be machined flush and perpendicular to the pipe wall. Any deviation from this placement, will tend to disrupt the flow and so induce erroneous readings.

A typical inaccuracy is for a component of the

velocity head of the fluid to be included in the pressure head. One of the ways that this can happen is for the raised edges surrounding the hole to scoop a fraction of the fluid flow into the orifice. Imperfections in the orifice perimeter can also induce vortices to be shed across the orifice and so oscillate the readings. Oscillations of up to ten millimetres in amplitude were noticed at the start of the experiments and even though these could have come from the natural turbulence, the need to check the tapings was justified.

The main error was from the tapping number 7 reading approximately 10 millimetres too high. This in absolute terms does not appear too serious until it is compared to a total headloss across the tapping locations of 50 millimetres.

The reasons for ignoring this error are two-fold. The first is that the highest water velocities used in this experiment are over twice those used in the main experiment. From Darcy's Pipe Friction Equation this would infer that the error would be quartered and thus very much smaller. The second and most important reason is that compared to the headlosses generated by the flow media, (potentially over two metres) this error represents less than 0.5% of the total reading and is therefore negligible in comparison.

A way of overcoming this error which was not used here, is to ignore the lowest and highest readings. It

is felt that the errors due to the interaction of the flow media with the manometer holes would be more significant than the errors discussed here. The decision was therefore taken to keep as many tapping points as possible operational.

2.4 CALCULATING DARCY FRICTION FACTOR

2.4.1 Results

While checking the accuracy of the manometer tappings the associated discharges were also recorded. This provided data to calculate the pipe friction factor for later use.

Although the Darcy Pipe Friction Equation is considered to have inherent inaccuracies (Ref. 10), it is used here to calculate the friction coefficient. There are three reasons for its use. The first is that it is simple and convenient to use. Secondly, the accuracies in the whole experiment are such that an exact solution is not required, and finally the results from this equation can easily be checked immediately by the side of the experiment.

Data obtained while checking the tappings is utilised in the Darcy pipe friction equation shown here:

$$Hl = Ff * \frac{l * Vel^2}{d * 2g} \quad (2.1)$$

where H_l = headloss across the manometer tapings,
 F_f = Darcy Pipe Friction Factor, dependant on
the roughness of the pipe wall and flow type,
 l = Length of the pipe involved, ($= 5$ metres),
 d = Inside Diameter of the pipe, ($= 0.1524$ m),
 Vel = Mean Velocity of the water flowing through
the pipe, ($=$ discharge / cross sectional
area),
 g = Gravimetric Constant
($= 9.81$ m / sec / sec).

From the data from the previous experiment (using
all of the manometer tapings) we have:

Headloss (m)	Discharge 3 (m / s)	Mean Water Velocity (m / s)
0.05565	0.0280	1.535
0.05539	0.0257	1.409
0.05462	0.0259	1.429

rearranging equation (2.1) we get:

$$Ff = Hl * d * \frac{2g}{I * Vel^2}$$

Substituting in the above values we have:

$$Ff1 = \frac{0.05565 * 0.1524 * 2g}{5 * 1.535^2} = 0.0141$$

$$Ff2 = \frac{0.05539 * 0.1524 * 2g}{5 * 1.409^2} = 0.0167$$

$$Ff3 = \frac{0.05462 * 0.1525 * 2g}{5 * 1.420^2} = 0.0162$$

Taking the mean of these values, we have:

$$Ff = 0.0157 \quad (2.2)$$

2.4.2 Conclusion

A typical value for the Friction Factor for a drawn μ PVC pipe under complete turbulent flow is 0.020 (Ref.11). The experimental value is in the same order of magnitude as the referred value and can be used in the processing of later results.

2.4.3 Discussion

The experimental value is found to be close to the referred value indicating that the experimental value is reasonable. It can therefore be used to subtract the headlosses due to fluid viscosity in the empty part of the pipe in the processing of later results.

It will be shown later that the headloss from the viscosity in the empty part of the pipe is small in comparison to the headlosses generated by the flow media. The use of the Darcy pipe friction equation is therefore justified, even though it is not the most accurate equation available.

The Colebrook-White Formula (Ref. 12) could have been used to obtain results of a greater accuracy, but the iterative nature of the calculation makes it cumbersome to use.

2.5 HEADLOSS RELATIONSHIP EXPERIMENT

2.5.1 Procedure

A number of different lengths of flow media are investigated by filling the pipe in increments of approximately 0.6 metres, to allow for a large spread of results. Six lengths are considered sufficient to enable accurate regression of the results. For each increment, at least ten discharges were recorded together with the associated headlosses between the manometer tapings.

The media lengths are measured by partially dismantling the test rig and carefully introducing a rod down the exposed upstream entrance to the pipe. The length of the media can be calculated by taking the complement of the 'distance to the downstream manometer tapping' and the 'length of the empty part of the pipe'. This is done after each set of experiments to allow for the possible compaction of the media plug under the force of the discharge. The next increment of media can then be introduced into the pipe before the apparatus is re-assembled.

Care is taken to ensure that the media does not upset the manometer tapping readings. It can happen if the media matrix (generated randomly during its initial placement) directs the flow away or towards, faster or slower, past the tapping holes. The pressure head will

be corrupted from the mean pressure head across the whole of the pipe by containing a component of the velocity head of a vortex, or jet of liquid.

To partially overcome the problem, each one of the individual tappings is compared to the mean of the others in its vicinity. If the individual readings do not approximate to the mean, then the flow media matrix is re-adjusted until it does. Unfortunately there can still be an overall error due to the individual errors not cancelling out each other. This is overcome by using the data from the set of discharges from the first increment of flow media closest to the tappings, as a control against all the subsequent readings.

2.5.2 Results

2.5.2.1 Approach to Results Processing

From elementary geophysics, it is known that the resistance to flow through a permeable substance is proportional to the velocity of that flow. Similarly, from Hydromechanics it is known that the resistance to flow through a pipe is proportional to the square of the velocity of the fluid passing through it. It is therefore reasonable to expect that the resistance to flow of the discharge passing through the loose matrix of the flow media elements contained in the pipe, is proportional to the velocity of that flow raised to a

power of a constant. It is the determination of the constant of proportionality and the power constant in this relationship that is the object of this experiment.

In mathematical form, the relationship between the headloss of a liquid passing through the flow media and the velocity of the liquid is:

$$Hl/lf = af * Vel^{bf} \quad (2.3)$$

where Hl = headloss across a flow media plug (metres),
 Vel = mean velocity through plug (metres/second),
 lf = length of flow media plug (metres),
 af = constant of proportionality,
 bf = power constant.

To regress this relationship using the approach described in Appendix B, we have to take the Logarithm of both sides, thus:

$$\log_e (Hl/lf) = \log_e (af) + bf * \log_e (Vel) \quad (2.4)$$

The Headloss experienced by the flow media plug, (divided by its length) can now be regressed against the velocity of the fluid through it to obtain the constants of the resultant relationship. As a measure of the accuracy of the relationship, the correlation coefficient is also determined.

2.5.2.2 Numerical Results

Due to problems involved with potential inaccuracies in the headloss manometer readings, the processing of the results proved to be quite complicated.

The flow rate and headloss results from the first increment of the flow media (in Table A.1) closest to the tappings, are regressed to find the relationship between the fluid velocity and headloss across it. The relationship found is:

$$Hl = 3.405 * Vel^{1.989} \quad (2.5)$$

(lf = 0.66m length of flow media)

with a correlation coefficient, cc = 0.9991 over a range of flows of Vd = 0.0 to 0.7620 metres/second

This equation is used to nullify the potential

error in the downstream tappings. It is done by subtracting the calculated headloss due to the first increment next to the tappings, from the total headloss across the whole length of the flow media. The length of the flow media resisting the remaining headloss, is found by subtracting the length of the first increment away from the total length of the media.

Darcy's Pipe Friction Equation (2.1) is used to eliminate the headloss due to the viscosity in the empty part of the pipe.

With the above two effects eliminated from the results, the regression can proceed. To compare results from different lengths of the flow media, the head losses are divided by their own lengths. This is finally regressed against the mean fluid velocity through the media.

N.B. Individual results taken are in Appendix A.

The resultant relationship is:

$$H_l / l_f = 7.385 * Vel^{1.860} \quad (2.6)$$

With a correlation coefficient, $cc = 0.9950$ over a range of flow of $Vel = 0.0$ to 1.535 metres/second

2.5.3 Conclusion

The two correlation coefficients in the above results section are very close to unity which (as discussed in Appendix B) suggests that the relationships found are accurate and significant. The difference in the constants derived from the regression substantiates the need to approach the processing of the results in the previously described manner. The different constants show that the first length of flow media shows a significantly different relationship to the rest of the increments immediately upstream. This is attributed to the proximity of manometer tapplings to the flow media corrupting the results.

The final relationship is described in the theory in chapter 5, and is used in the computer simulation described in chapter 6 to emulate a coil pump containing flow media.

2.5.4 Discussion

Due to the problems described earlier with the downstream tapplings, it is necessary to ignore the resistance due to the first increment of flow media. Besides the problems due to the inaccuracies in the construction of the tapplings, these are compounded by the interaction of the flow media components with the tapping holes themselves.

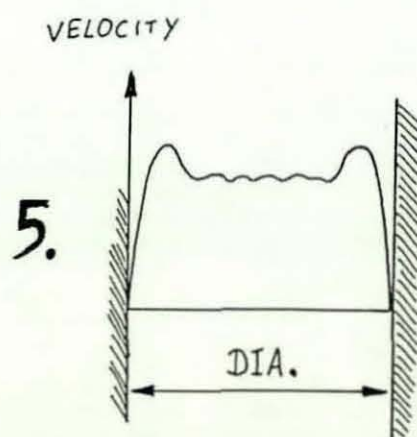
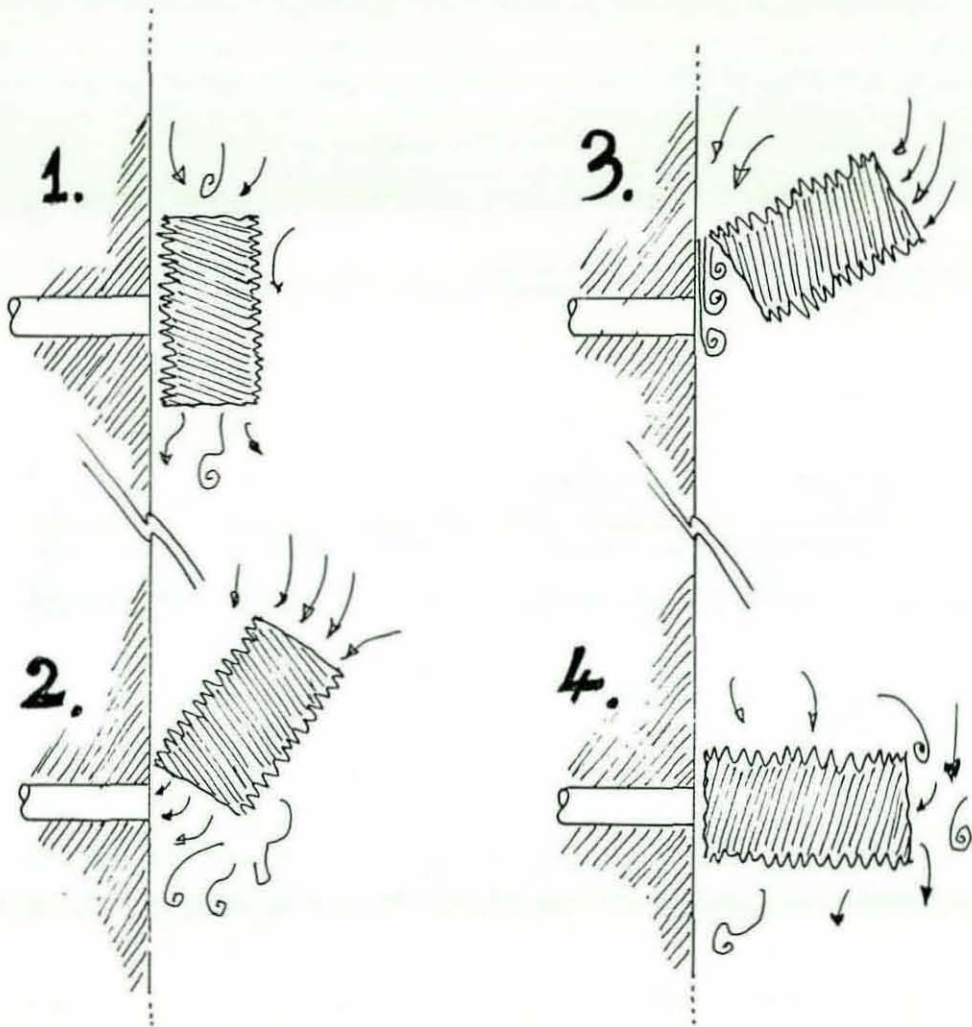


FIGURE 2.10, Flow Anomalies around Flow Media Element

An inaccuracy not taken into account here, is that the headloss across the flow media is not proportional to the length of flow media. To simplify the results processing, the headloss across a flow media plug is divided by its length. This give a value suitable for regression against the velocity of the fluid flowing through it. This hypothesis of non-proportionality is too complex to investigate with this simple equipment without introducing more manometer tappings. Therefore this hypothesis has been ignored, except to note that the accuracy of the above relations tend to discount it.

The flow media matrix used in these experiments consists of a large number of 30 millimetre diameter corrugated plastic pipes 50 millimetres long. These are arranged in a random manner and compacted by the force of the discharge passing through the matrix. The random nature of the matrix makes the tappings function difficult in terms of recording accurate results, as the flow through this matrix can be unpredictable. The readings can be corrupted for the following reasons:

1. The tapping holes can be masked by the side of a flow media element. The pressure at this point will then be unpredictable. (Figure 2.10a)
2. A flow media element close to the tapping point, may channel part of the flow towards or away from the hole. This will make the pressure

head in the tapping rise or fall due to a component of the velocity head being added or subtracted from the pressure head. (Figure 2.10b)

3. The flow around and through these elements is turbulent and due to the random nature of the flow media, this could cause vortices to be shed past the manometer holes. Consequently the pressure head will fluctuate at this point due to the varying velocity head of the water in the vortices. This is due to velocity being equal to the complement of the total head of the water (at any point) against the pressure head, and therefore as the velocity head varies, so will the pressure head. (Figure 2.10c)
4. A flow media element may shelter a tapping hole by being very close to and perpendicular to the wall. The open end of the flow media will then act as an enlarged tapping hole and the pressure head across this large hole can not be depended upon to be accurate. (Figure 2.10d)
5. The velocity profile across the pipe is hard to determine but it is thought to approximate to the profile shown in figure 2.10e. The lower

density of packing possible, near the boundaries of the flow media at the pipe wall, is thought to provide more open spaces than in the interior of the matrix. These open spaces will offer less resistance to flow and thus the velocities here will be higher than the mean. This will lead to a lowering of the pressure head at these points where a possible manometer tapping might be situated. Corruption of the results will then inevitably follow. This effect might be nullified by covering up both the upstream and downstream manometer points. This is impossible to do when different lengths of flow media have to be tested inside the pipe and so a problem remains.

All these possible errors may initially raise some doubts over the accuracy of the results taken, but the high correlation coefficient and the rigorous control experiments defend the results obtained.

It has been proved beyond reasonable doubt that the readings from the first increment of flow media have been corrupted by some or all of the errors described above. It also shows that these errors have been nullified by the elimination of the first increment of flow media from the rest in the results processing. This infers that the final relationship, relating the

headloss of a fluid passing through the media to the velocity of the fluid itself, is valid.

With hindsight, it would have been plausible to perform the experiments described in this chapter on the flexible ducting described in section 4.2.2. This would have enabled direct comparisons to have been made bearing in mind the similarity of the apparatus. An important feature of the experiment described in chapter 4 is that the flexible ducting is put under varying pressures. This has the possible consequences of varying the resistances to flow through the ducting and so must be investigated. Unfortunately, due to the nature of the fabric of the ducting, it would have proved impossible to position manometer tappings accurately enough to realistically measure the headloss across the flow media. A problem would also have occurred in supporting the flexible ducting to keep it straight.

Parallel research (Ref.13) has also made progress investigating the resistance to flow through porous granular media over a wide range of Reynolds numbers. This research has found that the headloss of the liquid passing through this material is proportional to the velocity raised to the power of approximately 1.85. This tends to support the values obtained above.

As an example, to show how the coil pump experimented upon in chapter 4 would be theoretically effected by the inclusion of flow media, consider the

following. If the pump is at a depth of immersion of 50 percent, then the length of flow media inside the helix is:

$$\begin{aligned} l_f &= n * (D + d) * \text{Pi}/2 \\ &= 12.848 \text{ metres} \end{aligned}$$

If the pump is rotating at 3 revolutions per minute, then the resistive head across the helix is:

$$\begin{aligned} H_l &= l_f * 7.385 * (\text{Ns} * (D + d) * \text{Pi}/60)^{1.860} \\ &= 12.848 * 7.385 * (3 * 1.0224 * \text{Pi}/60)^{1.860} \\ &= 3.161 \text{ metres of water} \end{aligned}$$

This shows that the inclusion of flow media is very significant when considering the design and power consumption of a coil pump.

N.B.: D = The Diameter of the Drum,

d = The Diameter of the pipe.

n = The number of coils in the pump

CHAPTER 3

INCREASED DISCHARGE EXPERIMENT

The aim of this experiment is to increase the pump discharge without increasing the depth of immersion of the drum to over 50 percent. This will prevent the shaft, drive chain and bearings from exposure to any corrosive properties of the liquid in which it is partly submerged.

A way to overcome the problem is to increase the entrance to the coils in such a way as to increase the liquid plug volume at the expense of the air plugs. The investigation of this is central to the purpose of this experiment.

N.B. To avoid repetition, the theories associated with the experiment have been included in Chapter 5, together with the rest of the theories describing the coil pump.

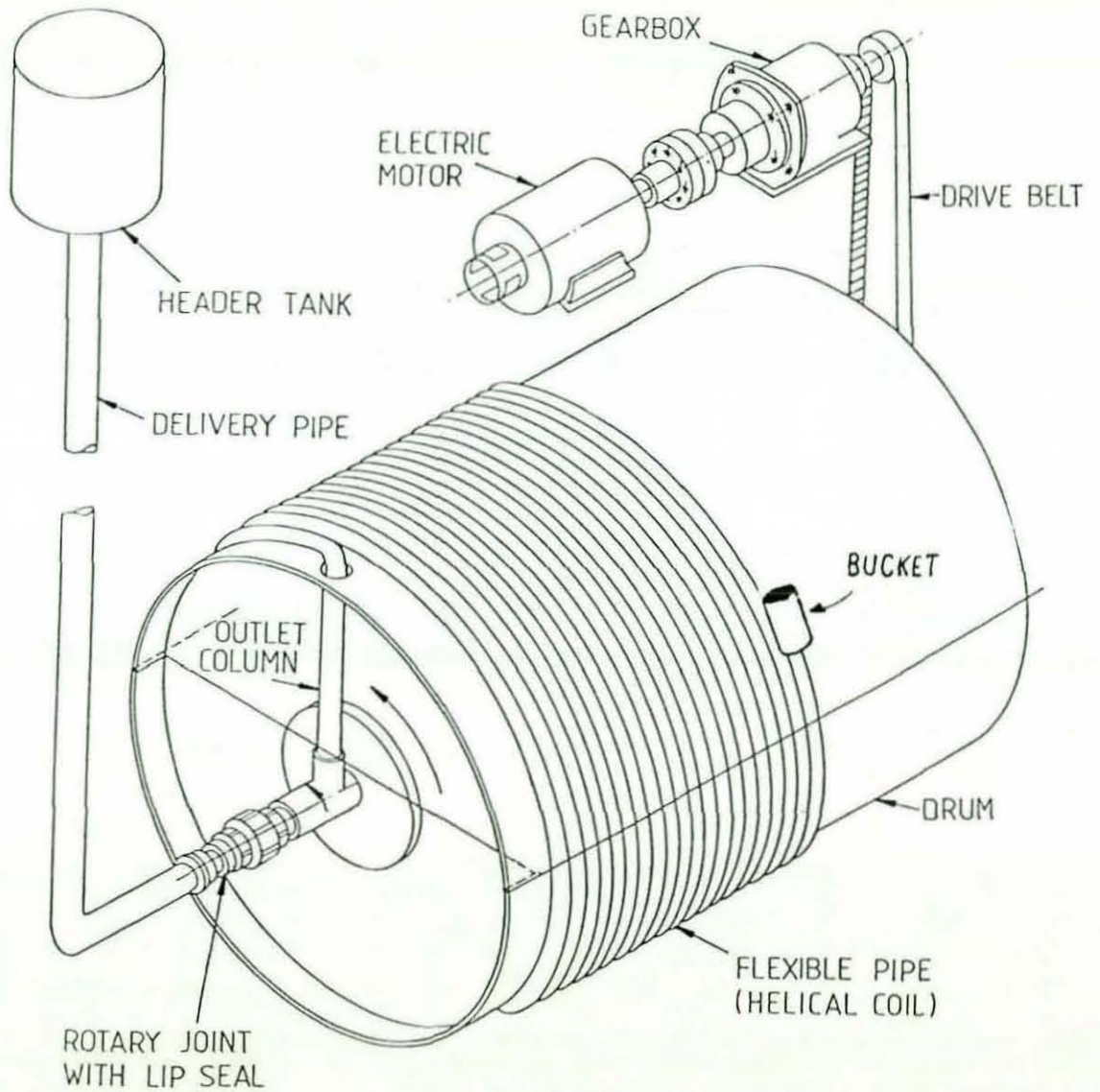


FIGURE 3.1, Increased Discharge Experiment

3.1 EQUIPMENT

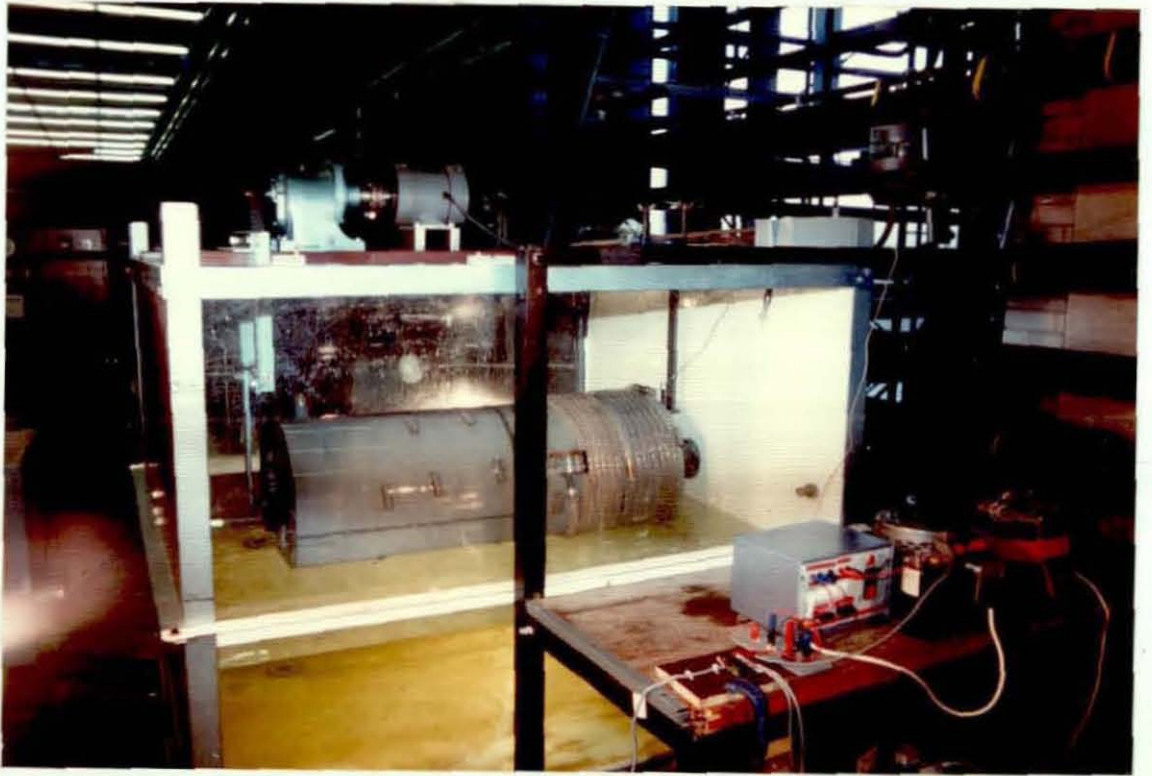
Figure 3.1 shows the layout of the Increased Discharge Experiment. The three main elements of the experiment consist of the Tank, Coil Pump and Head Lift apparatus which are each described in the following sections.

3.1.1 The Tank

The Tank had been constructed for a previous research project and so was made available for these experiments.

The dimensions of the Tank *were* 1.6 metres long by 1.1 metres wide, and 1.3 metres deep. An electric motor *was* situated on beams suspended over the top of the Tank. It *drove* the pump through a series of reduction gears and a drive belt to the main shaft on which the drum rotates.

A steady depth of immersion *was* achieved by allowing the discharge from the pump to circulate back to the tank. The depth of immersion *was* altered by introducing or draining liquid from the tank. The depth of immersion *was* read from a scale on the side of the transparent tank wall. The origin of the scale is situated at the same height as the drum shaft.



FIGURES 3.2, Coil Pump Drum Photograph

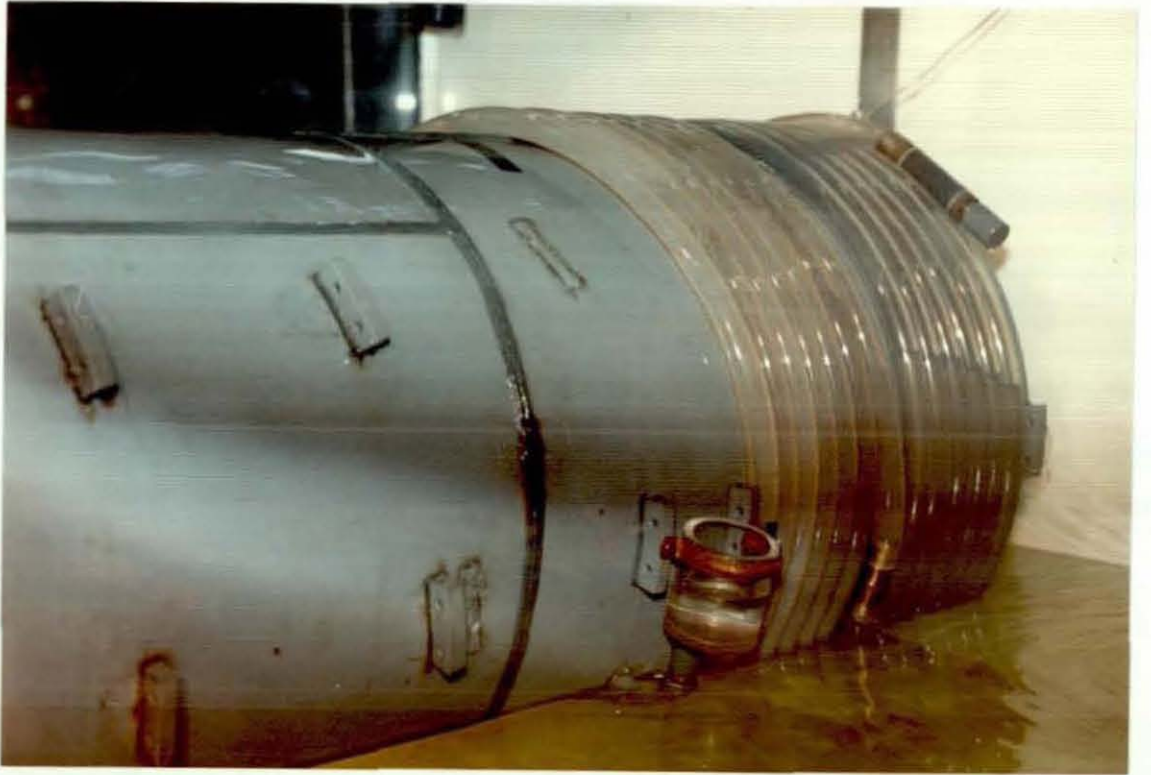


FIGURE 3.3, Coil Pump Bucket and Helix Photograph

3.1.2 The Drum

The diameter of the hollow drum, (figure 3.2) is 0.5 metres and the length is 0.8 metres. Liquid is free to enter or leave the interior of the drum through both ends. This prevents air from being trapped inside, so altering the stresses on the bearings and the forces on the electric motor, thereby effecting the pump efficiency. On the drum's surface are welded blocks of plastic in which holes have been drilled. These are used together with lengths of cord to secure the coils.

3.1.3 The Bucket and the Helix

The helix (figure 3.3) is constructed of transparent flexible piping. The mean internal and external diameters are 13.7 and 20.3 millimetres respectively. 14 Revolutions of the pipe are wound around the drum.

Attached to the inlet of the helix is a plastic scoop in the shape of a bucket. It had internal and external diameters of 38 and 50 millimetres respectively and an inside length of 50 millimetres. Three quarters of a revolution away from the inlet is a hole of 1 millimetre radius in the pipe wall (described in section 5.7.2.)

3.2 PROCEDURE

This procedure *was* formally regimented for consistent results and is laid out here:

1. The 'Bucket' device *was* secured to the entrance of the pump ready for the pumping to begin.
2. The Tank *was* filled to the required level.
3. The electricity supply *was* connected via a 'Variac', which *was* adjusted to control the speed of the motor.
4. The water plug levels inside the helix *was* allowed to reach equilibrium by rotating the drum at least twenty revolutions.
5. The values of drum r.p.m., external depth of immersion and the pump discharge *were* recorded over a set time.
6. The parameters *were* changed and the procedure repeated until all the data had been collected.

The experiment *was* finally shut down by emptying the tank and helix of liquid by rotating the pump backwards. This *prevented* the build-up of organic growths on the inside of the pipe wall. The power supply *was* then disconnected.

3.3 RESULTS

Appendix C contains four tables of results taken from this experiment, together with derived parameters used in later regressions and descriptions of the tables. From chapter 5, we have the following equations:

$$V_h = C_d \sqrt{2 * g * H_h} \quad (5.35)$$

and:

$$Vol_h = A_h * V_h * T_h \quad (5.32)$$

combining these, we get:

$$\frac{Vol_h}{T_h * A_h} = C_d \sqrt{2 * g * H_h} \quad (3.1)$$

where Vol_h = Volume of liquid passing out of the hole during each revolution,
 V_h = Velocity of liquid through the hole,
 T_h = Time for liquid to pass through the hole,
 A_h = Cross-sectional area of the hole,
 C_d = Coefficient of discharge of the hole,

g = Gravimetric constant, 9.81 m/s/s,
 Hh = Head difference across the hole.

This equation has been used together with the theory in Appendix B to regress the results in Appendix C, to find the constant 'Cd'. By calculating the result to the left hand side of the equation and comparing it with the right hand side, we obtain:

$$\frac{\text{Volh}}{\text{Th} * \text{Ah}} = 0.6291 - 0.3027 * \sqrt{2 * g * \text{Hh}}$$

With a Correlation Coefficient, cc = -0.5718

i.e. Cd = 0.3027

This result is not encouraging, as the negative correlation coefficient implies that the left hand side of the relationship is inversely proportional to the right. This is incompatible with the theory and the analysis will therefore have to be discounted. The absolute value of this Correlation Coefficient is also very low, which infers that this relationship is only marginally valid.

By entering values into equation (3.1) for each individual experiment, we can determine the coefficient of discharge for each experiment. The mean value of the coefficients is:

$$C_d = 0.0784$$

3.4 CONCLUSION

The value of the coefficient of discharge obtained from the linear regression described in Appendix B cannot be used because of the poor value of the correlation coefficient calculated. This is unfortunate as it does not confirm the associated theory in Section 5.7.

The coefficient of discharge obtained by taking the mean of the values calculated from individual experiments is low compared to values quoted from various text books (Ref.15) which vary from 0.97 to 0.99.

The experiment can still be considered successful even though quantitatively, answers cannot be produced. This is because it has been proved that by enlarging the inlet and introducing a small hole in the helix, the pump can sustain a higher discharge than in its normal arrangement. This advancement of the theory could prove decisive in improving the pump's efficiency.

3.5 DISCUSSION

The value of the coefficient of discharge from the regression might have to be discounted. This decision has been made on the basis of the poor value of the correlation coefficient. The limited success of the analysis is explained by examining the data taken. Only 9 experiments were completed; which, with hindsight, *was* too few. The spread of the parameters could also have been larger as it would have led to the regression having a more representative population.

By taking the mean value of the Coefficient of Discharge, an indication of its accuracy cannot be commented upon in a mathematical sense. However, it would seem that the value of 0.0784 is low compared with values quoted in various text books and so this value is also suspect.

The low value can be explained by the admission that the hole was not very accurately drilled to a radius of 1 millimetre. As the material is soft and pliable, it could have taken any cross-sectional area. Also, the roughness of the hole on the inside of the pipe, could have led to restrictions in the flow. The above value is therefore accepted with reservations.

A concept not investigated here, *was* the hypothesis that the enlarged inlet will impose a pressure on the first water plug. The effect that this might have is to elongate the first water plug. It has not been addressed here due to the problems of quantifying the pressure and translating this into its associated water plug elongation.

As described in Section 3.1.3, the hole in the pipe wall is situated three quarters of a revolution away from the bucket. The position of this hole has been decided upon by 'trial-and-error'. The positioning optimum could be investigated to minimise the liquid escaping from the hole whilst still allowing air to escape.

It is realised that more research should be done on this subject, especially as the experiment was successful in terms of confirming that enlargement of the inlet causes the discharge to increase.

CHAPTER 4

COIL PUMP POWER EXPERIMENT

This experiment has been performed to investigate the predictability and therefore the relationship between the power absorbed by the pump, and the parameters able to be varied on the apparatus. 168 individual experiments *were* performed on the apparatus, (displayed in Appendix D).

The rationale and justifications of the methods used to derive the relationships are discussed in this chapter. The validity of the relationships is discussed, within the boundaries of results taken, and conclusions are drawn.

4.1 EQUIPMENT

Figure 4.1 shows the layout of the Coil Pump Power Experiment. It is essentially a similar design to the coil pump in the previous chapter, and therefore the apparatus has been modified for this experiment.

The apparatus consists of the Tank, the Coil Pump, the Head Generator, and the Electronics. To avoid repetition, only a short description is given.

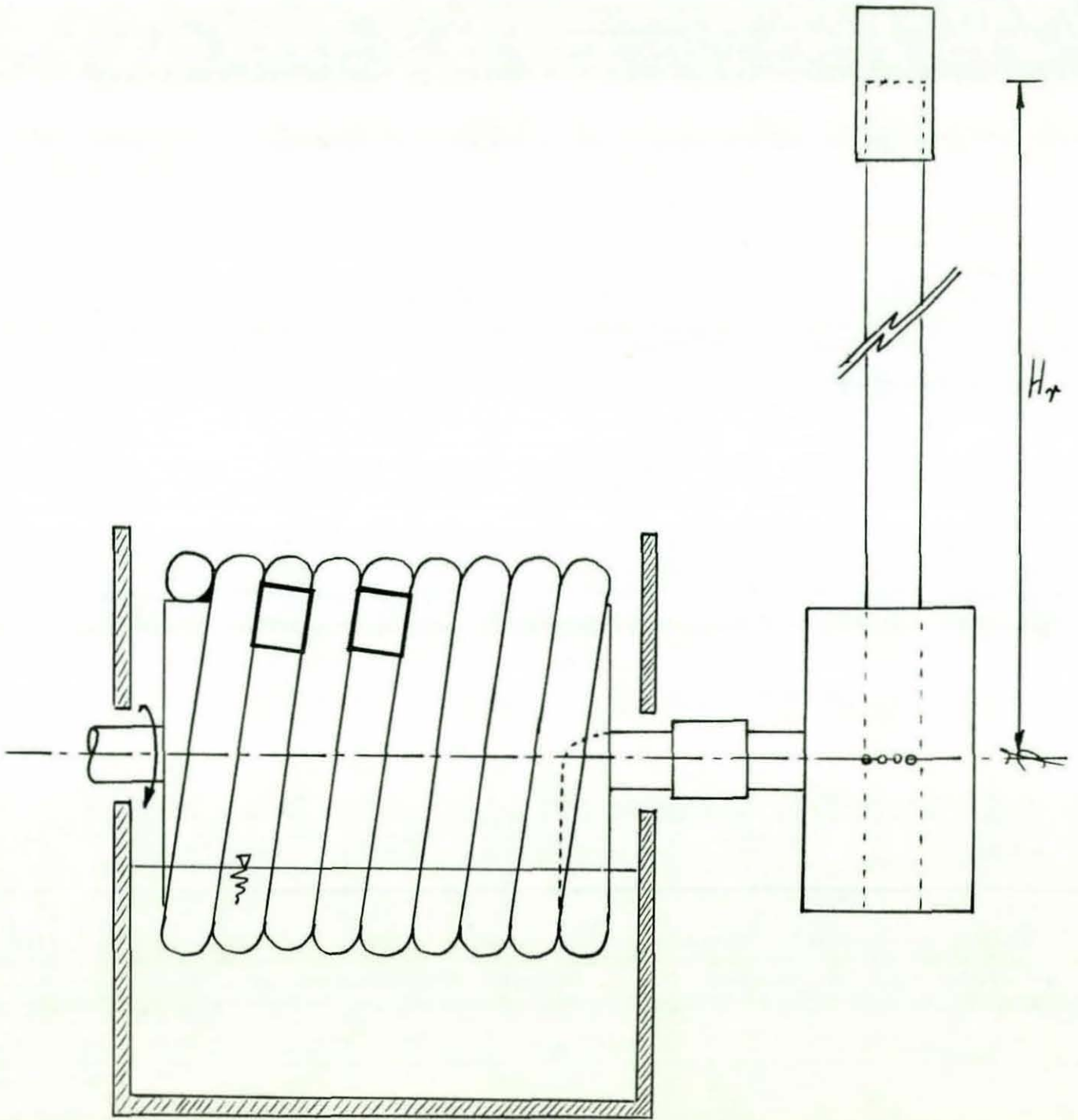


FIGURE 4.1, The Coil Pump Power Experiment Diagram

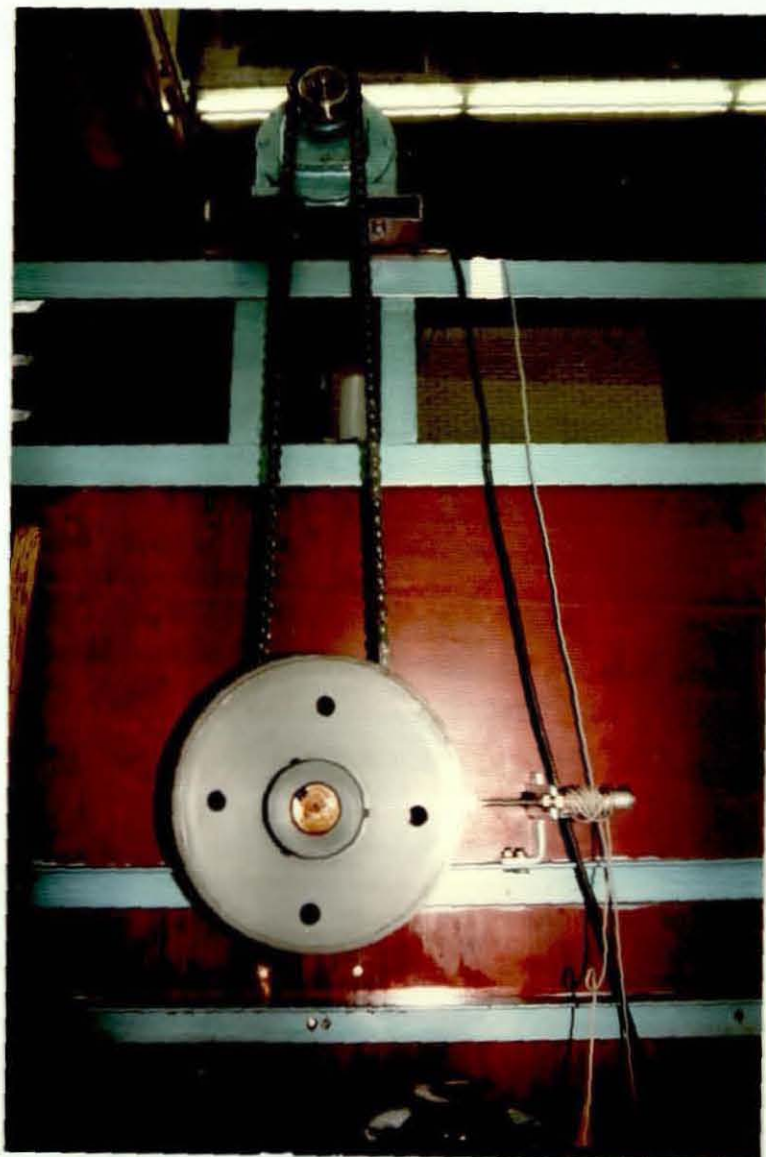


FIGURE 4.2, Drive Chain, Cam and Ether Photograph

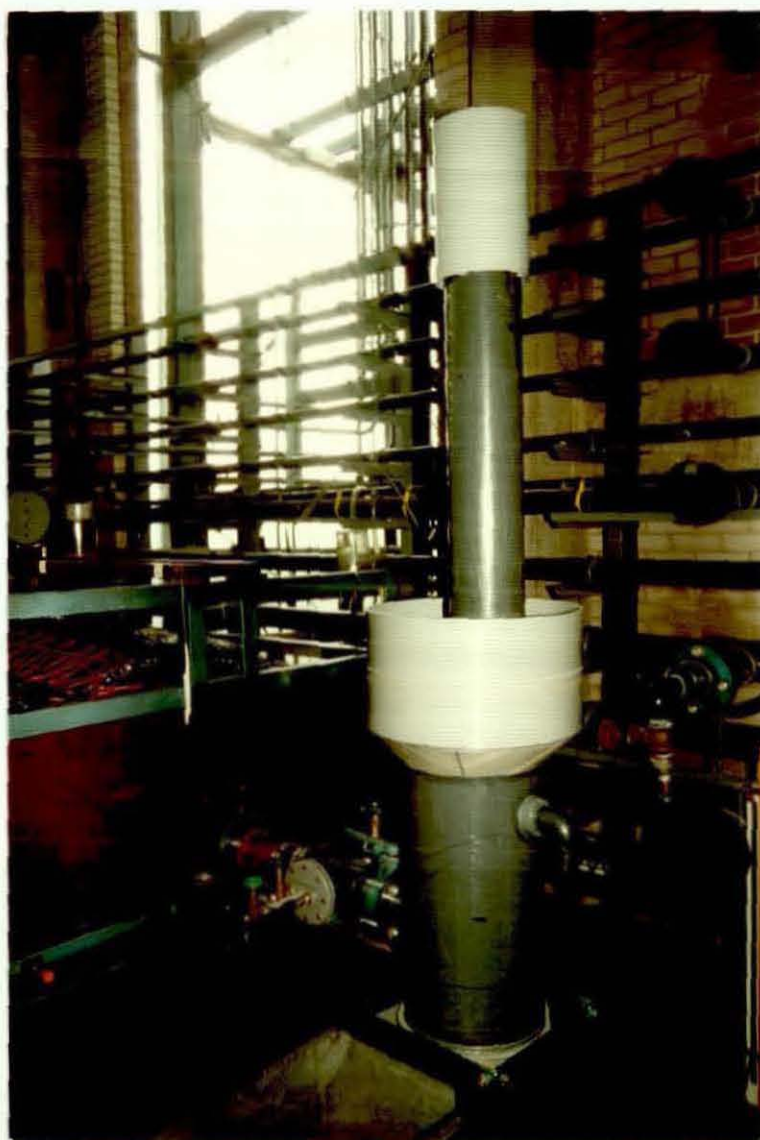


FIGURE 4.3, Head Generator and Shaft Bearing Photograph

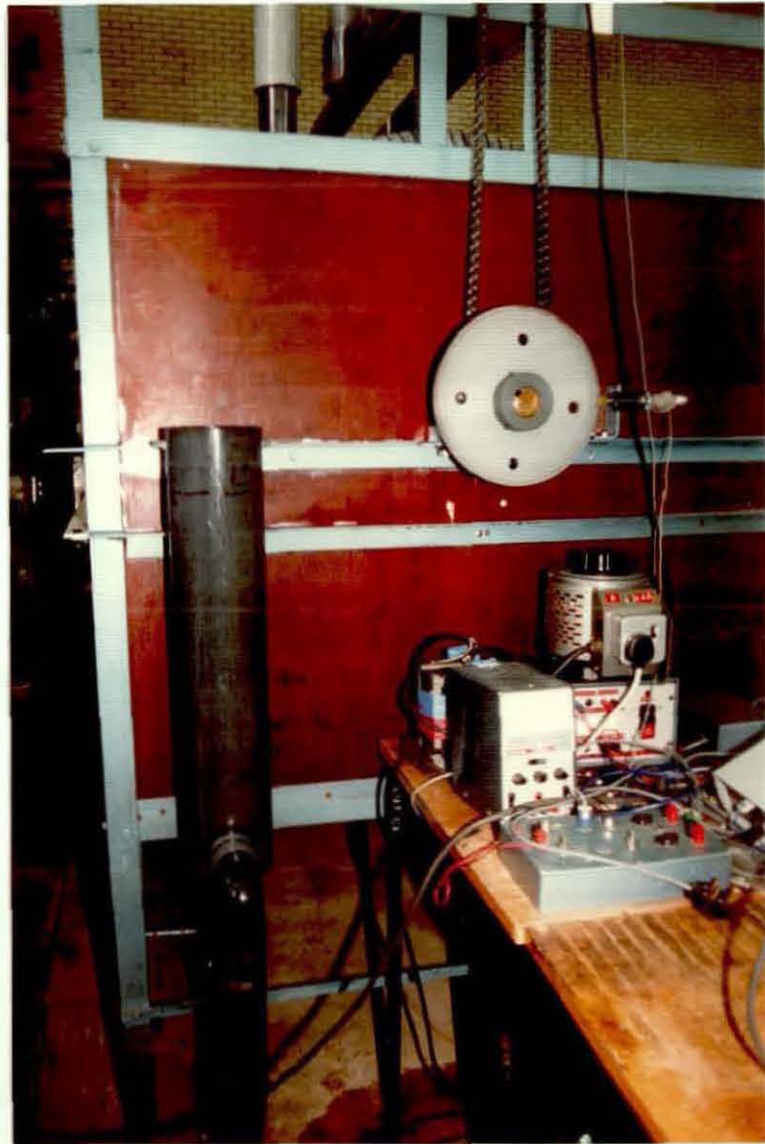


FIGURE 4.4, Variable Height Overflow Device and Variac

Photograph

4.1.1 The Tank

Due to the increased size of the coil pump used in this experiment the tank (figure 3.2) used in the previous experiment had to be altered. The electric motor (figure 4.2) that drives the coil pump, (situated on rails suspended over the top of the tank) has been raised from its original position to allow the larger helix to be fitted underneath. New larger bearings (figure 4.3) have been installed to take the weight of the heavier helix. A wider shaft has been installed to take the discharge from the helix, but the original reduction gear box remains. However, a larger, more powerful electric motor replaces the old one. A drive chain (figure 4.2) with sprockets also replaces a rubber and canvas drive belt.

A variable height overflow device (figure 4.4) has been fitted externally to the tank which enables a steady depth of immersion to be achieved. Due to the changing discharge demand (from the helix inlet) throughout a revolution, an excess of liquid has to be continually introduced into the tank. The overflow device stabilises the depth of immersion by letting the excess flow drain away. It has been made, so that the depth of immersion can be manually altered by sliding a section of vertical pipe up or down. Water escapes by flowing up and over the exposed end of the pipe.

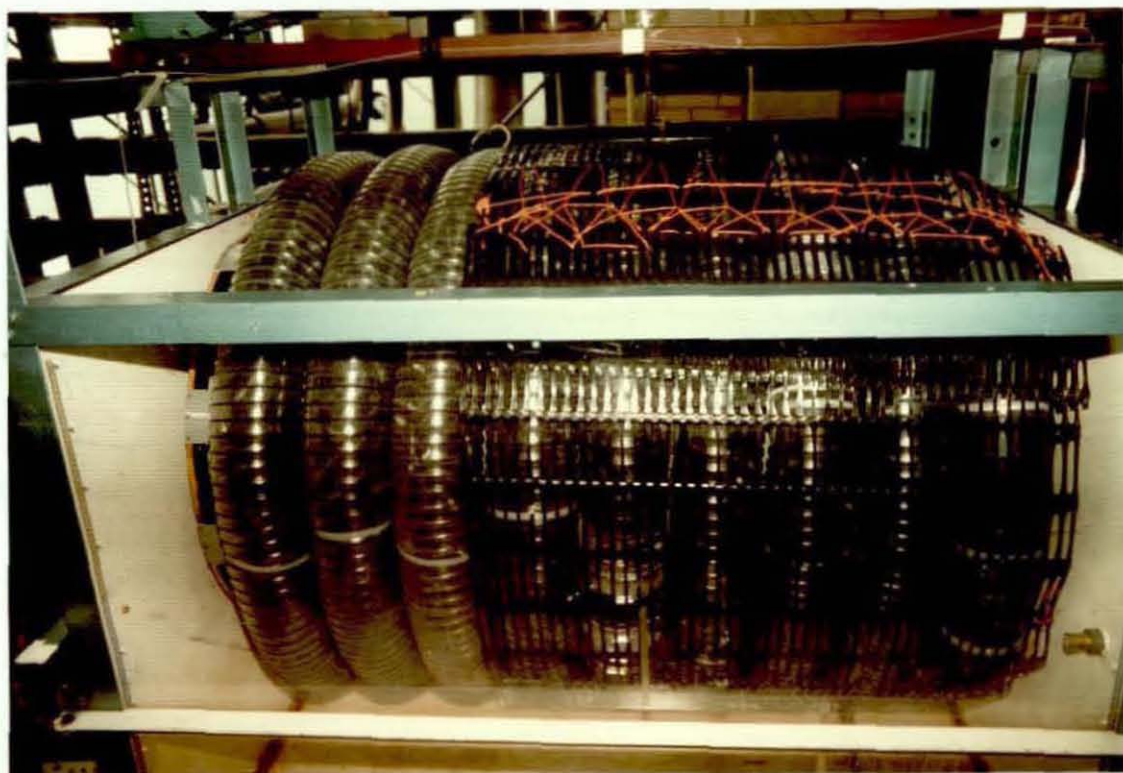


FIGURE 4.5, Helix Photograph



FIGURE 4.6, Helix Connector Photograph

4.1.2 The Coil Pump

The diameter of the drum (Figure 4.5) *was* 0.87 metres, and the length 1.2 metres. It *was* a larger drum compared to the one described in chapter 3, to maximise the tank volume; i.e. to allow more, larger coils.

Slotted plastic blocks have been welded to the surface of the drum in a spiral-like fashion to follow the path of the helix. These are used in conjunction with flexible plastic strips to secure the helix to the drum. Netting *was* wrapped around the helix to prevent the coils from moving while they are under pressure and the drum is in motion.

The helix *was* made of commercial flexible ducting. It consists of a skin of flexible translucent plastic, stiffened with a spiral of wire, enabling it to retain its circular cross-sectional shape whilst being wrapped around the drum.

The helix *was* split into three sections, two groups of two coils and a group of four coils. It enabled any combination of 2, 4, 6 and 8 coils to be attached to the drum. The placing of the flow media inside the coils is made convenient by the introduction of connectors (figure 4.6) which join the different sections of the helix together. The connectors contain netting inside to restrict the movement of the flow media to the sections where it has been placed.

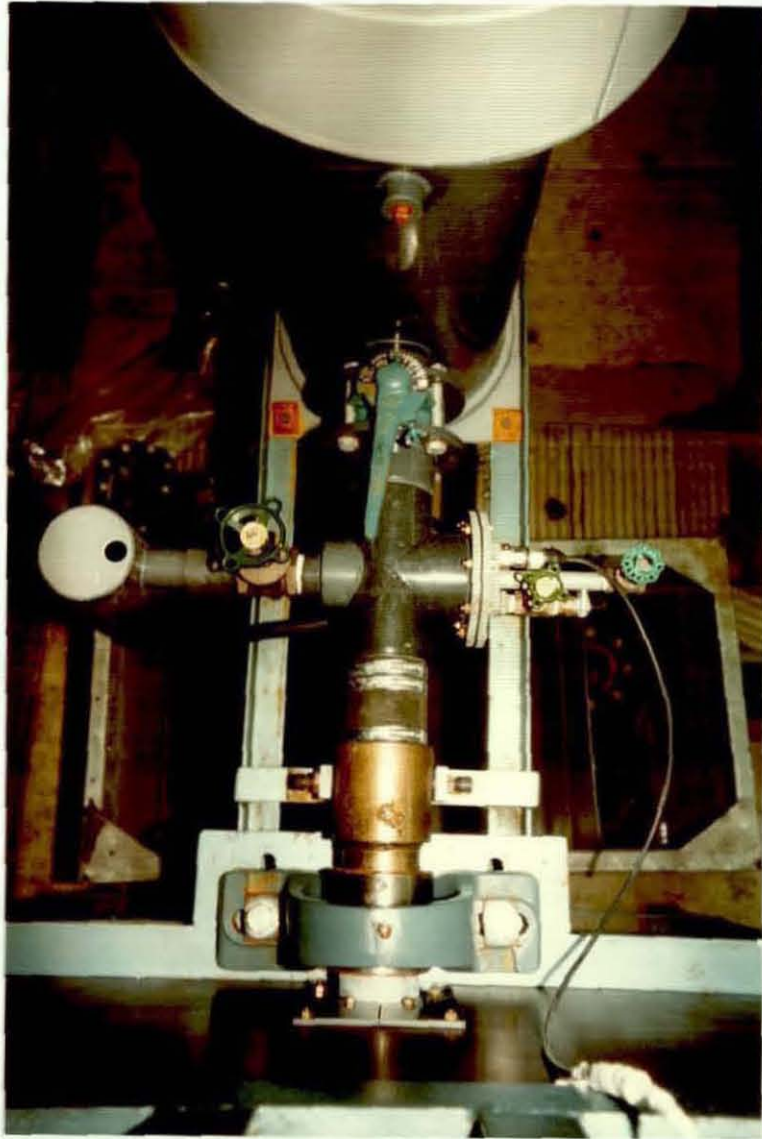


FIGURE 4.7, Rotary Valve and Pressure Transducer

Photograph

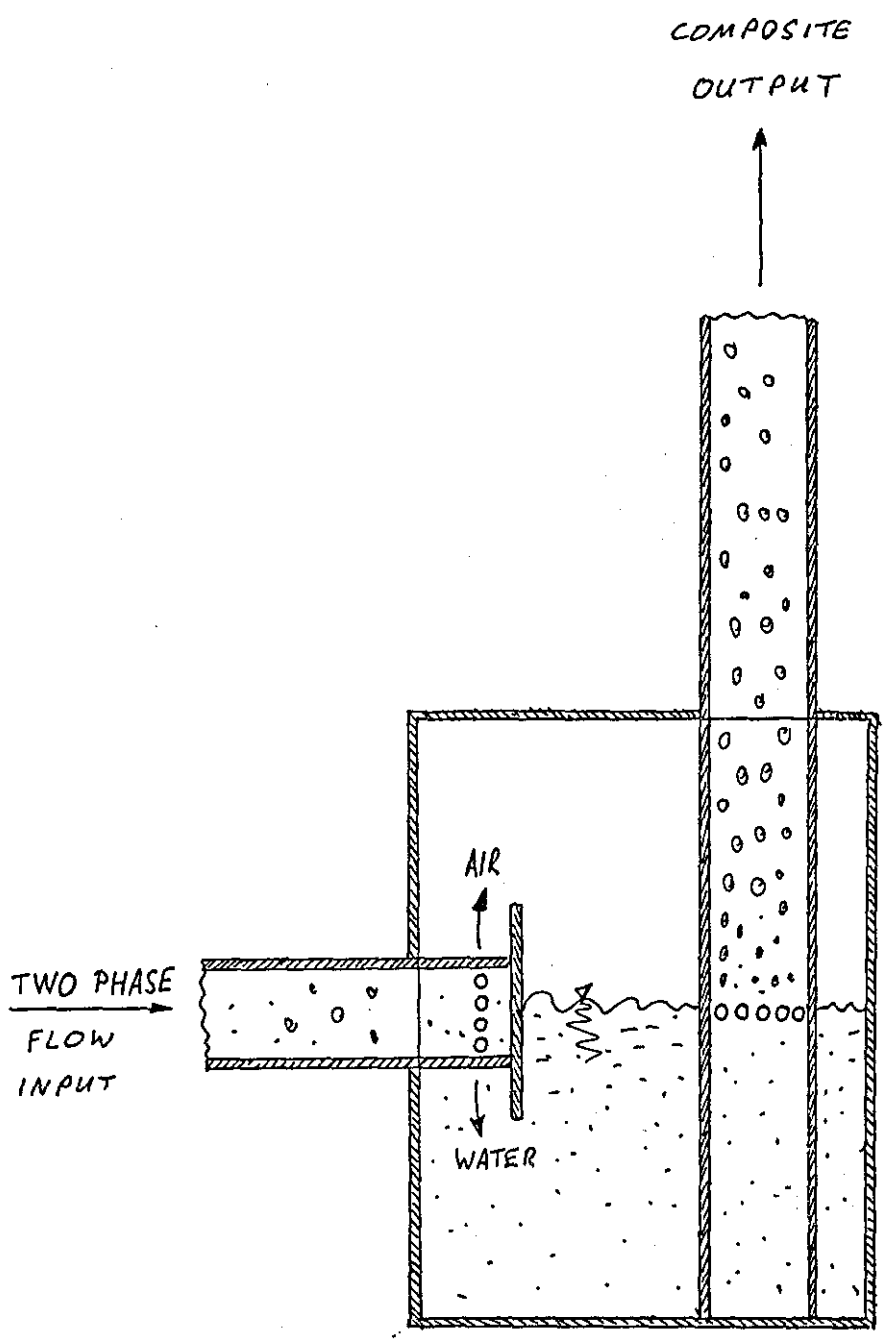


FIGURE 4.8, Head Generator Diagram

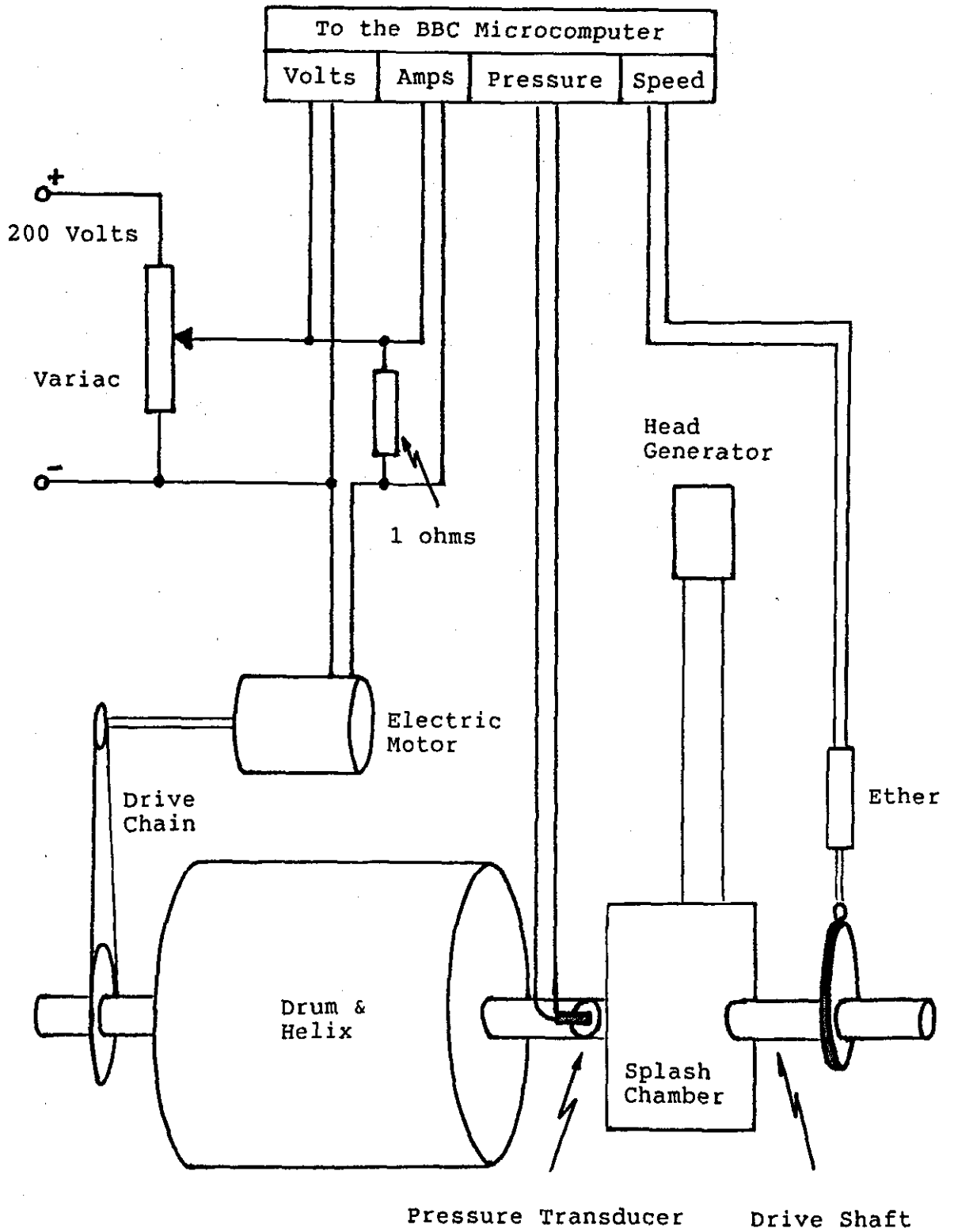


Figure 4.9, Data Logging Equipment

After the two phase flow passes through the helix, it is directed onto the central shaft of the pump. The flow leaves the shaft through a rotary valve (figure 4.7). The rotary valve maintains a water-tight seal between the shaft and the adjoining pipe, while allowing the shaft to rotate while the pipe is stationary. The discharge then travels along a horizontal pipe to be led off to the 'Head Generator' described in section 4.1.3.

4.1.3 The Head Generator

The head generator (Figure 4.3) consists of a chamber with an inlet from the coil pump shaft and an outlet vertically upwards. The chamber is designed to reduce the turbulence from the the two phase flow before directing it upward through the outlet. It is designed in such a way as to allow the maximum back pressure from the vertical pipe above the outlet to be sustained for as long as possible, throughout a pump revolution. The apparatus reduces the varying delivery head back pressure to a minimum, which would be present without this apparatus due to the air-plugs through the system.

A plate (figure 4.8) across the inlet prevents the water plugs from being immediately directed towards the outlet. The chamber calms the turbulence to let the discharge flow through the holes in the vertical pipe inside the chamber, to the outlet.

The holes in the vertical outlet pipe have been

introduced to reduce the size of the air bubbles in the vertical pipe. This prevents large air plugs forming in the pipe resulting in the loss of back pressure into the coil pump. To facilitate the measurement of the pressure, a transducer has been included near the inlet to the chamber.

Above the outlet of the chamber is a connected vertical pipe which maintains a column of water. This generates the back pressure on the chamber and the pump. The pipe can be changed between experiments to generate different heads. A chimneypot-like device (figure 4.3) has been installed at the top of the pipe and attached to this is a plastic sleeve. It directs the discharge towards a large graduated tank by the side of the experiment, where it is measured. Individual discharges and headlifts obtained can be seen in columns 5 and 7 respectively of figure D.2.

4.1.4 The Data Logging Equipment

Figure 4.9 Shows the overall set-up of the data logging equipment and where it interfaces to the rest of the apparatus. The following sections describe the data collection facility.

PRESSURE

4-15

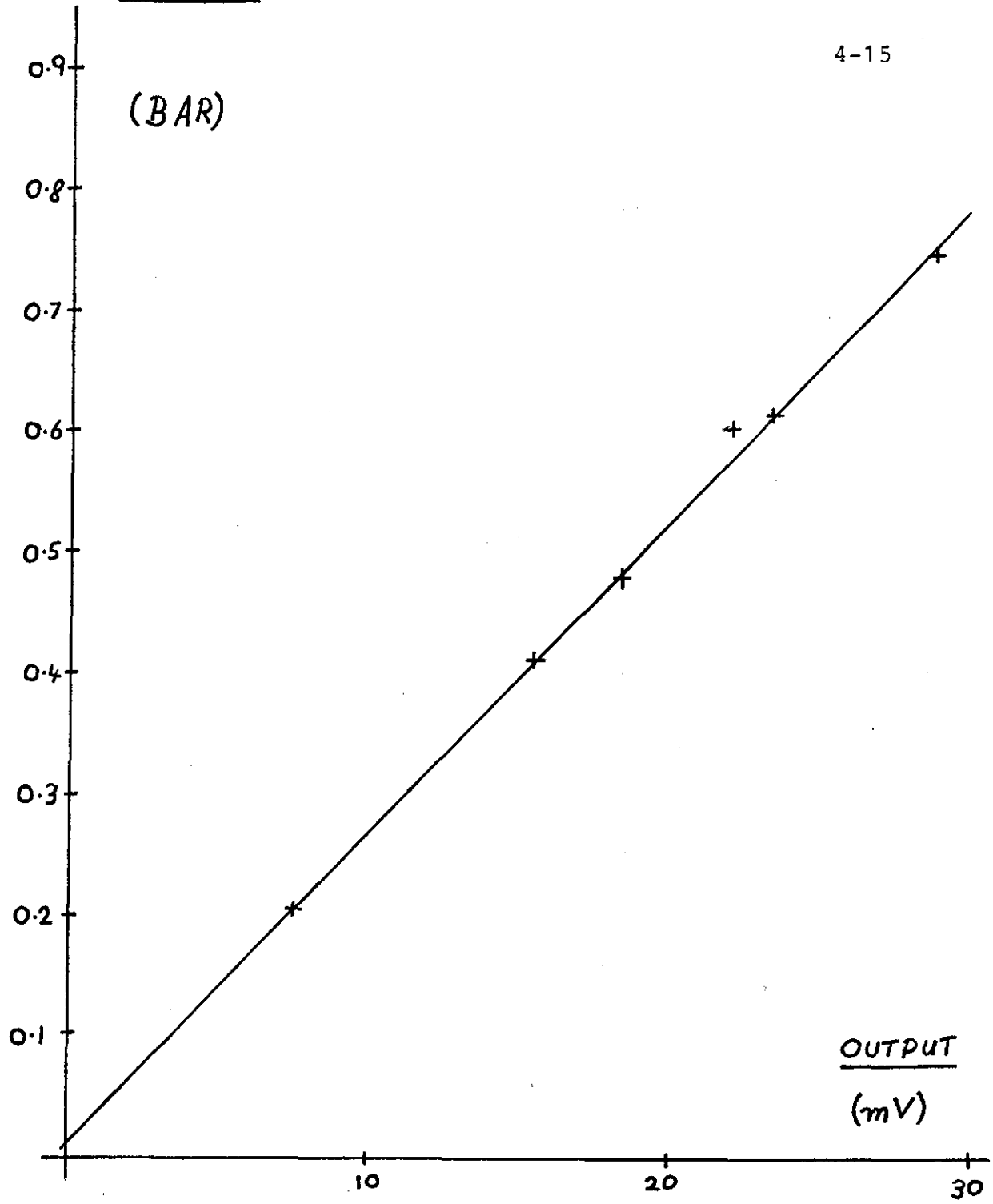


FIGURE 4.10, Graph of Pressure Against Voltage for the Pressure Transducer

4.1.4.1 Power Input

The Drum was driven by an electric motor through a set of reduction gears and a drive chain. The power supply was controlled by a large variable transformer called a Variac (figure 4.4). It controlled the voltage across the motor and therefore the speed at which it will turn. The power was recorded by measuring the voltage across the motor and the current through it.

The voltages across the motor can reach 200 Volts. Therefore this has to be stepped down by a factor of 2 for compatibility with the Analogue to Digital port of the BBC Microcomputer, which was used for data logging in this experiment.

The BBC cannot directly read current and so a 1 Ohm resistor has been introduced in series with the motor to record the voltage across it. A direct comparison of current against voltage can then be obtained. This was fed into the second Analogue to Digital port. The mean power input for each experiment can be seen in column 2 of figure D.1.

4.1.4.2 Pressure Output

The voltages gained from the pressure sensor, to measure the pressure of the discharge from the pump, are amplified to provide signals for the BBC to record. This sensor has been previously calibrated to provide a relationship of the pressures imposed on the sensor,

against the amplified voltages gained. Figure 4.10 shows the relationship obtained and the resulting equation is:

$$\text{Hr} = 0.33 + (0.77 * \text{VOLTS})$$

(Pressure Head, (from the operational amplifier)
metres of water)

The voltage is fed into a third channel of the Analogue to Digital ports of the BBC. This equation translate the volts to pressures. The mean pressure for each experiment can be seen in column 3 of figure D.3.

4.1.4.3 Angular Velocity Of The Pump

An electrical device called an Ether (figure 4.2), in conjunction with a cam attached to the pump shaft, is used to record the angular velocity of the pump.

An Ether is a variable resistor, with a rod passing inside a spiral of resistance wire. As the rod passes in or out of the ether tube, so the resistance across the device either rises or falls. A steady voltage is applied across the input side of the Ether and, when the pump is in motion, a varying voltage can be read from the output side. The voltage input is set so that the output remains within the bounds of 2.5 and zero volts for compatibilty with the computer port.

The cam that the Ether follows has been machined so that if the pump maintains a constant angular velocity through its cycles, the motion of a cam follower will describe a simple harmonic function (i.e. a sine wave).

This varying voltage is fed into the fourth channel of the Analogue to Digital Ports of the BBC. It used (when combined with the time variable described later) to accurately determine the angular velocity of the pump. The mean value for each experiment can be seen in column 1 of figure D.1.

4.1.4.4 The BBC Microcomputer

Initially there were problems with the accuracy of the data collected. The Analogue to Digital ports for this computer are designed to cope with joy-sticks and paddles and are therefore of a low accuracy. This was remedied by replacing the components with ones of superior quality. A side effect of the upgrade allows the range of voltages to be expanded from 1.8 volts to 2.5. This allows higher voltages from the sensors to be entered so increasing their accuracy.

A fifth source of data in the form of Time (in milli-seconds) is received from the computer's internal clock. It references all the other sources of data.

To summarise, the five types of data item stored onto disk are:

1. Volts from the Pump Motor (divided by 100),
2. Amps from the Pump Motor,
3. Pressure Output (volts - amplified but not corrected from its calibration),
4. Orientation of the drum (in the form of volts to be processed later),
5. Time (milli-seconds).

The rate at which readings are taken is calculated to give the computer adequate time to record results over ten revolutions of the experiment. As 800 sets of readings are the maximum able to be taken over this time, then a set of readings have to be taken approximately every 4.5 degrees of revolution of the pump. The decision to take this many readings has been taken on the basis of the memory restrictions of the computer.

Once the readings had been taken, the data was transferred from memory onto a file on a floppy disk. It was subsequently transferred on to the University Mainframe Computer for analysis.

4.2 PROCEDURE

Below is a description of the parameters which can be varied on the apparatus:

1. The height to which the pump lifts the discharge. This was found by measuring the height from the centre-line of the pump shaft, to the top of the vertical pipe installed over the outlet of the splash chamber (figure 4.3). This was varied from zero to 3 metres in increments of half metre intervals. Individual values are displayed in column 7 of figure D.2.
2. The rotational speed of the pump. This was varied by adjusting a 'Variac' (figure 4.4). It was envisaged that the maximum speed for production models will be 3 r.p.m. These can be varied in an analogue manner but are kept to values of approximately 1, 2 and 3 r.p.m. Individual values are displayed in column 1 of figure D.1.
3. The number of coils wrapped around the drum. A maximum of 8 coils were fitted around the drum. The helix was split into 3 sections of 4, 2 and 2 revolutions (figure 4.5). It enabled any combination of 4, 6 or 8 coils to be fitted to the drum. Individual values are displayed in column 6 of figure D.2.

4. The depth of immersion of the pump, adjusted by altering the variable height drain situated externally to the tank (shown in figure 4.4). Immersions are restricted to below the underside of the shaft. This prevents water from leaking out of the tank through the holes in the walls through which the shaft passes. Although the adjustment is analogue in nature, depths of approximately 100, 200, 300 and 400 millimetres below the centreline of the shaft are adhered to. Individual values are displayed in column 4 of figure D.1.
5. The flow media inclusion option. The helix connectors (figure 4.6) easily facilitate the inclusion of the flow media. This option is displayed in column 11 of figure D.3. If the individual values are equal to zero, then flow media has not been included in the coils, otherwise the values refer to the theoretical head calculated by equation (2.6).

The experiment has been devised to inter-relate the factors influencing the power consumption of the pump.

4.2.1 Procedure for Each Experiment

The procedure is structured for consistent results and is laid out here in chronological order:

1. The required number of coils are wrapped around the drum together with the flow media installed inside, if desired. Netting is then wrapped around the coils to prevent them moving while the drum is in motion and under pressure.
2. The tank is filled up to the required level.
3. The variable height drain is adjusted to the required depth of immersion.
4. A computer program written to capture the data is loaded from disc, and the pump is set in motion to the required speed.
5. Once the water levels internal to the helix have reached equilibrium, the program is executed to collect the data.
6. After ten revolutions, the collected data is loaded onto floppy disc for later transfer to the University Mainframe Computer. While this is in progress, the experimental parameters can be altered ready for the next experiment.

Non-Flow Media Experiments

Number of Coils, n	Headlift (Metres) Hr
8	3.0
	2.0
	1.0
	0.0
6	2.0
	1.5
	1.0
	0.0
4	1.5
	1.0
	0.5
	0.0

Recurring Sub-Group	
Rotational Speed Ns, (rpm)	Depth of Immersion DOI (mm)
1	100, 200 300, 400
2	100, 200 300, 400
3	100, 200 300, 400

Flow Media Experiments

8	0.0
	0.5

FIGURE 4.11, Experiment Organisation Table

4.2.2 Parameter Organisation in the Experiments.

These have been split into two main groups, depending upon whether flow media is present. The organisation of these is displayed in figure 4.11 and elaborated on below:

1. Non-Flow Media Experiments. These are split into 3 sections dependant on how many coils are wrapped around the drum. These sections are split into 4 groups representing each of the heights to which liquid is lifted. To each group of experiments is applied a sub-group. The sub-groups consist of 12 experiments made up of a combination of 3 rotational speeds and 4 depths of immersion, making in total 144 non-flow media experiments.
2. Flow Media Experiments. These were limited by the time available for research. Only 24 experiments were completed out of a planned series of 48, on a helix of 8 coils filled with flow media. Two different pumping heights were applied, with combinations of 4 depths of immersion and 3 rotational speeds.

Figure 4.11 portrays the organisation of the parameters for both groups of experiments. The core of 12 experiments on the right hand side is the recurring sub-group and is therefore only displayed once. The decisions made on the values used in the structure of the organisation of the headlifts in the experiments were made on the basis of 2 restrictions. The first is the maximum head to which the pump can lift with the number of coils wrapped around it. The second restriction is due to the limited strength of the fabric of the coils. This restricts the pressure to which the helix can pump to 3 metres.

4.3 RESULTS

The object of this experiment is to prove that relationships can be found to predict the power absorbed by the pump. To this end, over two thirds of a million items of data were recorded throughout the whole of this experiment. It is possible that rigorous analysis could enable precise relationships to be developed. Unfortunately time, Computer power and storage constraints has forced the compression of the data into a subset for processing on an Apple IIe Microcomputer. This data consists of a sequential file containing the mean power, outlet pressure and time of each revolution, for each experiment completed.

For convenience and optimisation of access time, the sequential file has been converted to a random access file. During this process it has been found that there is still too much data to be held on a single disc. This problem has been solved by taking the mean value for each of the parameters over all the revolutions for each experiment and storing these values in the disc file. At this point it reduces the disc access time to an acceptable level for regressing results to form relationships; i.e. 4 minute to load the results for approximately 150 experiments. It is these values which form the basis for the regression described later, and are displayed in Appendix D.

An environment has been developed on the computer consisting of software tools and utilities to process the data so that relationships can be formed. The data and the relationships derived can be displayed in two ways; i.e. either in graphical or mathematical form.

4.3.1 Processing The Results

The process by which a series of parameters are combined to form relationships is called multiple regression. Various combinations and permutations of experimental parameters have been combined using this process to relate to the power absorbed by the coil pump. This power (equal to the applied power minus the obtained power) is an important feature and is easily derived. It has therefore been used to process the results.

It has been found that there are two partial equations, which when combined describes the power absorbed by the pump for experiments 145 to 168. These two partial equations represent the two most distinctive power loss values envisaged to be present in the apparatus and can be represented thus:

$$\begin{array}{l} \text{Power} \\ \text{Absorbed} \\ \text{Expt. 145-168} \\ \text{(Theoretical)} \end{array} = \text{Power1} + \text{Power2} \quad (4.1)$$

Where Power1 = Theoretical Power absorbed by the first partial equation,

Power2 = Theoretical Power absorbed by the second partial equation.

The first partial equation represents the power losses due to the hydraulic resistances to flow of the discharge through the coil pump, and due to the immersed pump rotating in its vat. This powerloss is proportional to the speed of rotation of the coil pump and to the height to which the pump is lifting its discharge. With the constant of proportionality present the following equation describes the power absorbed due to the non-flow media hydraulic resistances to flow:

$$\text{Power1} = K1 * Ns * Hr \quad (4.2)$$

Where K1 = Constant of Proportionality for Non-flow Media Hydraulic Resistances,

Ns = Speed of Rotation of the coil pump,

Hr = Height to which the discharge is lifted.

The second partial equation represents the powerloss absorbed due to the hydraulic resistance of the discharge due to the inclusion of the flow media inside the coils. The powerloss is proportional to the speed of rotation of

the coil pump raised to the power of 1.860. With the constants discussed below present, the following equation describes the power losses due to the presence of the flow media in the coil pump:

$$\text{Power}_2 = K_2 + K_3 * N_s^{1.860} \quad (4.3)$$

Where K_2 = Equation Flow Media Constant
 K_3 = Constant of Proportionality of the Flow Media Resistances.

Equations (4.2) and (4.3) can now be combined with (4.1) to form the following equation:

$$\begin{array}{l} \text{Power} \\ \text{Absorbed} \\ \text{Expt. 145-168} \\ \text{(Theoretical)} \end{array} = K_1 * N_s * Hr + K_2 + K_3 * N_s^{1.860} \quad (4.4)$$

Equation (4.4), which fully describes the powerloss due to the coil pump containing flow media, can now be used in the process of Multiple Regression to derive its constants. Associated with the partial equations will be their individual correlation coefficients, together with

the overall correlation coefficient. The coefficients describe the accuracy, and hence the validity of the whole relationship. The multiple regression produces the following equation for experiments 145 to 168:

$$\begin{array}{l} \text{Power} = 5.916 * N_s * H_r + 3.11 * N_s^{1.860} \\ \text{Absorbed} \\ \text{Expt. 145-168} \quad \quad \quad - 0.485 \\ \text{(Theoretical)} \end{array} \quad (4.5)$$

With 0.979 = Overall Correlation Coefficient,
 0.761 = First Partial Equation Correlation
 Coefficient,
 0.951 = Second Partial Equation Correlation
 Coefficient.

The overall correlation coefficient displays a value close to unity which infers the whole equation accurately predicts the power absorbed by the pump for experiments 145 to 168. Of the two partial equations the second one exhibits a high correlation coefficient and is therefore the dominant partial equation relative to the first in terms of accurately contributing quantitatively to the overall power absorbed by the coil pump. The second partial equation can therefore be said to accurately describe the power absorbed by the flow media. As the correlation coefficient of the first partial equation is relatively low, it would therefore be advantageous to investigate this further so as to be confident of its

accuracy and therefore its inclusion in the overall equation.

The final investigation comprises taking the first partial equation and generating values for the first 144 experiments, representing the power absorbed by the pump not containing any flow media. These values are then linearly regressed against the actual values exhibited by the apparatus to determine the accuracy of the first partial equation. From this investigation the following equation has been formed relating the experimental results to the theoretical values generated:

$$\begin{array}{l} \text{Power} \\ \text{Absorbed} \\ \text{Expt. 1-144} \\ \text{Non-flow Media} \\ \text{(Experimental)} \end{array} = 1.104 * \begin{array}{l} \text{Power} \\ \text{Absorbed} \\ \text{Expt. 1-144} \\ \text{Non-flow Media} \\ \text{(Theoretical)} \end{array} + 3.702 \quad (4.6)$$

With a Correlation Coefficient of 0.967

The high correlation coefficient shows that there is a strong relationship between the the theoretical equation and the experimental data for the first 144 experiments. This therefore ties in the results from the flow media and non-flow media experiments.

4.4 CONCLUSION

The multiple regression performed in the previous section generates equation (4.5). This can be considered to be an accurate and valid relationship due to its associated correlation coefficient having a value close to unity. This equation describes how the various parameters able to be varied on the apparatus predict the power absorbed by the flow media containing pump for experiments 145 to 168. An important feature of the equation is that it can be split into two partial equations which describe the two most dominant powerlosses present in the apparatus. The first partial equation describes the hydraulic powerlosses due to the non-flow media resistance, and the second is flow media related.

The first partial equation has had to be investigated further due to the low correlation coefficient describing its accuracy in equation (4,5), so as to be confident of its accuracy. To this end, the regression described by equation (4.6) has been performed on the first 144 experiments. This proves that by generating theoretical power absorbed values and comparing them against their associated experimental ones, this partial equation is accurate in describing quantitatively the hydraulic powerlosses of the pump without any flow media included. This is demonstrated by the high correlation coefficient associated with the linear regression thereby proving that the first partial equation is accurate and valid.

4.5 DISCUSSION

This experiment has been designed to collect and process results with the use of computers. Over two thirds of a million items of data were collected and due to the reasons given in section 4.3, these could not be processed to full potential. This processing could potentially have resulted in very precise relationships describing the coil pump power absorption throughout a revolution instead of just the mean power absorbed as concentrated upon here. The types of processing which could have been attempted include Numerical Integration and Fast Fourier Transforms (Ref. 18). These are obvious directions which could be profitable to pursue in the future.

4.5.1 The Approach to Regressing the Data

Multiple Regression is a development of the principles of Linear Regression. The main advantage the former has over the latter is that it can relate more than one pair of parameters together. This process has been used in this case to relate the speed of rotation of the pump, linearly and raised to the power of 1.860, and the height to which the pump is lifting its discharge, to the power absorbed by the pump.

An advantage of Multiple Regression is that it gives correlation coefficients for all the partial equations as

well as for the whole equation. This allows an appreciation of the accuracy of the constituent parts of the whole equation, thus enabling further investigation of questionable partial equations.

When examining the correlation coefficient associated with equation (4.5) it is found that the whole equation exhibits the high correlation coefficient of 0.979. This proves that this equation is very accurate in predicting the power absorption of the coil pump containing flow media for experiments 145 to 168.

When investigating the correlation coefficients representing the partial equations, it can be seen that the one representing the flow media hydraulic resistance is dominant in terms of accuracy relative to the other partial equation. This is demonstrated by comparing the correlation coefficient of the flow media resistance partial equation of 0.951 to the correlation coefficient of the non-flow media losses of 0.761. Two conclusions can be drawn from this data, the first is that the partial equation representing the flow media resistance to flow is valid and accurate, and thus does not need to be investigated further to confirm its accuracy. The second conclusion is that the partial equation representing hydraulic resistances present in the coil pump unrelated to the flow media needs to be analysed to further establish its validity.

The first partial equation is further validated by generating theoretical power absorption values to compare

with the values obtained from the first 144 experiments. These are then linearly regressed to derive equation (4.6) and its associated correlation coefficient of 0.967. This coefficient quantitatively describes the accuracy of the first partial equation predicting the non-flow media hydraulic resistances to flow. As the value of this coefficient is very close to unity this support the accuracy of the first partial equation.

The above validation helps to justify the accuracy and validity of equation (4.5) in predicting the total hydraulic power losses of the coil pump, and thus this experiment can be thought to be successful.

4.5.2 Observations Made During Experimentation

During the experiment, it has been found that the coil wall cannot withstand the applied operating pressures and will often spring a leak while the helix is pumping to over 3 metres. This leads to a change of performance and invalidation of the assumptions made to substantiate the basic theories involved. The radial distortion of the assumed circular shape of the helix to an oval is noticeable when it is bent around the drum. Such errors do not help the accuracy of the results but as it is not possible to assess their effect, they can only be noted.

An observation associated with the above, made while experimenting, is that the flexible ducting longitudinally changes shape depending upon the applied pressure.

At atmospheric pressure, the skin has a serrated longitudinal profile, but as the internal pressure increases, the skin becomes increasingly tauter. Consequently, it is envisaged that the resistance to flow will decrease as the pressure increases. It would be advantageous to include the resistive properties of the flexible ducting as a separate variable as this would increase the confidence of the realism of the equation, and the understanding of the concepts involved.

Throughout the whole experiment the phenomenon of "Blowback" (Ref. 7) has not been encountered. This phenomenon can be described as where the majority of the water and air plugs in the helix dramatically leave the helix through the inlet. This has been attributed to the fact that large diameter coils allow bubble-back and therefore acts as an escape valve to prevent blowback.

It has to be mentioned that the efficiency of the electric motor providing the propulsion for the coil pump has not been taken into account in the calculations. Its efficiency is approximately 60 percent, but is dependent upon the applied torque. Due to these unknowns, the efficiency of the motor and the coil pump has to be treated as one unit.

4.5.3 Summary

It has been shown that equation (4.5) successfully describes the power absorption of the helix experimented upon in this chapter. The approaches used to collect and process the results have been formulated so that consistency can be achieved with future experiments. This enables characteristics to be compared so that the performance of a pump can be predicted in any given situation.

CHAPTER 5
-----COIL PUMP THEORIES

The Theories relating to the coil pump have been developed and modified over a long period of time. This chapter combines the theories found by previous research with those developed by this project.

5.1 GENERAL HELIX THEORIES

The following sections describe the general theories that control the actions of the air and water plugs as they pass through the helix.

5.1.1 The Pressure Build-up Inside The Helix

Irrespective of whether the pump is rotating, the pressure head inside the helix is generated by means of a cascading manometer. This can be thought of as a number of manometers in series, of which the water/air plugs in each of the manometer loops may or may not be spilling / bubbling into the previous one.

Figure 5.1 shows a cascading manometer which can be thought of as equivalent to an 'unwound' coil. Assuming there are no internal resistances to flow throughout a revolution the head difference across the helix is balanced by the sum of the head differences

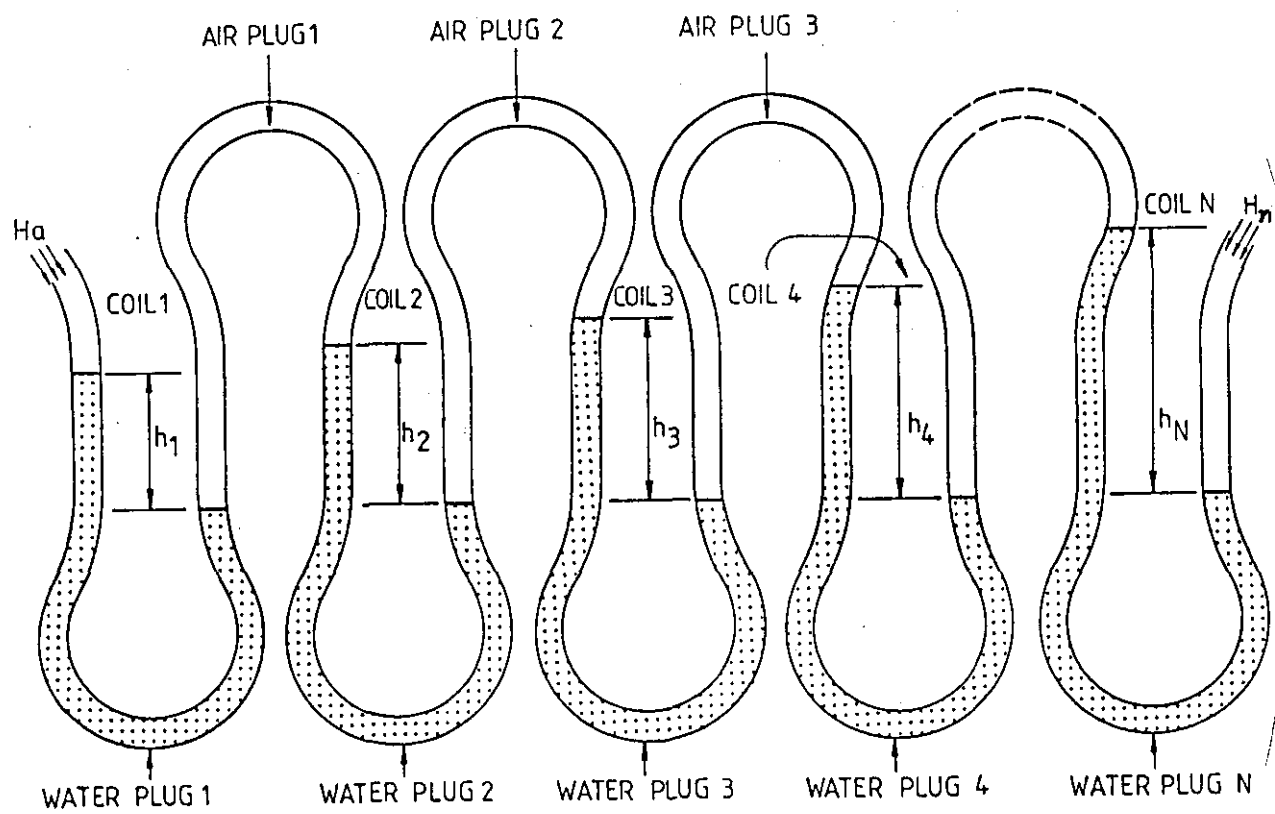


FIGURE 5.1, A Cascading Manometer

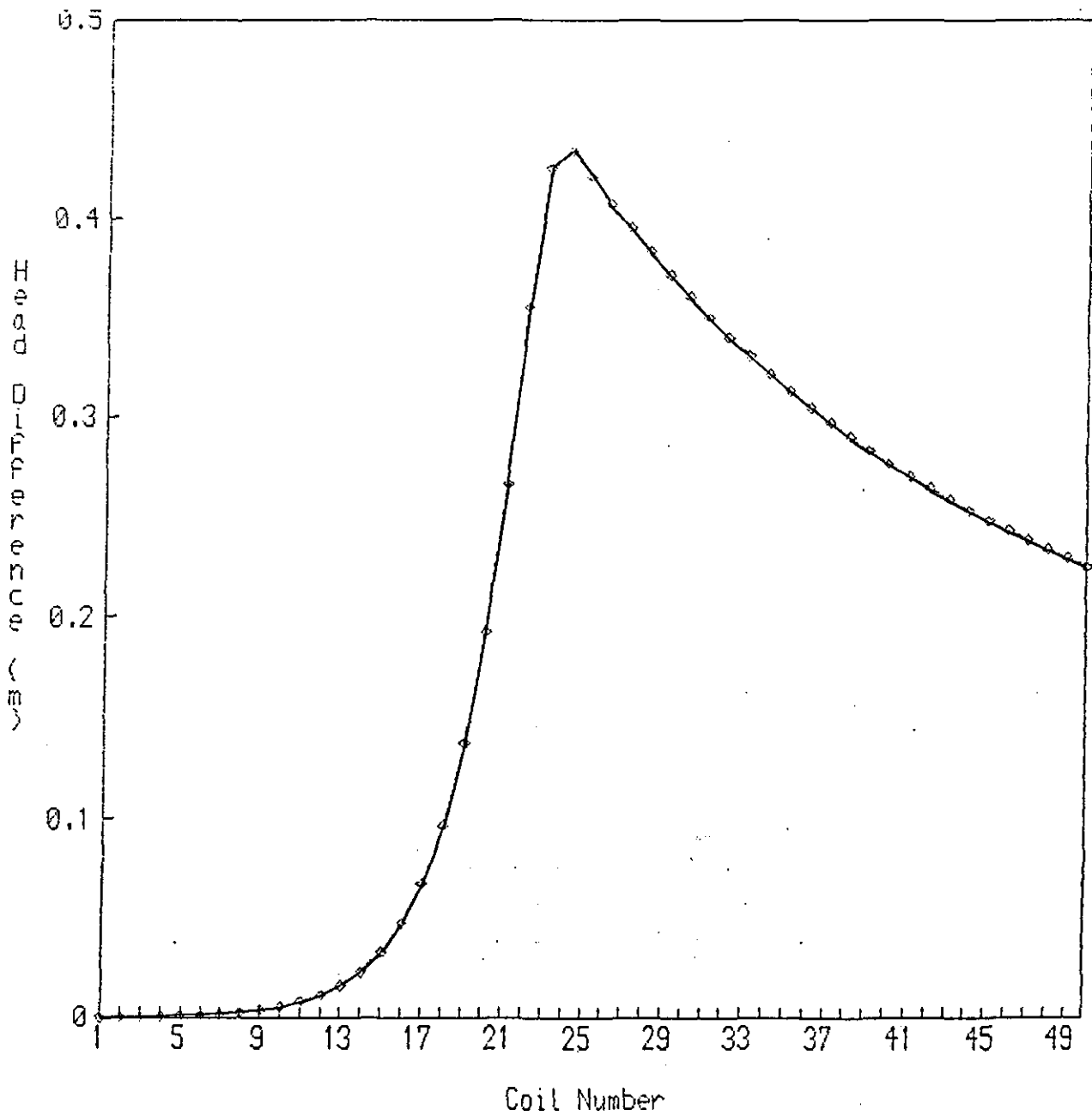


FIGURE 5.2, A Coil Pump Head Difference Profile

across all the water plugs, i.e.:

$$H_n - H_a = h_1 + h_2 + \dots + h_x + \dots + h_n \quad (5.1)$$

where H_n = absolute pressure head at the outlet,

H_a = atmospheric pressure head,

h_x = head difference across the xth water plug,

and n = number of manometer loops or coils.

The head differences of the cascading manometer in figure 5.1 can be shown in a more graphical manner as seen in figure 5.2. This head difference profile and the many others displayed in this chapter describe the actions of the helix and how the water plugs contribute to the headlift pressure. The area under the graph can be thought to be equivalent to the total headlift pressure across the helix.

5.1.2 Air Plug Contraction

The compressibility of air has an important effect on the pump. It is this which allows the air plugs to compress thus allowing the water plugs to rotate away from the outlet.

From previous research (Ref. 16) we can use the standard gas law equation to calculate the air plug lengths inside the helix. If ' H_x ' is the absolute pressure of the air plug in the xth coil, and ' V_{olx} ' is

the volume of that plug at that pressure, then:

$$H_a * Vol_1^{1.15} = H_x * Vol_x^{1.15}$$

or, assuming a constant pipe diameter:

$$H_a * La_1^{1.15} = H_x * Lax^{1.15} \quad (5.2)$$

where Lax = length of the xth air plug under pressure head H_x .

If ' Lrx ' is the reduction in the length of xth air plug as the pressure rises from ' H_a ' to ' H_x ', then:

$$Lrx = La_1 - Lax$$

substituting this into equation (5.2):

$$Lrx = La_1 - \left(\left(H_a * La_1^{1.15} \right) / H_x \right)^{1 / 1.15}$$

$$\text{or } Lrx = La_1 * \left(1 - \left(H_a / H_x \right)^{0.869565} \right) \quad (5.3)$$

$$\text{and } \bar{\Phi}_x = Lrx / (R + r) \quad (5.4)$$

= rotation of preceding water plug relative to the trailing edge of the xth air plug.

5.1.3 General Resistances to Flow

There will always be a resistance to the flow passing through a helix. The resistive headloss across each water plug has to be subtracted from the head difference each plug exhibits, to obtain the useful head difference utilised by the helix.

As the resistance to flow inside the helix is small and cannot be separated experimentally from the friction in the bearings on the pump shaft, this headloss is ignored when calculating the profile of the helix.

5.1.4 Flow Media Resistance

Flow media can be included inside the helix to facilitate the treatment of waste water. From the experiment in chapter 4 the following equation can be formed to predict the headloss in a single coil:

$$hrx = lwx * af * Velx^{bf} \quad (5.5)$$

where hrx = flow media resistance head of the xth coil

lwx = length of the xth liquid plug,

- af = proportional coefficient of resistivity of the flow media, equal to 7.385 in the experiment in chapter 2,
- Velx = discharge velocity through the flow media,
- bf = power coefficient of resistivity of the flow media, equal to 1.860 in the experiment in chapter 2.

This equation is used in later sections to calculate the resistance to flow in a helix which could potentially be full or partially full of flow media.

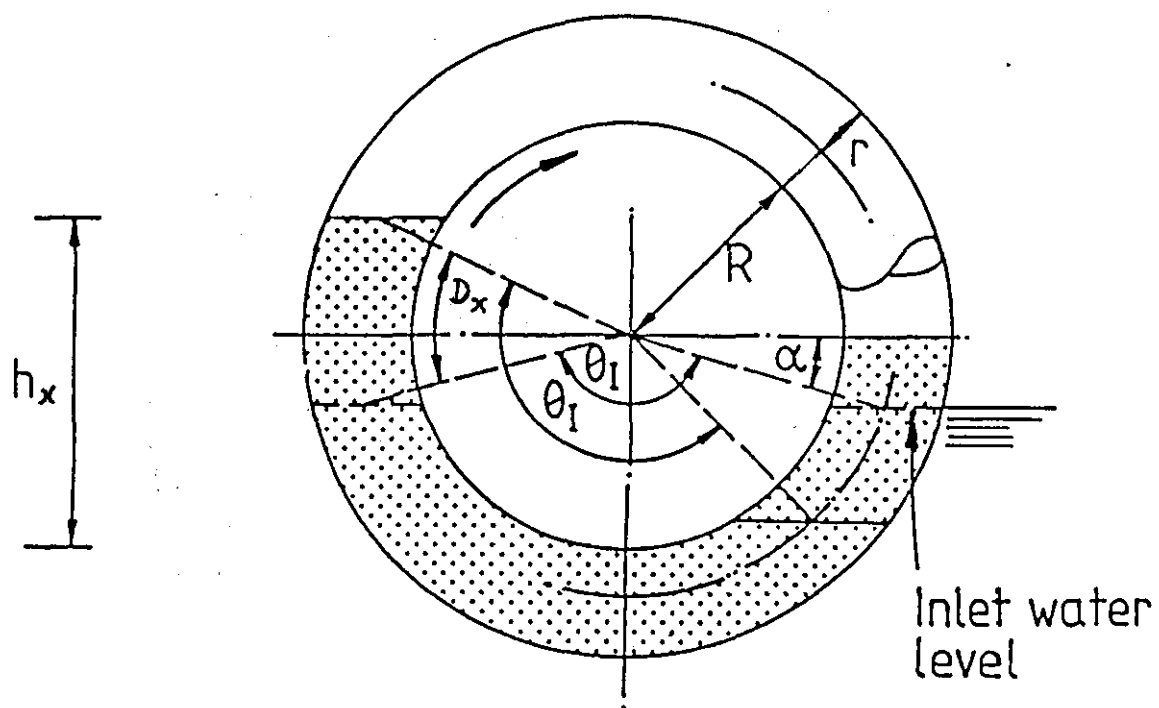


FIGURE 5.3, A Rotated Water Plug

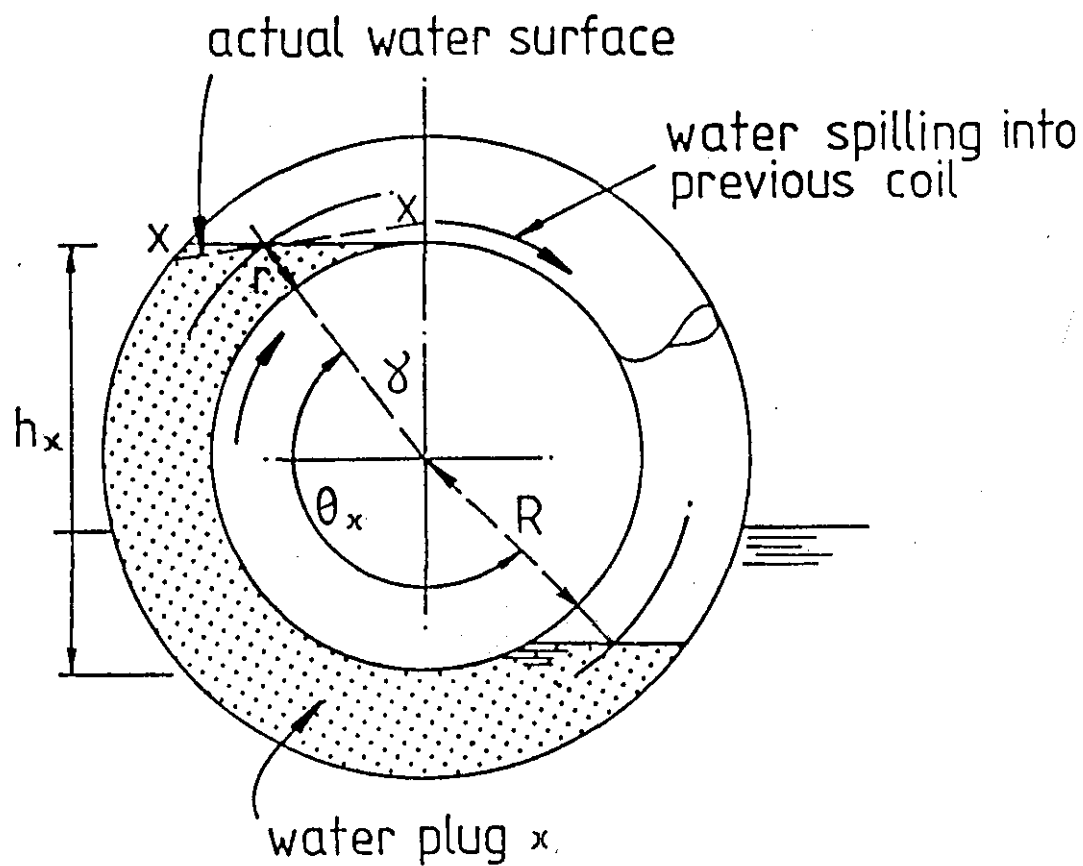


FIGURE 5.4, A Rotated Water Plug About to Spill

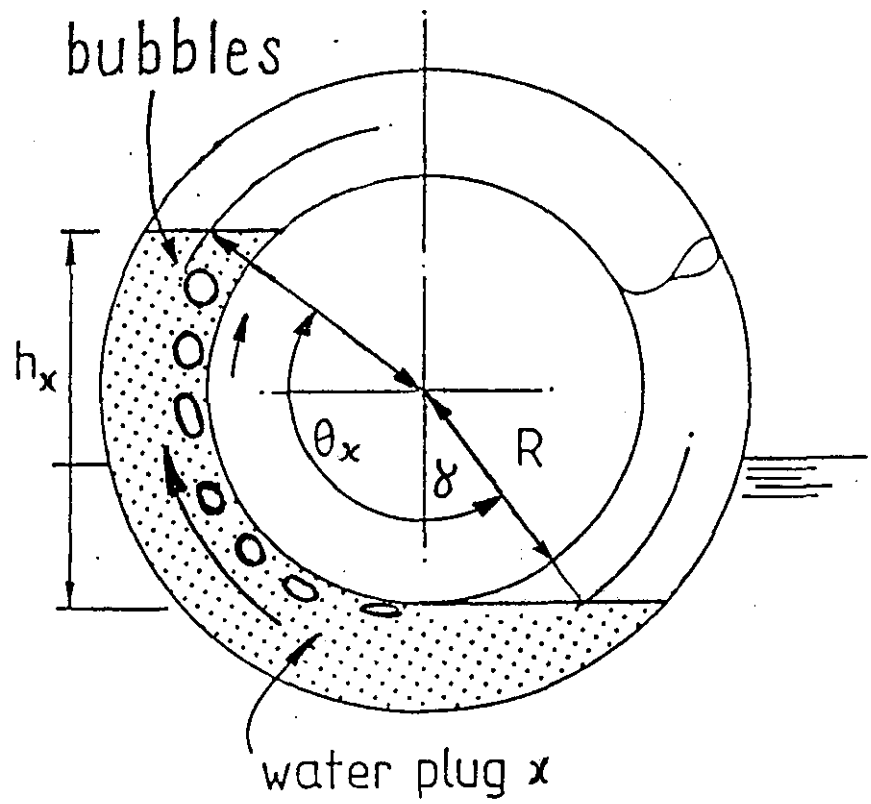


FIGURE 5.5, A Rotated Water Plug About to Bubble

5.1.5 Water Plug Level Development

Consider the pump rotating by visualising the helix as a stationary pipe with plugs of air and liquid moving along it. The initial orientation of the plugs as they enter the helix are that the water plugs lie at the bottom of first coil, and the preceding air plug occupies the space above the water plug.

As the air plugs travel through the helix they progressively become more compressed due to the increased pressure build-up towards the outlet. The water plugs (shown in figure 5.3) will also progressively rotate further away from the outlet relative to their original orientation.

A water plug will progressively rotate until either:

1. It reaches the outlet.
2. If it tries to rotate any further then the trailing edge of the water plug will spill back over the crown of the coil into the following water plug, Figure 5.4.
3. If it tries to rotate any further the leading edge of the water plug will reach the soffit at the bottom of the coil, and the preceding air plug will bubble through the water plug to the following air plug, Figure 5.5.

These last two restrictions effect the passage of the air and water plugs through the helix. The critical factor which governs which one of two last restrictions is reached first is determined by the depth of immersion in which the helix is sitting.

If the depth of immersion is above fifty percent then the water plugs will spill back, otherwise the air plugs will bubble back. This is because, in the former case the water plugs entering the helix are longer than the air plugs, as shown in figure 5.4. It follows that, as the water plug rotates its trailing edge will reach the crown of the coil before the leading edge reaches the soffit. If the water plug rotates any further, it will spill.

The converse is true that if the air plug is larger than the water plug as shown in figure 5.5 then the trailing edge of the air plug will reach the soffit of the coil before the leading edge is near the crown. If the plug rotates any further, it will start to bubble back.

The following sections describe in full the consequences of the above restrictions and how they effect the development of the head differences throughout the helix.

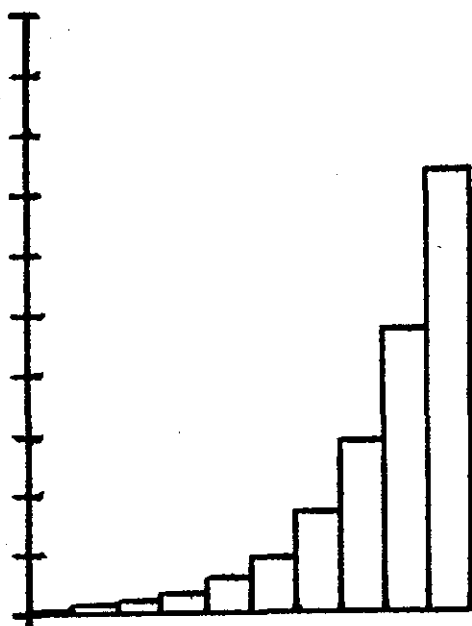


FIGURE 5.6, A Typical Low Headlight Profile

(not drawn to scale)

5.2 THE HELIX AT BELOW 50% D.O.I.

As described above, for a helix below 50% depth of immersion, the air plugs in this helix will always tend to bubble before the water plugs spill. Three different profiles are exhibited according to whether the helix is pumping to low, medium or high headlifts. These profiles, and how they can be calculated are described in the following sections.

5.2.1 Low Headlift Pumping

The definition of a helix pumping to a low head is that no air is being bubbled through the water plugs. A typical head difference profile displaying this pattern can be seen in figure 5.6. It can be seen from this diagram there is an exponential rise in head differences towards the outlet. As the outlet pressure is known it is logical to start at this point when describing the theory.

If the water plug nearest to the outlet is complete then (from figure 5.3) we can describe the pressures across the water plug with the following equation:

$$H_n = H_{n-1} + h_n - h_{rn}$$

This can be expressed in a more general form so as to be able to describe any of the coils in any circumstances in the helix with the following equation:

$$H_x = H_{x-1} + h_x - h_{rx} \quad (5.6)$$

From figure 5.3, we can derive the equation to predict the head difference across an individual coil:

$$h_x = (R + r) * (\text{Cos}(\theta_1 - Dx) - \text{Cos}(\theta_1 + Dx)) \quad (5.7)$$

where θ_1 = half of the angle the first water plug subtends at the centre of the axis,
 = $\text{ArcCos}(\text{DOI} / (R + r))$ (5.8)

Dx = rotation of the xth water plug from its original position,
 = summation of all the individual rotations of all the following water plugs due to the compressions of their air plugs.

$$= \sum_{x=1}^n \phi_x \quad (5.9)$$

If we ignore the headlosses due to resistance to flow, the approaches used to calculate the head difference profile from the above equations can be discussed.

It can be seen from the complexity of the above equations and from the following discussion that an iterative process has to be used. This is because the outlet pressure is known but the final water plug rotation is not, as it depends upon all the previous ones which are also unknown.

By initially guessing the rotation of the first water plug and calculating from the inlet forward, a head difference profile can be calculated from the rest of the rotations and head differences. The total head generated by this profile is compared with the desired outlet head and the rotation of the first plug is adjusted to calculate a closer profile. This iteration continues until the convergence leads to an acceptable error between the desired and theoretical total head generated.

The above approach is also used to calculate the profile for non-spilling coils in a helix with a depth of immersion greater than 50 percent.

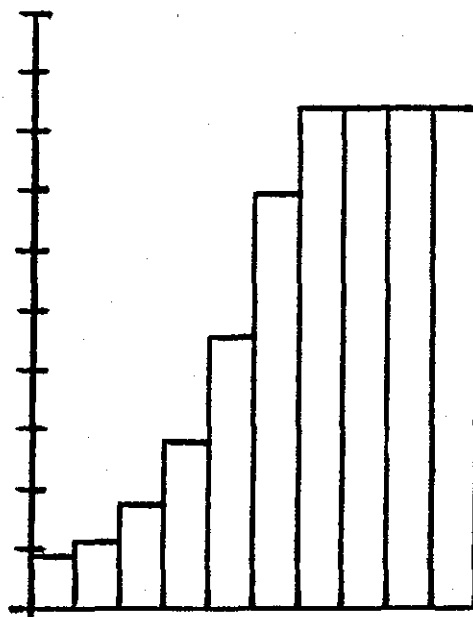


FIGURE 5.7, A Typical Bubbling Medium Headlift Profile

(not drawn to scale)

5.2.2 Bubbling Medium Headlift Pumping

The definition of a helix pumping to a medium head is that at least one but not all of the water plugs are being bubbled through. A Typical head difference profile of this pattern is shown in figure 5.7. It can be seen from this diagram that there is an exponential rise in head level differences towards the outlet until a threshold is reached. At this point, the water plug in this coil has generated the maximum head difference through the action of bubbling alone. The phenomenon of air bubbling through a water plug limits the rotation of the water plug and so limits its head difference.

The iteration mentioned in the previous section can be utilised to find out if a helix has crossed the threshold from low headlift pumping to medium. If the calculated value of rotation of the final water plug exceeds the maximum possible, it implies the last water plug is being bubbled through.

The limiting factor which determines the extent to which the i th water plug may rotate can be expressed by the following identity:

$$D_i = \theta_i - \gamma \quad (5.10)$$

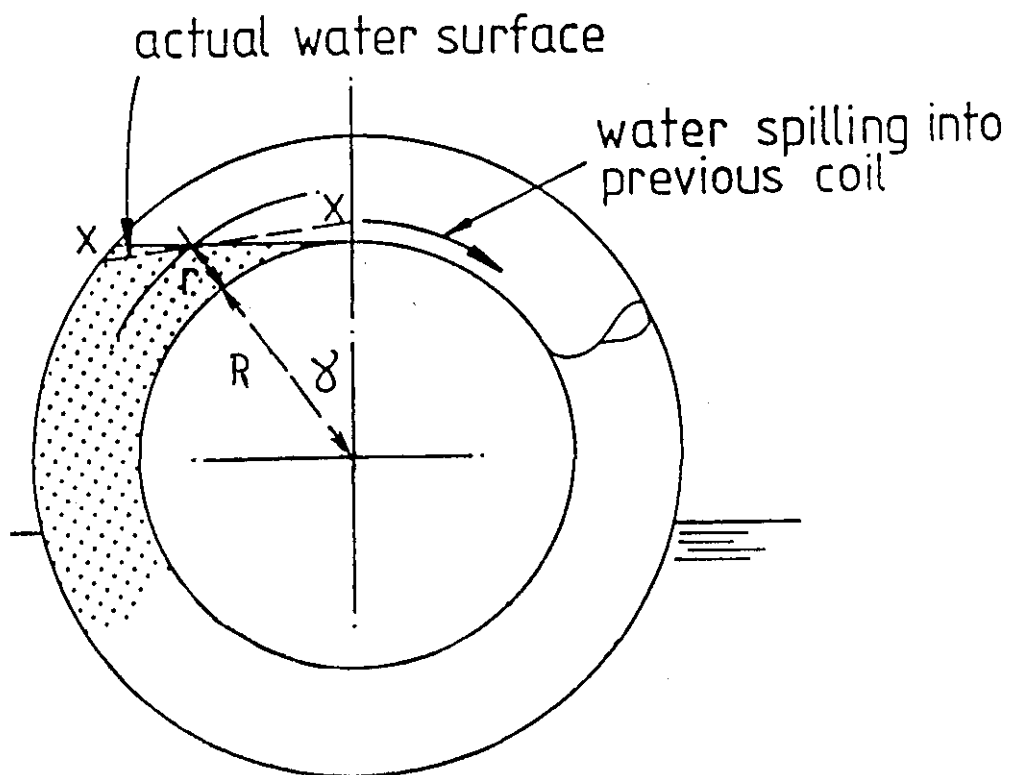


FIGURE 5.8, The Restricting Rotation Angle

Where ' γ ' is defined in figure 5.8 and can be expressed as:

$$\gamma = \text{ArcCos} \left(R / (R + r) \right) \quad (5.11)$$

This is the angle which the centre of the leading edge of the i th water plug (which has reached the *crown* of the coil) subtends with the vertical, at the centre of the drum.

If the calculated ' D_i ' is greater than ' $\theta_1 - \gamma$ ', the iteration copes with this limitation by equating ' D_i ' to ' $\theta_1 - \gamma$ '. This limits the head able to be generated by this water plug. The consequence of this limitation is to induce the following plugs to rotate further to cope with the desired total headlift needed.

By including the above restriction in the rotation of the water plugs, then as the headlift increases from a low headlift pumping situation, the head difference profile reaches the one displayed in figure 5.7.

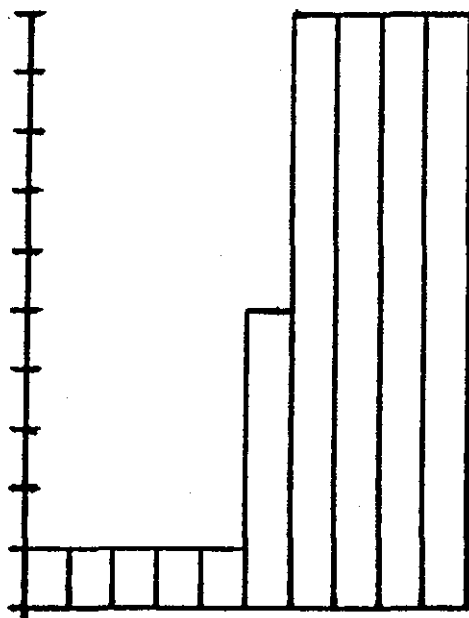


FIGURE 5.9, A Typical High Headlift Profile

(not drawn to scale)

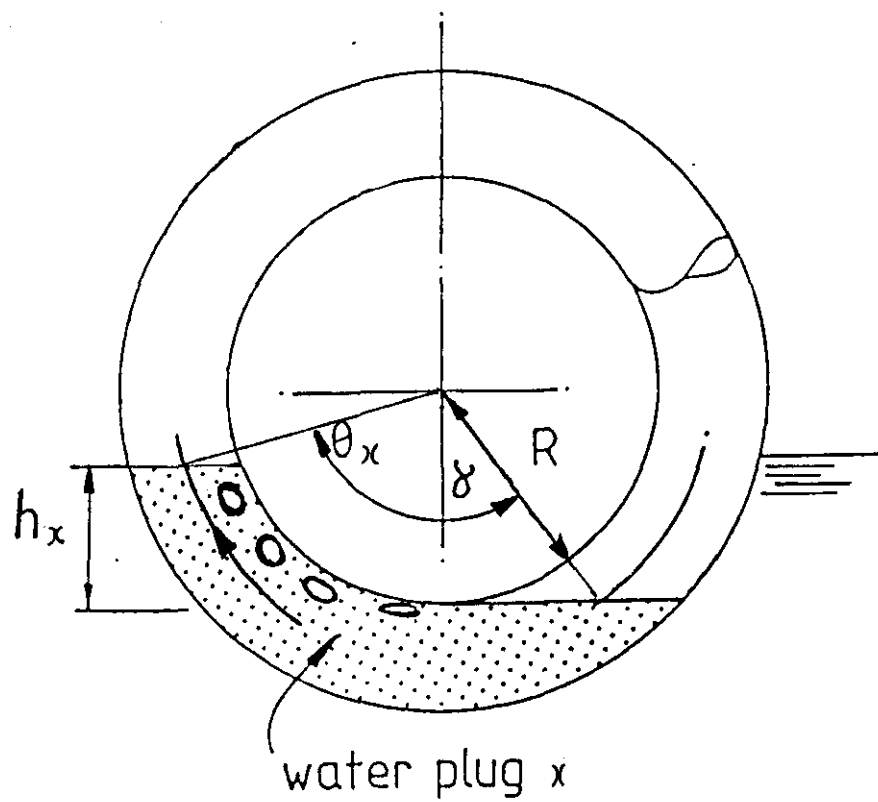


FIGURE 5.10, A Bubbling First Water Plug

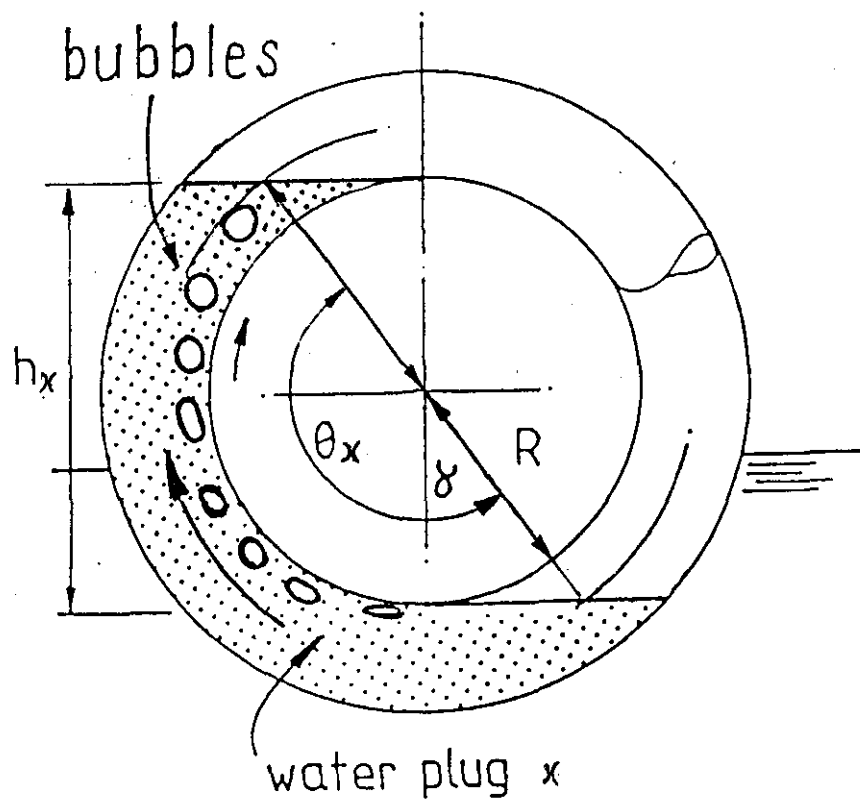


FIGURE 5.11, A Bubbling and Spilling Water Plug

5.2.3 High Headlift Pumping

The definition of a helix pumping to a high head is that all the water plugs are being bubbled through. A typical head profile can be seen as figure 5.9. This diagram shows a helix where all but one of the coils are exhibiting one of two discrete head level differences.

All water plugs in this helix are being bubbled through. The water plugs exhibiting a high head difference are spilling into the following water plugs, as well as being spilt into by the preceding water plugs. The head difference these water plugs generate remains constant due to the air depressing the leading edge of the water plug to the soffit. The trailing edge also constantly spills due to the preceding water plug spilling into this. The excess water from the preceding water plug will spill over from this water plug into the following one.

The remaining water plug, whose head difference is at neither of these two levels, is bubbling and being spilt into but is not spilling itself. It is the head difference from this coil, which has to vary to cope with the variations of head desired between the discrete levels provided by the other coils. The head varies throughout the revolution to take up the continually changing demand of the headlift, as discussed in section 6.1.4.

The head difference from the bubbling only water

plugs can be found from the diagram in figure 5.10. As this water plug enters the inlet of the helix it is already being bubbled through. The result is that the leading edge is already depressed to the soffit while the trailing edge is still at the external depth of immersion. It consequently leads to a water plug of reduced length compared to the water plugs in the previous two sections, and therefore the head that it generates is also reduced. The head difference from a bubbling only water plug can be found by:

$$h_u = R - DOI \quad (5.12)$$

The head difference from the bubbling and spilling water plugs can be found from figure 5.11, and is:

$$h_v = D \quad (5.13)$$

The head difference of the remaining coil, which is being spilt into but is not itself spilling is:

$$h_w = H_n - H_a - H_u - H_v \quad (5.14)$$

where H_u = head generated by bubbling water plugs

$$= i * h_u \quad (5.15)$$

H_v = total head generated by bubbling
and spilling water plugs

$$= (n - i - 1) * h_v \quad (5.16)$$

i = number of bubbling only water plugs.

By rearranging equation (5.14) and adding (5.15) and (5.16), we can obtain an equation that describes a helix both bubbling and spilling, i.e.:

$$H_n - H_a = (i * h_u) + ((n - i - 1) * h_v) + h_w \quad (5.17)$$

The head difference profile for a desired headlift is calculated by varying the number of bubbling only water plugs 'i' in equation (5.15) until the following identity is true:

$$h_u < h_w < h_v \quad (5.18)$$

This ensures the head difference for the water plug being spilt into but is not spilling itself is physically possible.

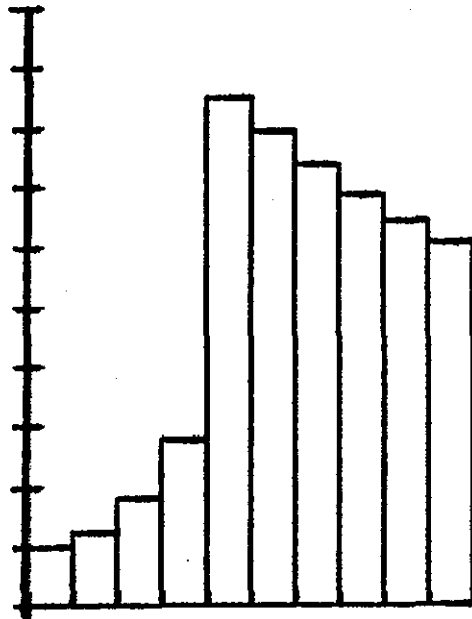


FIGURE 5.12, A Typical Spilling Medium Headlift Profile

(not drawn to scale)

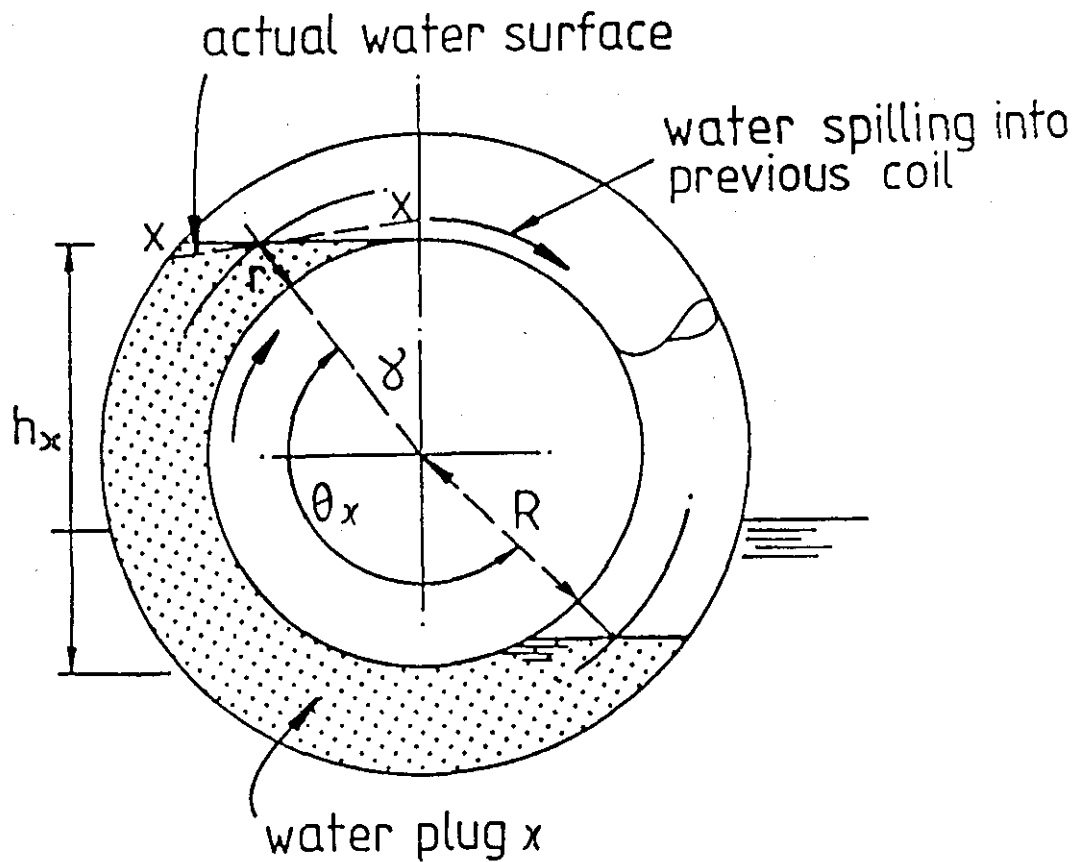


FIGURE 5.12, Spilling and being Spilt into Water Plug

5.3 THE HELIX AT OR ABOVE 50% D.O.I.

As described in section 5.1.3 for a helix above 50% depth of immersion, the water plug will tend to spill before the air plugs bubble. The water plug head differences exhibit three different profiles according to whether it is pumping to low, medium or high headlifts. These different profiles and how they can be calculated is described in the following section.

5.3.1 Low headlift Pumping

The definition of a helix pumping to a low head is that it does not require any of the water plugs to be spilling. This definition is very similar to the definition of a helix pumping to a low headlift at a depth of immersion of below 50%. As the same can be said of the theories and the calculations, then section 5.2.1 can be used to calculate the head difference profile of the pump described in this section.

5.3.2 Spilling Medium headlift Pumping

The definition of a helix pumping to a medium head is that at least one but not all the water plugs are spilling. A typical head difference profile is shown in figure 5.12. It can be seen from this diagram that there is an exponential rise in head level differences towards the outlet. At some point, there is a maximum

head difference and after this point, there is a decay towards the outlet. The maximum point is the last water plug which is not spilling or being spilt into. The preceding water plug is being spilt into, and all those preceding that are being spilt into and are themselves spilling.

The spilling is caused by the air plugs being compressed to such an extent that they cause the water plugs to rotate over the crown of the coil in which they are in. The head difference of the spilling water plugs is therefore a function of the volume of their associated air plugs.

Figure 5.13 shows a water plug which is both spilling and being spilled into. The head difference generated by the water plug is:

$$h_x = R - (R + r) * \text{ArcCos} (L_{ax}/(R - r)) \quad (5.19)$$

The calculations are approached by starting at the outlet because the required head is known. From this, the length of the last air plug can be calculated using equation (5.3) and so the head difference generated by the last water plug can be calculated from equation (5.19). By using equation (5.6) we can then calculate the pressure head of the penultimate air plug.

These calculations continue towards the inlet until the water plugs cease to spill. This can be found from the following identity:

$$L_{ax} + L_{w1} > 2 * n * (R + r) \quad (5.20)$$

That infers that there is a point at which the water and air volumes inside a particular coil become too large for a spilling situation to occur. This is done by taking the length of the smallest water plug possible; i.e. one which has not been spilt into, and adding it to the length of an air plug being tested. If this length is longer than the centreline perimeter of the coil then it indicates the length of the air plug is too long to allow the water plug to spill.

Calculating the head difference of the water plug being spilt into but is not spilling itself is impossible as the amount of water introduced to the plug is unknown. This calculation can be circumvented by assuming that at some point in a revolution, the water plug is just about to be spilt into by the preceding water plug. At this point in the revolution there are no water plugs with unknown volumes.

The calculations from the exponential rise in head differences can then proceed in the same way as the previous section. There are only two differences to the

calculations; the number of coils is reduced to the number that are not spilling, and the pressure head is reduced to the pressure at the plug which is first spilling.

5.3.3 High Headlift Pumping

There comes a point at which the helix in the previous section cannot create a higher headlift pressure with the profile and theory discussed. This point is when all the coils are spilling back and so the first water plug is spilling out of the inlet. The only way to increase the head differences is to restrict the air from passing through the outlet and so force the coils to bubble-back. This will create the situation described in section 5.2.3 and so to avoid repetition will not be reiterated here.

Ways to prevent the escape of air from the outlet are discussed in section 5.8.3.

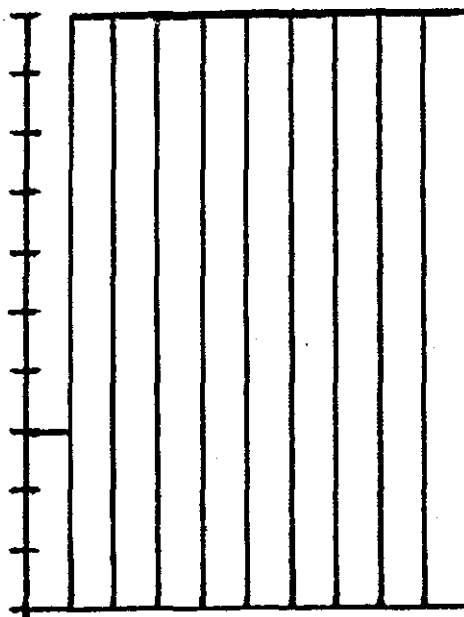


FIGURE 5.14, A Typical Maximum Headlift Profile

(not drawn to scale)

5.4 MAXIMUM HEAD LIFT PUMPING

We can calculate the maximum head attainable from any given pump by taking equation (5.17) and holding the number of bubbling only water plugs ('i') to a minimum of one. The first water plug is left just bubbling, due to the restrictions discussed in sections 6.13, and therefore this coil is only relied upon to maintain a minimum head difference throughout the whole of the revolution. The head difference profile can be seen in figure 5.14 and the equation describing this is:

$$H_n - H_a = h_u + (n - 2) * h_v + h_w \quad (5.21)$$

'h_w' can be maximised from equation (5.18) to get:

$$h_w = h_v \quad (5.22)$$

Substituting equation (5.22) into (5.21), we get:

$$H_n - H_a = h_u + (n - 1) * h_v \quad (5.23)$$

For the helix to reliably maintain its maximum headlift pressure throughout the whole of a revolution, the head difference from the water plug nearest the outlet has to be ignored due to factors discussed in section 6.1.1. This factor has been ignored in the previous sections as the helix is not lifting to its maximum achievable.

Equation (5.23) can be modified by ignoring the last spilling and bubbling water plug; i.e. the maximum reliable headlift pressure available throughout the whole of a revolution is:

$$H_n - H_a = h_u + (n - 2) * h_v \quad (5.24)$$

The flow media resistance has been left out of the calculations in this section as the idea of having a helix pumping to its maximum lift is mutually exclusive with the concept of a waste water treatment unit.

5.5 FLOW MEDIA HELIX PUMPING

From equation (5.6) we have the general equation which describes the head differences across a water plug:

$$H_x = H_{x-1} + h_x - h_{rx} \quad (5.6)$$

So far, the effects of flow resistance have been ignored, but with the inclusion of the flow media inside the helix it has been shown that there is a significant increase in resistance to flow. By ignoring inlet losses and resistance to flow through the empty parts of the helix, we can combine equations (5.5) and (5.6) to form:

$$H_x = H_{x-1} + h_x - l_{wx} * a_f * V_{elx}^{bf} \quad (5.25)$$

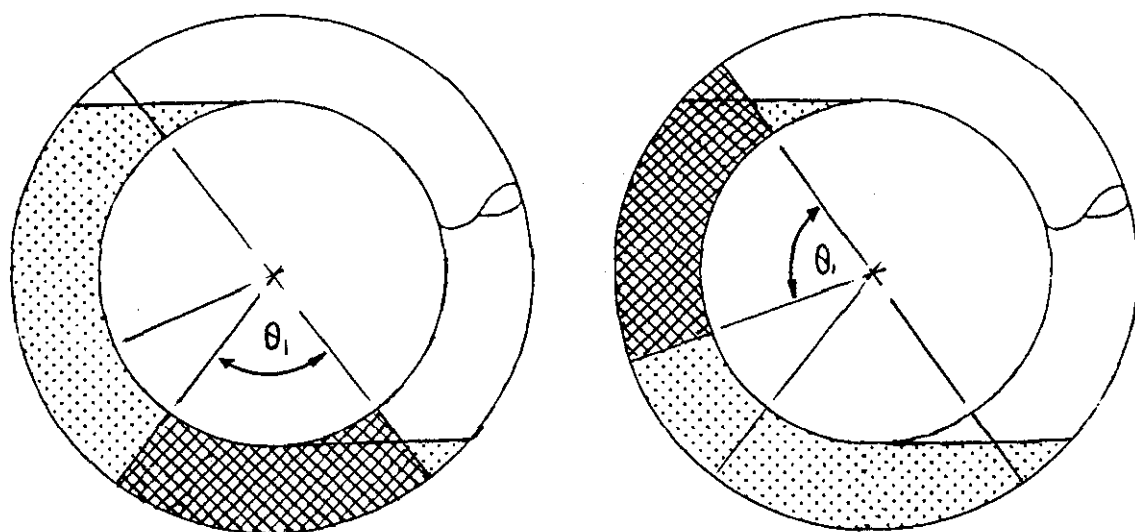


FIGURE 5.15, The velocity of a Bubbling and Spilling

Water Plug

The only variable which cannot be directly calculated by the above theory is the water plug velocity. This is different depending upon whether or not the plug is spilling and/or bubbling. The following calculations describes the mean velocity throughout a revolution:

1. A non-bubbling, non-spilling water plug has a velocity through the media of:

$$V_x = (2 * \pi - \dot{\phi}_x) * (R + r) * N_s / 60 \quad (5.26)$$

This shows that the velocity is equal to the velocity of the helix minus the velocity of the plug due to its rotation through its increased head difference capacity.

2. The velocity of a bubbling, non-spilling water plug is:

$$V_x = 2 * \pi * (R + r) * N_s / 60 \quad (5.27)$$

As the rotation of the water plug stays the same throughout the revolution, equation (5.27) is a

simplified version of equation (5.26).

3. The velocity of a spilling water plug (which might or might not be bubbling), is complicated by the fact that the spilling effect significantly reduces the velocity of the water plug through the helix. Figure 5.15 shows two coils; in the left hand figure is a coil at the start of a revolution, and in the right hand figure is the same plug at the end of the revolution.

The hatched area in the figures is the equivalent water plug volume that is accepted at the inlet. It is only this area that does not spillback between the start and the end of the revolution. We can therefore use this part of the plug as a reference to calculate the velocity of the water plug through the media.

From the diagram:

$$V_x = (P_i - 2\theta_i) * (R + r) * N_s / 60 \quad (5.28)$$

The equations in this section can be included with theories in the previous sections to provide a basis upon which the head difference profile for a coil pump in any given circumstance can be calculated.

5.6 THE DELIVERY PIPE

The theory behind the delivery pipe is not central to the concepts covered by this thesis, but a description is included here for completeness.

The definition of a delivery pipe is one which raises the water plugs to a level higher than the equivalent pressure head generated by the helix. This is done by limiting the diameter of the pipe to approximately 2 to 3 centimetres. It enables the air/water plug interfaces to remain intact, allowing the water plugs to be pushed up the delivery pipe to a height, extra to the outlet head, corresponding to the combined heights of the pressurised air plugs inside the delivery pipe.

A full description of the theories involved can be read in reference 16.

5.7 THE PUMP DISCHARGE

5.7.1 Introduction

Previous research (Ref. 16) has studied the discharge of the pump, finding that theoretically, the mean pumping rate for a coil pump is:

$$Q = N_s * A * L_{w1} \quad (5.29)$$

where A = cross sectional area of the pipe,

L_{w1} = length of a liquid plug taken in
at the inlet.

With no dynamic losses, ' $L_{w1} = 2 * \theta_1 * (R + r)$ ', where ' θ_1 ' is determined by equation (5.8). However, in reality ' L_{w1} ' is reduced due to inlet restrictions, and in previous research it has been found that the above equation over-estimates the theory by six percent.

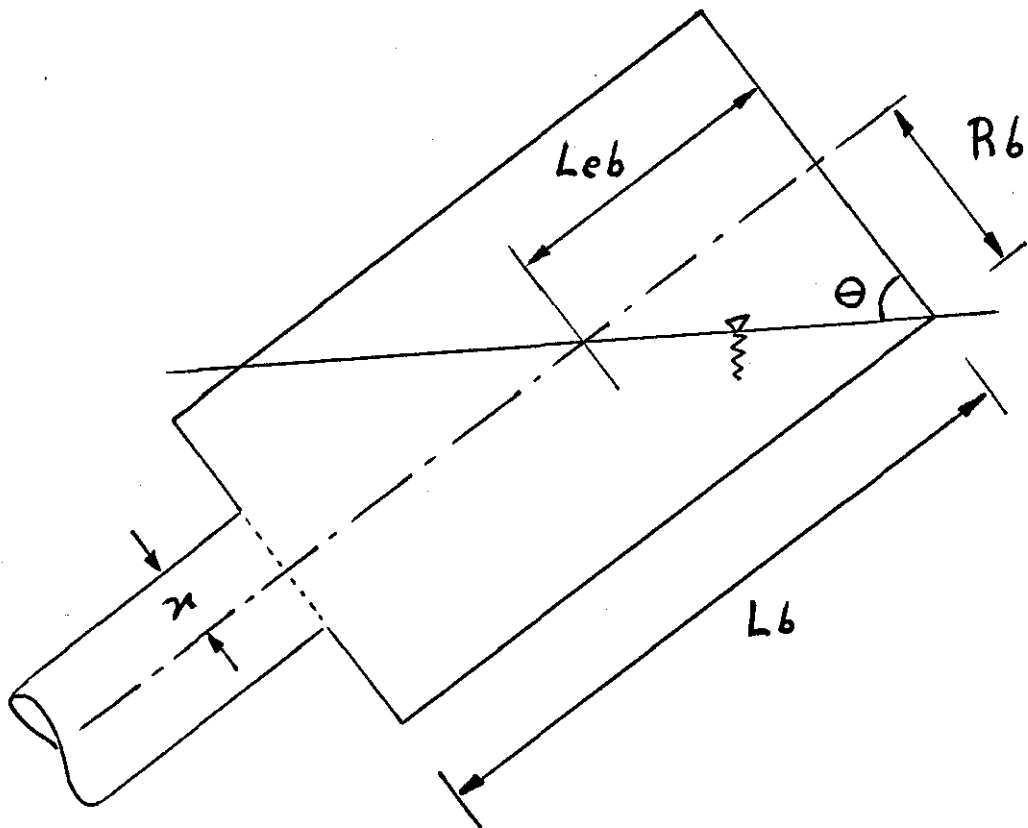


Figure 5.16 Diagram to find the Bucket Volume

5.7.2 Increasing the Discharge

5.7.2.1 Introduction

To increase the discharge of a coil pump, for a given immersion, diameter of helix and rotational speed, the volume of each water plug has to be increased. This has been investigated in the experiment in chapter 3 by increasing the size of the inlet.

The device discussed in this thesis is an open ended cylinder attached to the helix inlet (Figure 5.16). The effect this has is to hold extra water while the inlet of the helix rotates above the surface of the tank water. As the water in the helix travels away from the inlet, the water in the cylinder follows, thus adding to the length of the existing water plug and increasing the discharge. A side effect is that as the extra water is added to the trailing edge of the water plug, the orientation of the plug is rotated away from the outlet. This will cause the water plugs to spill prematurely thus reducing the performance of the pump. The effect is minimised by introducing a hole three quarters of a revolution away from the inlet. It lets excess air escape from the preceding air plug thus equalising the leading and trailing water levels. Unfortunately some of the water also escapes thus decreasing the initial internal depth of immersion. These effects are discussed in the following sections.

5.7.2.2 Liquid Plug Volume Increase Calculation

The volume of liquid scooped up by the 'bucket' device is affected by the depth of immersion in which the drum is sitting. i.e.:

$$\text{Volb} = \text{Ab} * (\text{Lb} - \text{Leb}) \quad (5.30)$$

Where Volb = volume of liquid scooped up by the bucket,

Ab = cross sectional area of the bucket extra to that of the inlet to the helix,

Lb = length of the bucket,

Leb = length representing the reduction in volume of the liquid the bucket scoops up due to the orientation of the bucket relative to the surface of the liquid in the tank,

Lb - Leb = mean length of the liquid scooped up inside the bucket over its cross sectional area.

The bucket used in this experiment is cylindrical in shape and so the diagram shown in figure 5.16 is used to calculate L_b , i.e:

$$L_b = R_b / \tan(\theta) \quad (5.31)$$

The detailed equation for the volume of the bucket in this experiment is:

$$Vol_b = \pi * (R_b^2 - r^2) * (L_b - (R_b/\tan(\theta))) \quad (5.32)$$

5.7.2.3 Calculating the Discharge Through the Hole

The disadvantage of having the hole is that as well as letting out the air, it also lets out the discharge. This can not be helped but can be limited by making the hole as small as possible. As air is less viscous than water, there will be little problem in letting enough air escape. The problem arises in calculating the smallest hole possible in order for this to happen so as to limit the water escaping. As the experiment in Chapter 3 does not explore the optimum diameter for the hole, it is outside the bounds of discussion here.

Calculating the water loss through the hole is

simple in nature and is analysed here. The analysis is used to check the theory against the practical results obtained from the experiment in Chapter 3.

By using Torricelli's equation from basic Hydrodynamics, it has been established that the velocity through an orifice is related to the headloss across it by the equation:

$$V_h = C_d \sqrt{2 * g * H_h} \quad (5.33)$$

where g = gravitational constant,

C_d = constant for the orifice in question,

V_h = velocity of the water through the hole.

H_h = head difference across the hole.

If the hole is in contact with the water plug for time ' T_h ', then the volume of water passed through the hole in one revolution is:

$$Vol_h = A_h * V_h * T_h \quad (5.34)$$

where Vol_h = volume of water passing through the hole in one revolution,

A_h = area of the hole,

V_h = water velocity through the hole.

5.7.2.4 Calculating the Increased Discharge

By developing Equation 5.29, it can be said that the discharge of a pump without a bucket is:

$$Q = Vol1 * Ns$$

Where Vol1 = volume of the first water plug in a normal pipe.

The discharge from a modified helix can be found by incorporating the volume of water scooped up by the bucket into the above equation to produce:

$$Qb = (Vol1 + Volb + Volh) * Ns \quad (5.35)$$

where Qb = discharge of a helix with a bucket attached,

Volb = volume of water captured by the bucket,

Volh = volume of water lost through the escape hole.

5.7.2.5 Calculating the Increased DOI

The increased discharge brings an increased depth of immersion inside the coil. This can be found from the following equation:

$$DOI_e = \sin((\pi - 2 * \theta_{pe}) / 2) * R \quad (5.36)$$

where θ_{pe} = half the angle subtended by the extended plug, at the centre of the drum,

DOI_e = internal depth of immersion inside the helix measured from the centre of the drum downward.

This will give an indication as to how effective the modifications to the pump prove to be. This depth of immersion can then be used, together with theories discussed in the rest of this chapter, to predict the performance of the pump.

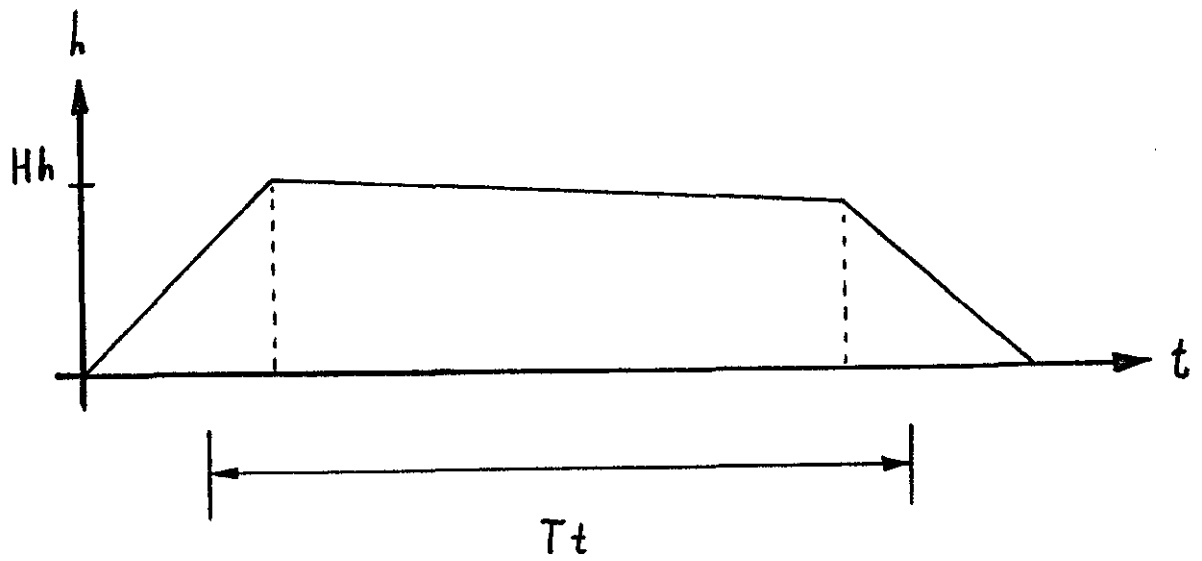


FIGURE 5.17, Head Difference Across the Pipe Hole

5.7.2.6 Discussing the Accuracy of this Theorem

Equation (5.34) assumes that the head across the hole and therefore the velocity through it will be constant. It also assumes that the hole is in contact with the tank water at the same time as it is in contact with the water plug, thereby producing a constant flow pattern.

As the water flows out of the plug the head difference across the hole reduces. Because the equations use the initial head difference the results calculated will be too high. It is assumed the volume of water lost is small in comparison to the total water volume in the plug, and therefore this error can be neglected.

There will also be an error due to the rapid changes in head difference across the hole when the orifice is rotating above the tank water surface, but still in contact with the water plug. It will effect the results in the same way as the error described in the previous paragraph. It is also assumed that the effect will be insignificant.

Another error is where the orifice is venting water to the atmosphere. This could produce a different resistance to flow through the hole compared to when it is venting to the tank water. As this effect is unknown, it too is neglected.

Figure 5.17 shows the relationship between the head

difference across the orifice against the rotation of the drum for a typical plug. It shows the head rising as the hole approaches the tank water level, a slight fall-off of head as the orifice passes through the tank water, and a reduction of head as the orifice leaves the external water level.

The equivalent time for the water to escape at full flow through the hole is also shown in the diagram. It has been reduced arbitrarily in comparison with the total time the water has to escape to correct for the errors in the assumptions made previously.

The constant ' C_d ' can be found by experimentation and this is the object of the experiment described in chapter 3.

Further research to increase the accuracy of the relationships described here is discussed in section 7.3.

5.8 THE HEAD GENERATOR

5.8.1 Introduction

This is a device (shown in figures 4.3 and 4.8, and described in Chapter 4, section 4.1.3) which allows the two phase flow exiting the helix to rise predictably up the delivery pipe, without the excessive variations in back pressure experienced inside the delivery pipe (described above). This predictability is important for the experiment described in chapter 4. A constant back pressure on the outlet of the helix is desired as this simplifies the results processing due to one less phenomenon to account for.

If the air plugs are allowed to escape up the vertical pipe unmodified, two actions occur which lead to a reduction in the back pressure generated by the vertical pipe. The first is that the air plug travels faster up the pipe than the water plug. The second is that the rising air plug stays mainly in one bubble.

The problem of a whole air plug rising faster than the water in the vertical pipe is that it tends to push the water column above it prematurely out of the outlet. This leads to the loss of head generated for part of a revolution until the next water plug enters the vertical pipe.

The air plug remaining in one piece is a major problem as this leads to a loss of space available for

the water in the pipe to generate the full back pressure for the duration the air plug is in the pipe. This would not occur if the air plug were to be split into a number of small separate bubbles.

The above two problems can be limited by the use of the head generator. The theories associated with the device are discussed in the rest of this section.

5.8.2 Prevention of Loss of Head

The prevention of the loss of head in the vertical pipe due to the above two features is done by splitting the air plug into many small bubbles. It enables the head generated above the mass of bubbles to be maintained and developed amongst and below the bubbles.

Bubbles are generated by introducing the air plug to the vertical pipe through a series of small holes drilled in the pipe at the same level as the centreline of the helix (as shown in figure (4.8)). The two phase flow will experience a headloss through the holes but it is envisaged that this will not be significant.

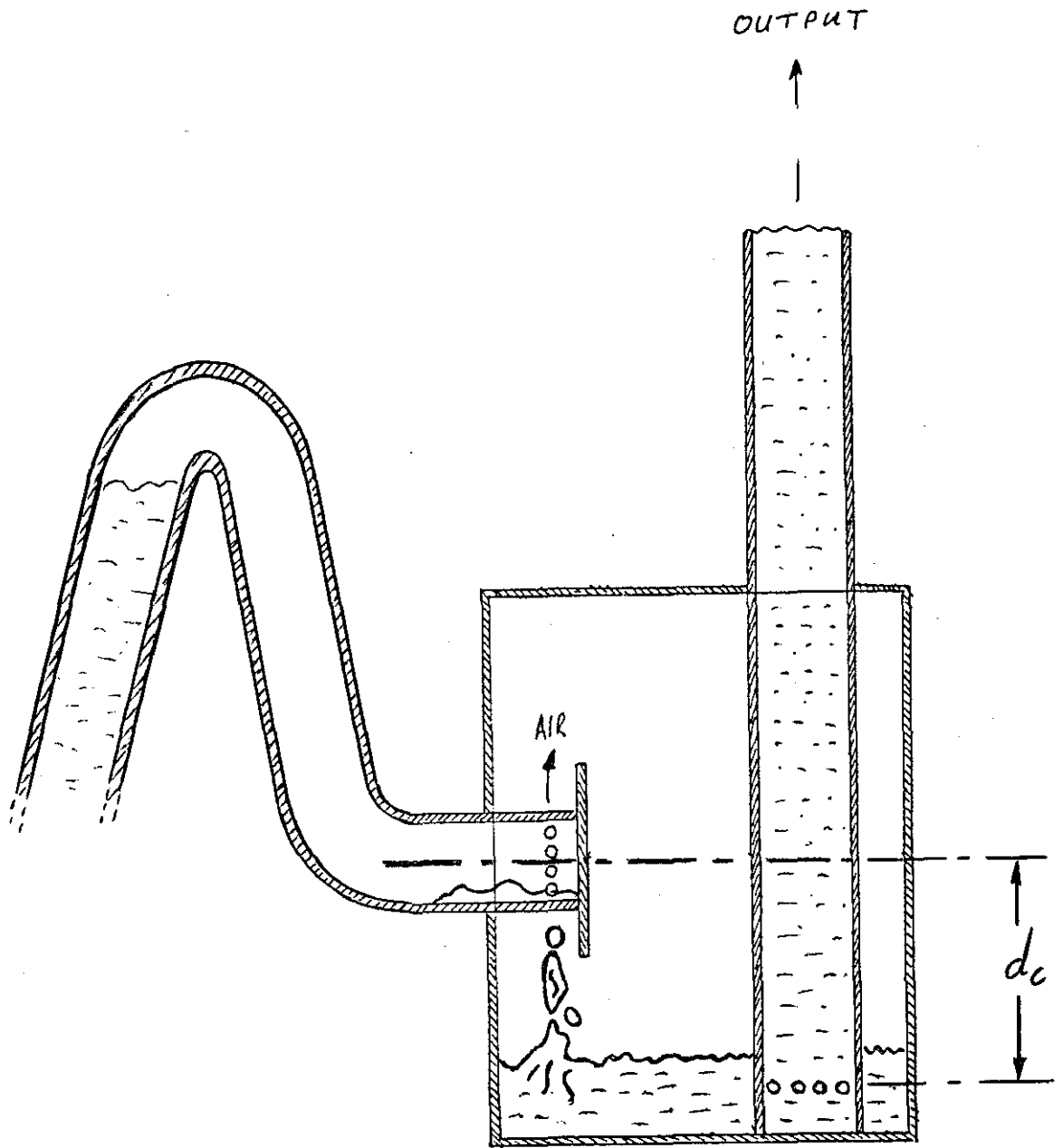


FIGURE 5.18, The Helix and Head Generator

5.8.3 Prevention of Air Escaping

It is difficult for a helix at a depth of immersion greater than 50 percent to generate high head lifts unless bubbling also occurs. This can be achieved by preventing the air escaping up the vertical pipe. It is done by lowering the holes drilled in the vertical pipe to a position below the level of the centre line of the drum.

When an air plug enters the Splash Chamber, it lowers the water level inside towards the level of the holes, thus increasing the head the helix has to pump against. If the level of the holes is sufficient to force the helix to bubble back then the helix will exhibit water plugs that are both spilling and bubbling and therefore be able to respond to pumping to high headlifts.

The level to which the holes have to be lowered can be found by considering the helix in motion in figure 5.18 with the head generator accepting an air plug. Consider the situation where the volume inside the chamber is restricted so that part of the air plug entering the chamber forces the water level down close to the holes, while the rest is still inside the helix. The increase in back pressure generated by the lowering of the water level will force the air to bubble back through the following water plug. It is done by restricting the volume inside the chamber to less than

the volume of an air plug under the headlift pressure. The level of the holes in the vertical pipe has to be a minimum of the diameter of the drum below the centreline of the helix. This distance ensures there is a sufficiently large increase in headlift when air plug enters the chamber for it to bubble through the following water plug, i.e:

$$Volc < Vola \quad (5.37)$$

$$dc > D \quad (5.38)$$

where D = diameter of drum,
 dc = depth of holes in the vertical pipe
 below the centerline of the helix,
 $Volc$ = volume of splash chamber,
 $Vola$ = volume of last air plug,

If these two identities are utilised in the design of the Splash Chamber then air will be prevented from escaping out of the outlet, and high headlifting is then achievable.

Unfortunately, The above theories preventing the flow of air through the helix makes it unsuitable for it to be used as a wastewater treatment process. This is because the oxygen in the air (captive in the helix) will be exhausted by the bacteria and so will die.

CHAPTER 6

THE COMPUTER SIMULATION

A computer simulation has been developed to visually substantiate the theories described in Chapter 5. The utilisation of a computer to simulate the internal actions of a pump is the logical way to perform the many calculations necessary for the realistic interpretation of the theory. A computer has been used in order to take advantage of its facility for presenting data, especially graphics. This facilitates the visualisation of the internal workings of the coil pump.

The first computer simulation of the coil pump was developed by Annable (ref 7). It is the development of this model and the inclusion of the new theories that have led to the simulation developed for this thesis. Appendix F contains the listing of the computer simulation. The program has been written in Microsoft Graphics Basic for an Apple IIe Microcomputer.

6.1 ASSUMPTIONS AND APPROXIMATIONS OF THE SIMULATION

The assumptions and approximations of this simulation have been discussed here to put its validity and accuracy into perspective.

6.1.1 Single Snapshot per Revolution

The calculations are only performed once per revolution and thus it must be assumed that the pump can sustain its performance over the entire revolution. As this assumption might be invalid then the simulation should take a conservative bias to ensure a pump can realise its simulated performance. The possible ways a designer might accomplish this include:

1. The required headlift could be increased,
2. A single coil could be subtracted from the total actually used in the helix,
3. The compressibility of air could be reduced decreasing the rotation of the water plugs,
4. Reducing the diameter of the drum; reducing the head differences that the coils could sustain.

If one, or any combination of these measures are implemented then this would offset the possibility of the helix being unable to support the required head. None of the above suggestions has been implemented in this simulation as more research has to be undertaken to determine the most realistic approach to take.

6.1.2 The Spilling Interface

As described on section 5.3.2, when a helix is spilling but not bubbling, there is a coil which is being spilt into but which is not spilling itself. This complicates the simulation as the length of the water plug and therefore the head difference able to be generated by this plug is indeterminate. To overcome this problem, it is assumed that the orientation at the helix is such that the coil in question is on the point of just being spilt into. This avoids the problem originally posed and so enhances the accuracy of the simulation.

6.1.3 The First and Last Coils

It is assumed in simulation that the first and last coils can sustain their head differences throughout the whole of a revolution. Realistically, when the first water plug is in the process of entering the inlet it will be unable to sustain its head difference, as calculated in the simulation. This argument can also be applied to the last water plug, which will be unable to sustain the calculated head difference when it is in the process of leaving the helix.

The above assumptions are unimportant when the helix is not pumping to near its maximum possible head. This is because the rest of the helix will be able to absorb the difference between the calculated and actual

head differences from the first and last coils.

To avoid the possible consequences of ignoring this assumption, one of the suggested ways of lending a conservative bias to the simulation (described in section 6.1.1) could be adopted to assist in supporting the calculated head differences of the first and last coils. This will only be implemented if the helix is pumping near its maximum.

6.1.4 The Level Oscillations -----

It is suspected that the oscillation of the head differences referred to in section 1.3.2 is caused by the phenomenon described in the previous section. During a revolution, the first and last coils contribute a continually varying head. The remaining coils therefore have to support the remaining head, which will also be continually varying if the required headlift remains constant. It is proposed that the varying head applied to the majority of the coils will cause the oscillations described in the referred section.

As the cause of this phenomenon is associated with the one described in the previous section, then the recommended action described in this section should be adopted.

6.2 THE HIGH-LEVEL FLOW OF PROGRAM LOGIC

This section describes the progression of the execution of the logic through the simulation. As the helix can be subjected to a variety of different situations this is reflected in the discussion of the various ways the coil tries to react to these different situations.

The theories described in chapter 5 have been combined with observations made, to form the construction of the execution of the logic. The approaches adopted by the original simulation referred to in section 1.3.4 have also been applied here, but developed further to include the bubbling plus the bubbling and spilling profiles discussed in this thesis. In particular, the idea that different types of profiles are investigated in turn, to attempt to form a profile to sustain the required headlift, is central to understanding the high-level logic of the simulation. It is also important to appreciate that within each profile explored, the whole range of heads it is able to generate is investigated, starting with the lowest head available, to find a suitable profile.

Once the parameters of the coil pump and its environment have been entered and variables to be used in the simulation have been initialised, the process of finding a suitable profile is begun.

The selection of the order of profiles to be

explored is important to the logic of simulation. The approach taken, is to assume that the helix is initially pumping without a headlift, so as to fill the coils with air and water plugs. The headlift is then increased to the required value and each profile is investigated in turn until a satisfactory one is found, or it is determined that the helix cannot sustain the head required. The determination of the order in which the profiles are tried depends upon the range of heads it is considered to be able to lift. The non-bubbling non-spilling profile is tried first as this supports only a very low range of headlifts compared to the other profiles.

If the non-bubbling, non-spilling profile cannot support the required head then a profile pumping to a medium range of headlifts is investigated. If the pump is below 50 percent depth of immersion, then the bubbling, non-spilling profile is investigated to discover whether it can provide a suitable profile. Conversely, if the depth of immersion is above 50 percent, then the non-bubbling, spilling profile will be examined.

If one of the profiles generating a medium range of headlifts cannot cope with the required headlift, the bubbling, spilling profile will be investigated in an attempt to produce a high headlift.

Whichever profile has been found to be suitable, is displayed in either graphical or tabular form.

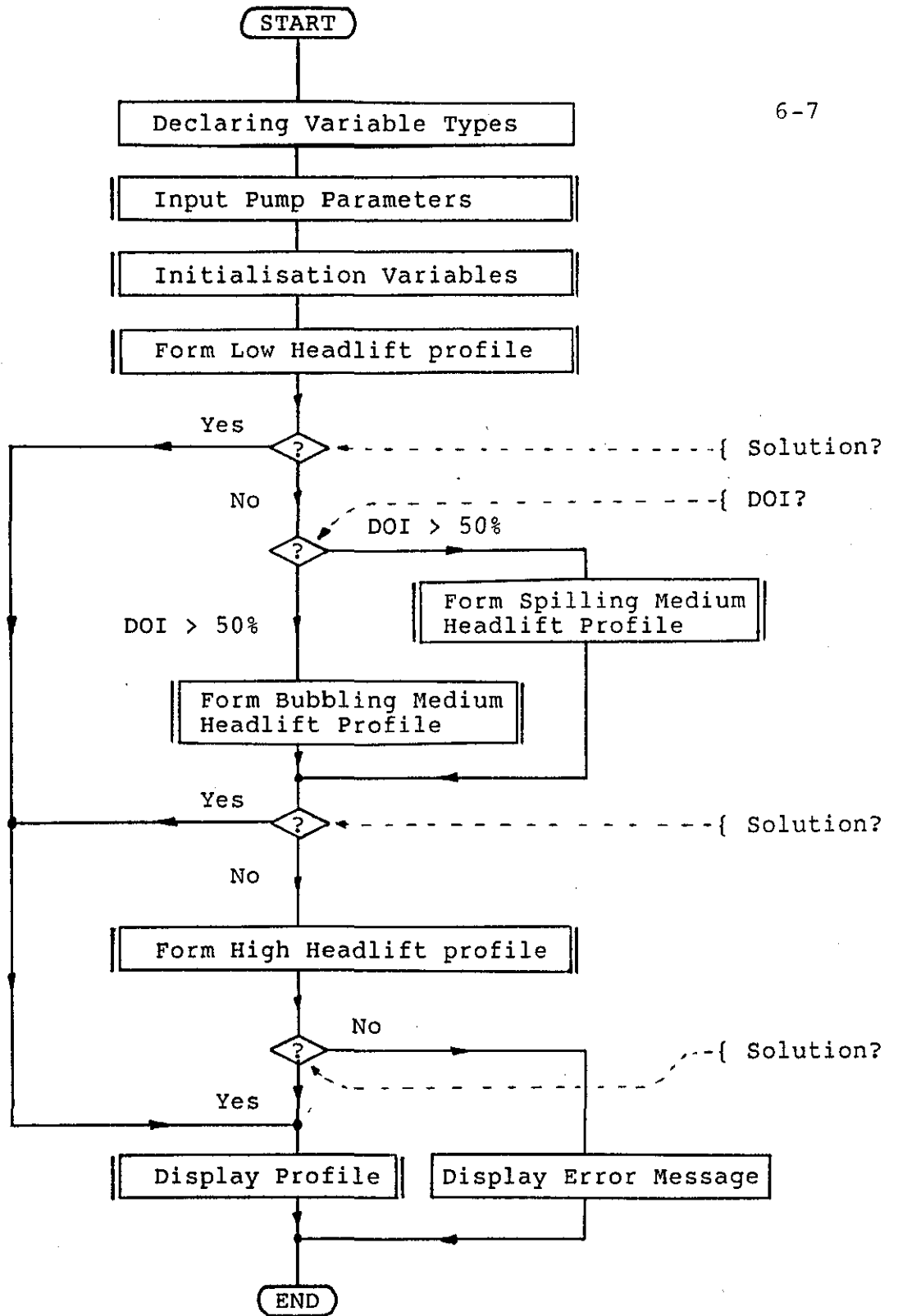


FIGURE 6.1, Control Procedures Flowchart

6.3 FUNCTIONAL DESCRIPTION OF THE PROCEDURES

The following sections provide a functional description of the procedures in the simulation.

6.3.1 Control Procedure

This procedure controls the flow of logic throughout the program as discussed in section 6.2. A flowchart of the logic can be seen in figure 6.1. After declaring variable types, the input procedure (section 6.3.2) is called to allow the user to enter the required parameters. Once the initialisation procedure (section 6.3.3) has been called to calculate useful variables, a number of other procedures are called until an appropriate profile has been found.

Each procedure represents a profile for either low, medium or high head lifting, for either above or below 50 percent depth of immersion. These are called in turn, starting with the low head lifting procedure (section 6.3.4). If this procedure cannot provide a suitable profile then another one is called to produce a medium head lift profile (section 6.3.5 or 6.3.6). As before, if this procedure cannot provide a suitable profile then yet another (6.3.7) is called to provide a high head lift profile. If a suitable profile can be found it is displayed, otherwise a message is displayed to say that the helix cannot pump to the required head lift in the current environment.

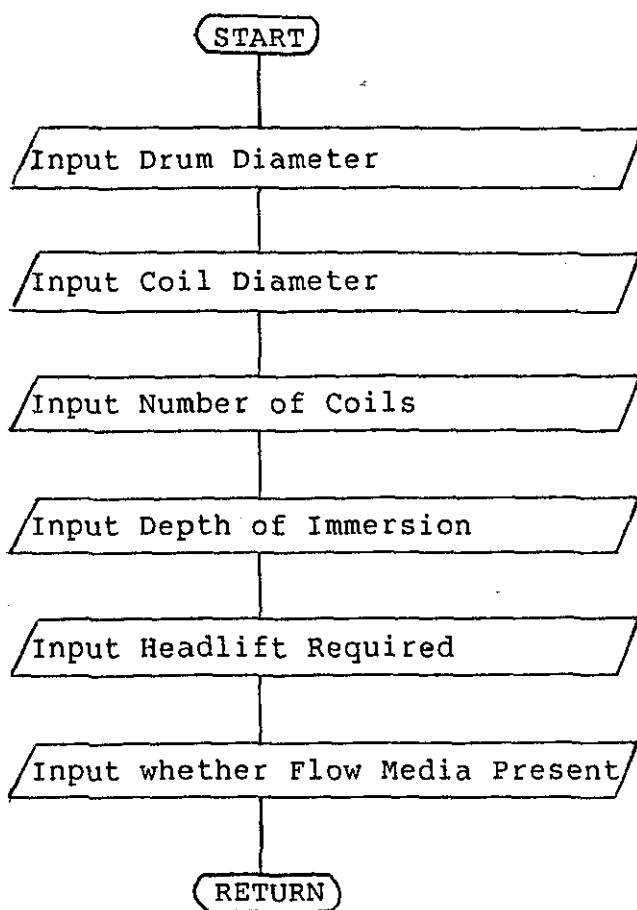


FIGURE 6.2, The input Procedure Flowchart

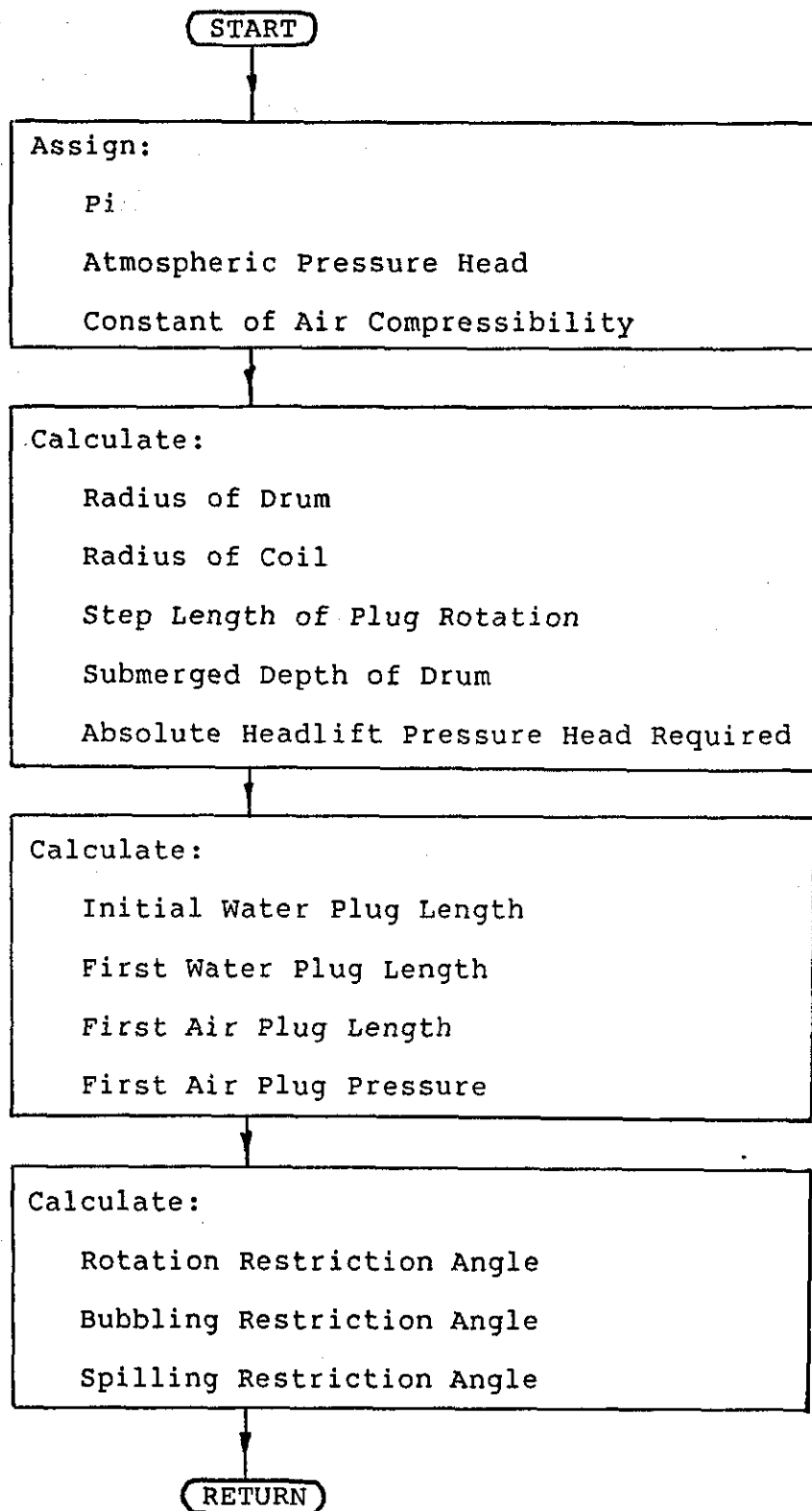


FIGURE 6.3, Initialisation Procedure Flowchart

6.3.2 The Input Procedure

To adequately describe the situation, the variables entered must reflect the dimensions of the pump and its environment. A flowchart of the logic can be seen in Figure 6.2. The variables considered to be important for the simulation described in this chapter are:

1. The diameter of the drum,
2. The diameter of the coils,
3. The number of coils,
4. The depth of immersion,
5. The head lift,
6. Whether flow media is present.

6.3.3 Initialisation Procedure

This procedure uses the parameters described in the previous section to initialise constants and calculates variables to be used in the following procedures. A flowchart of the logic can be seen in figure 6.3.

Firstly, the constant 'pi' is assigned together with the mean atmospheric pressure (equivalent to a pressure head of 10.182 metres of water), and the reciprocal of the compressibility of air (refer to Equation 5.3). The radii of the drum and coils are then calculated from their diameters.

The variable which controls the step length of rotation for the first coil is set to a value optimised

to allow a small increase in head generated by the pump to be calculated (in sections 6.3.4, 6.3.5 and 6.3.6), while keeping the number of iterations to a minimum. The depth to which the drum is submerged is converted from a percentage of the drum diameter to the submerged depth of the drum. The absolute head to which the helix is required to pump is calculated from the product of the atmospheric head and the required headlift.

The angle at the centre of the drum the initial water plug subtends is calculated from equation 5.8. This value is also used later to determine the initial air plug lengths. The first water and air plug lengths are calculated for later use. The absolute pressure head experienced at the inlet to the helix is substituted into the first position of the array storing the cumulative absolute pressure heads generated by the water plugs.

The angle from the vertical to which the leading or trailing edge of a water plug must reach, for it to be on the point of either bubbling or spilling respectively, is calculated from Equation 5.11. This value is used to determine the angles through which a water plug must rotate before it spills or it is bubbled through.

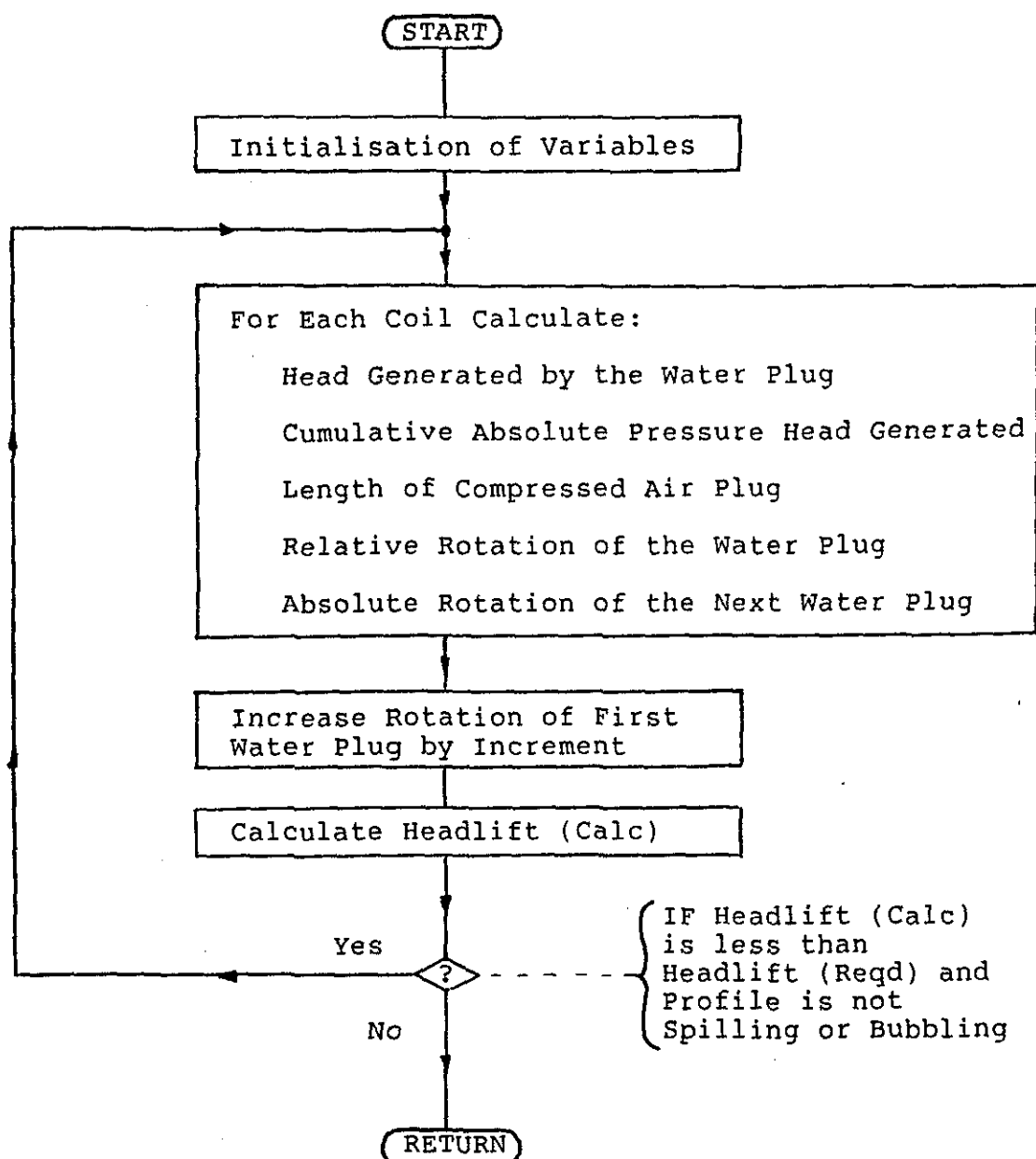


FIGURE 6.4, Non-Bubbling, Non-Spilling Procedure

6.3.4 Non-Bubbling, Non-Spilling Procedure

This procedure uses the theories described in section 5.2.1 to calculate the head difference profile for a helix that is neither bubbling or spilling. A typical head difference profile of this type can be seen in figure 5.6. A flowchart of the logic can be seen in figure 6.4.

After the initialisation of the relevant variables, control is passed to a loop. The looping continues until either a profile capable of pumping to the required head is found, or this profile has been invalidated. The validity of the profile depends upon whether the rotation of the last water plug causes it to bubble or spill. If either of these two phenomena occur, then other types of profiles are investigated.

The control loop surrounds the logic to create the characteristic profile of the exponential rise of head differences along the helix. For each coil in turn, the head generated by the left and right hand sides of the current water plug is calculated (Equation 5.7). The velocity of the current water plug is calculated (Equation (5.26)) and this is used to calculate the resistive head (Equation (5.25)) due to the inclusion of flow media, if present. The product of these three heads is stored and also added to the cumulative head of the previous coils to calculate the total head generated by the profile up to the current coil (Equation 5.6).

The length of the current air plug is calculated (Equation 5.2) from the first one, and by comparing the absolute pressures of this and the first air plug. The reduction in length between this and the previous air plug is calculated (Equation 5.3) to find the rotation achieved by the current water plug (Equation 5.4) relative to the previous water plug. The total rotation of the next water plug is found from the summation of all the incremental rotations (Equation 5.9) up to the current coil. This is important as it is used to determine the head generated by the next water plug. It is also important in deciding whether the next coil is spilling or bubbling and as such, controls whether the profile is suitable for the required head.

Once the total headlift generated by the helix has been calculated the execution is passed back to the control loop. At this point, a decision is made on whether to continue looping, or to return to the main control procedure. If looping again it will do so with a slightly increased rotation of the first water plug. This will induce the next profile to provide a larger required headlift for the control loop to examine again. Control is eventually passed back to the control procedure when either a suitable profile has been found or it has been proved that this profile is unsuitable for the required headlift.

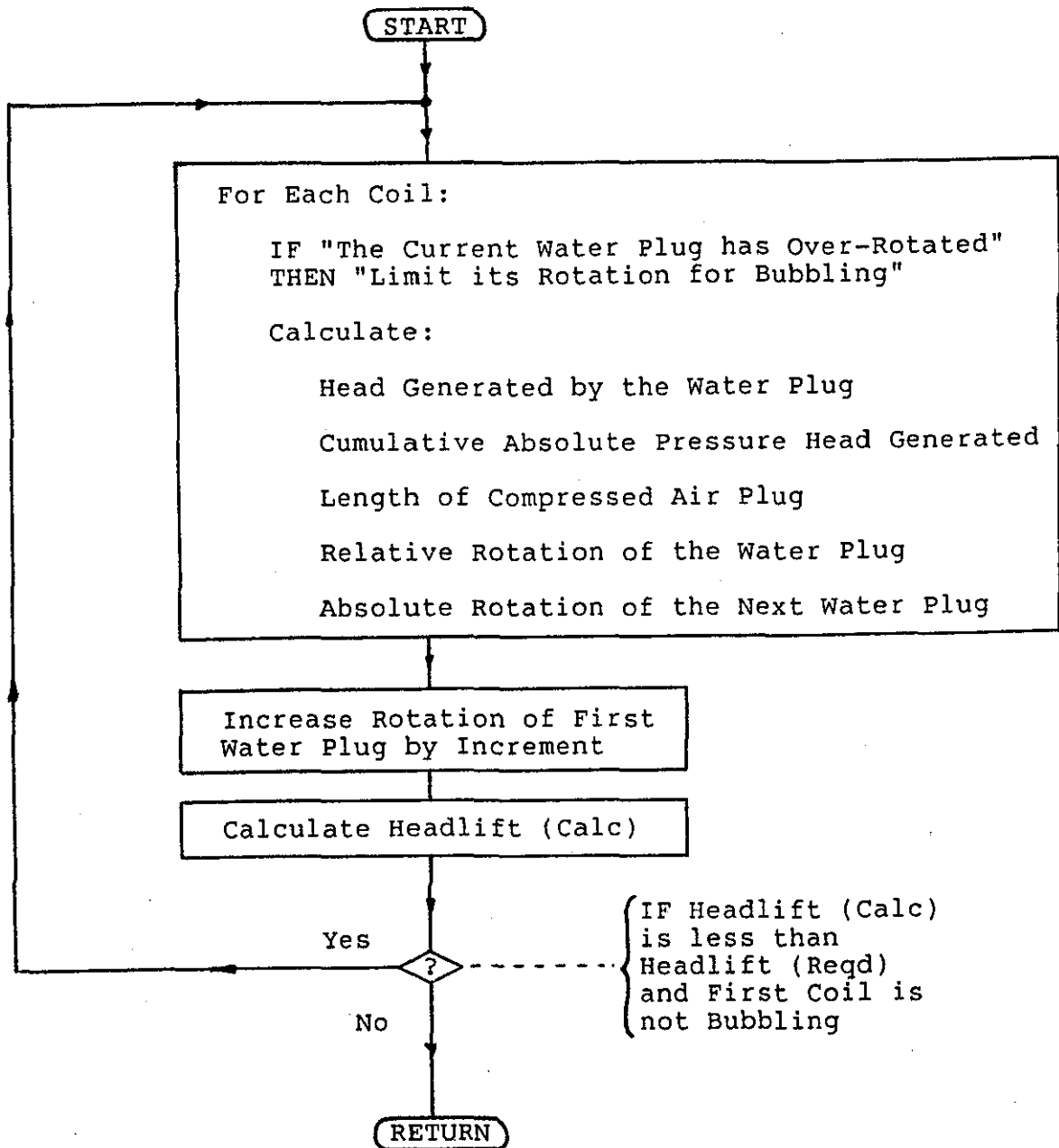


FIGURE 6.5, Bubbling, Non-Spilling Procedure Flowchart

6.3.5 Bubbling, Non-Spilling Procedure

This procedure uses the theories described in section 5.2.2 to calculate the head difference profile for a helix that is bubbling but not spilling. A typical head difference profile of this type can be seen in figure 5.7. A flowchart of the logic can be seen in figure 6.5. The total headlift generated by this profile is considered to be mid-range in comparison to the maximum headlift achievable. This procedure is called from the control procedure immediately after the previous procedure if it has been found that this has not been able to provide a suitable profile.

This procedure is similar to one discussed in the previous section in terms of the control loop surrounding the head difference profile logic. However there are modifications to reflect the differences in profile of the two situations. To avoid repetition, only the differences in the two procedures will be discussed here.

There is no initialisation of variables in this procedure as the values generated from the previous procedure are still valid. This is due to the profile being similar, differing only in the addition of a plateau towards the outlet of the helix.

The control loop differs from the previous procedure in the logic that decides whether or not to exit the loop. The exit conditions are dependent upon

whether a profile calculated can provide the required head without the first water plug starting to bubble. If the first coil rotates to the extent that it starts to bubble it will invalidate the profile under investigation. This is because the bubbling will depress the leading edge of the water plug causing its length to decrease. This reduces its capacity to sustain its head difference, and the discharge of the helix.

As there is a limit to which any bubbling-only water plug can generate a head difference, this has to be taken into account when forming a head difference profile. If any water plug is judged to be bubbling, then its rotation is restricted to the maximum possible, as calculated in the initialisation procedure. The restriction of the rotations causes the characteristic head difference plateau towards the outlet end of the helix, as shown in Figure 5.7.

The differences described above enable the simulation of a bubbling helix pumping to the mid-range of its ability relative to the maximum head lift capabilities.

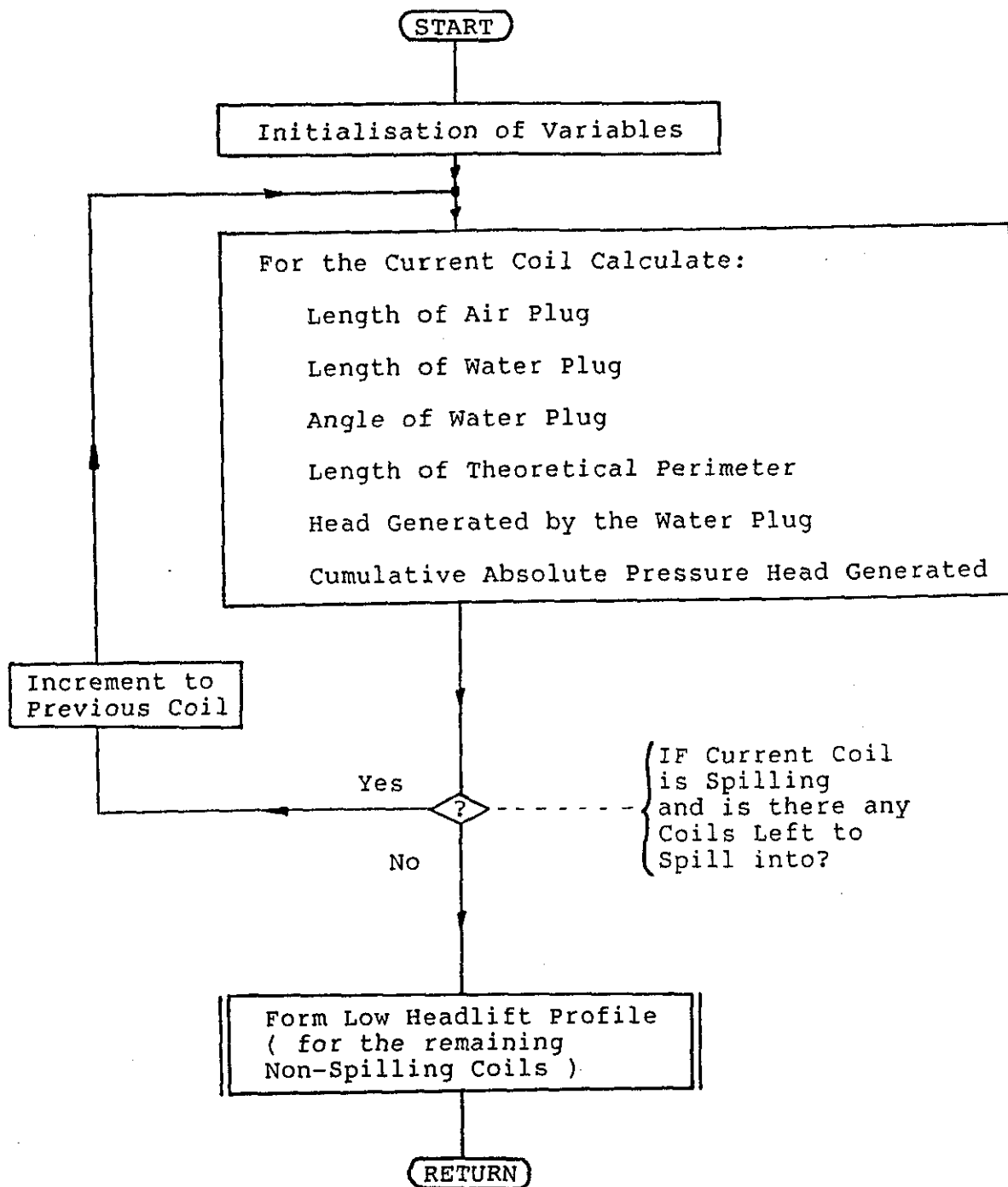


FIGURE 6.6, Non-Bubbling, Spilling Flowchart

6.3.6 Non-Bubbling, Spilling Procedure

This procedure uses the theories described in section 5.3.2 to calculate the head difference profile for a helix that is spilling but not bubbling. A typical head difference profile of this type can be seen in Figure 5.12. A flowchart of the logic can be seen in figure 6.6. The total headlift that can be generated by this profile is considered to be mid-range in comparison to the maximum headlift achievable. This procedure is called from the control procedure immediately after the "non-bubbling, non-spilling" procedure, if it has been found that this has not been able to provide a suitable profile.

The functionality of this procedure is split into two major sections to reflect the two distinct parts of the profile. The following description reflects the execution of this procedure.

The progression of the logic starts with the calculations generating the spilling part of the profile from the outlet backwards. This continues until either the end of the spilling part of the profile has been found, or the calculations determine that the whole helix is spilling. If the latter is true, it indicates that this profile is unsuitable to sustain the required head. If some of the coils are not spilling, then the "non-bubbling, non-spilling" procedure described in section 6.3.4 is called. This calculates the first part

of the profile for the remaining coils towards the inlet of the helix. This procedure generates a profile from the head difference between the inlet and start of the spilling profile. The logic is executed in this way as the required head at the outlet is known, unlike the rotation of the first water plug. This makes it possible to calculate the spilling profile from the reduced lengths of the air plugs under pressure.

The execution of the first part of this procedure proceeds with the initialisation of variables pertaining to this procedure. As the first part of the procedure calculates the spilling profile of the helix from the outlet backward, then the total head of the last coil is initialised to the head required. The variable holding the current coil number is assigned to the last coil, and the test perimeter variable is assigned to zero to conform to the logic of the following control loop.

The execution continues by forming the spilling profile. This is similar to the previous ones in terms of consisting of a control loop surrounding the head difference profile logic. The spilling profile will be calculated until either the inlet is reached, or the coil currently being investigated is found not to be spilling. For each coil, the calculations (Equation 5.3) involve finding the length of the current air plug. The theoretical water plug length is calculated by subtracting the air plug length from the perimeter of the coil. The angle this water plug subtends at the

centre of the helix is calculated by dividing the length of the water plug by the radius of the drum.

The test perimeter variable is assigned. This variable describes the length of the compressed air plug length combined with the length of the first water plug. This variable is used by the control loop logic to decide whether the current coil is spilling by comparing the test variable with the actual perimeter of the current water and air plug.

The head generated by the left and right hand sides of the water plug is calculated from Equation 5.19. The velocity of the current water plug is calculated (equation (5.28)) and this is used to calculate the resistive head (equation 5.25)) due to the inclusion of flow media, if present. The product of these three is subtracted from the cumulative head of the following coils to calculate the total head generated by the profile up to the current coil (Equation 5.6). The variable holding the current coil number is decremented so that the next coil to be investigated is the next one in the direction of the inlet.

The control loop tests whether the test perimeter variable is longer than the actual coil perimeter calculated from the current water and air plugs. If this identity is true, it implies the current coil is too short to support both the air and water plugs at this pressure without the water plug spilling. This situation indicates that the coil is contributing to the

spilling profile and so the control loop will step to the next coil for further investigation.

Once the first part of the procedure has formed the spilling profile, the execution of the logic exits from the control loop, proceeding to the second part of the procedure which calculates the non-bubbling, non-spilling part of the profile. It does this by calling the "non-bubbling, non-spilling" procedure which is described in section 6.3.4. This procedure has been designed to develop a profile for the whole helix, for the total head required. Therefore the relevant variables have to be temporarily reassigned to reflect the current objective. This consists of developing a profile for the remaining pressure head, not supported by the spilling part of the profile. Control is passed back to the control procedure to display the total profile in either graphical or tabular form.

If the control loop determines that the whole of the helix is spilling, then the helix is generating its maximum headlift with the current type of profile. If the maximum headlift generated by the profile does not compare to that required, then control is passed back to the control procedure to allow another profile to be investigated.

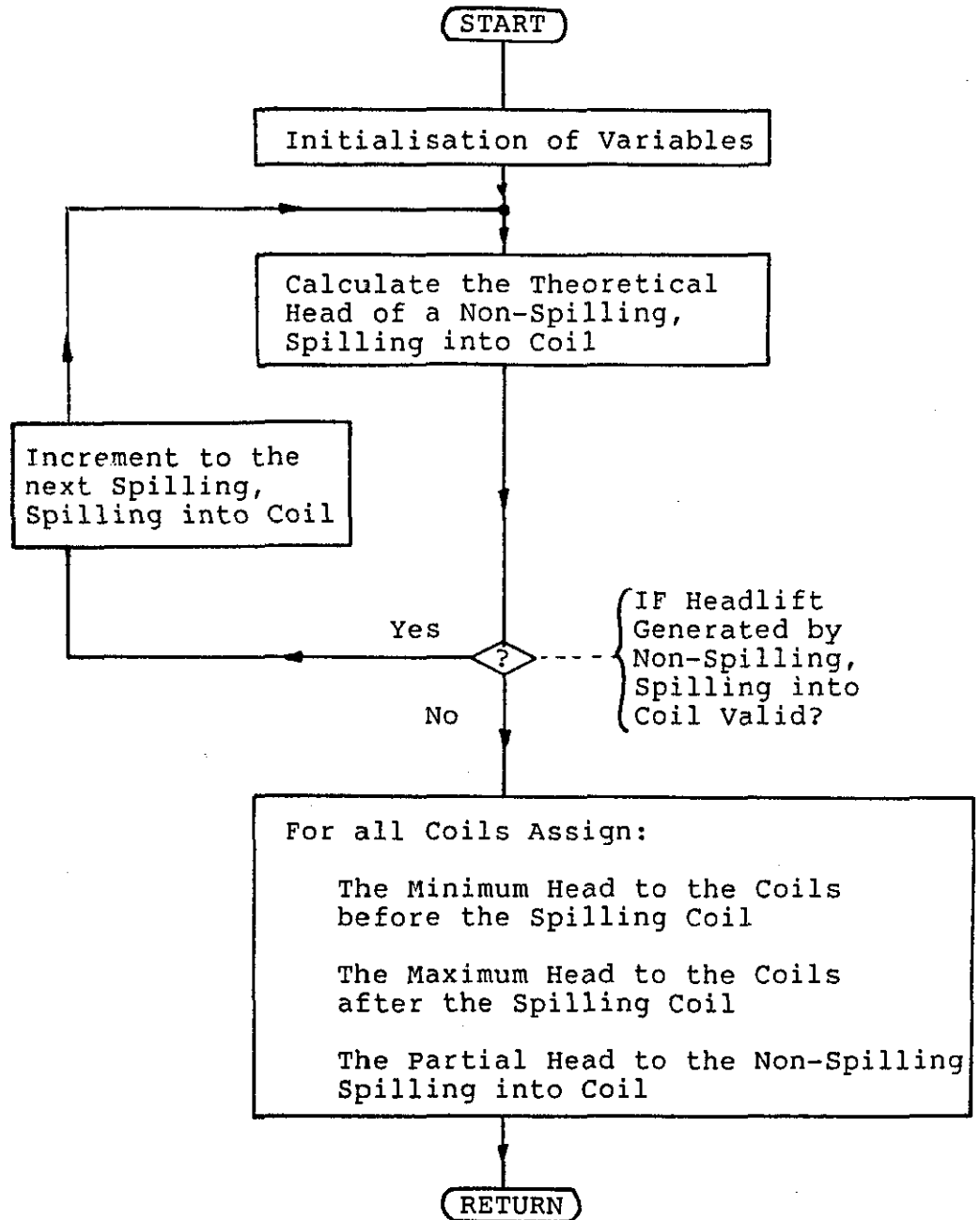


FIGURE 6.7, Bubbling, Spilling Procedure Flowchart

6.3.7 Bubbling, Spilling Procedure

This procedure uses the theories described in section 5.2.3 to calculate the head difference profile of a helix that is both bubbling and spilling. A typical head difference profile of this type can be seen in Figure 5.9. A flowchart of the logic can be seen in Figure 6.7. The total headlift that can potentially be generated by this profile is considered to be at the high end of the range in comparison to the maximum headlift achievable. This procedure is called from the control procedure immediately after the previous procedure, if it has been found that it has not been able to provide a suitable profile.

The functionality of the procedure is dissimilar to any of the other procedures in this simulation as the profile this generates is completely different to the others. The profile consists of a lower plateau of bubbling-only coil head differences (Equation 5.12), and a higher plateau of bubbling and spilling coil head differences (Equation 5.13). These are separated by a single coil which can have a head difference anywhere between these two plateaus. It represents a coil which is bubbling and being spilt in to, but which is not spilling itself.

Various variables pertinent to this procedure are first calculated. The minimum head difference a bubbling only water plug can sustain is calculated from

equation (5.12), and the maximum head difference a bubbling and spilling water plug can sustain is calculated from equation (5.13). The velocities of these two types of plugs are calculated from equations (5.27) and (5.28), and from these, the resistive flow media heads are calculated using equation (5.25).

The execution of the logic continues with a control loop, inside of which, is the logic to determine how many coils belong to which plateau, and head generated by the intermediate coil. If a profile can be found to develop the required head lift, then the appropriate head difference is applied to each of the coils. Control of the execution of the program is finally passed back to the control procedure for the profile to be eventually displayed in a tabular or graphical manner.

The control loop logic controls whether to exit the loop. The logic will allow the execution of the loop to terminate if the head generated by the intermediate coil is physically possible by being between the maximum and minimum coil plateaus (Equation 5.18).

The logic inside the control loop consists of decrementing (from the outlet to the inlet) the variable labelling the current intermediate coil, and then executing the calculation (Equations 5.17) to find the head generated by the intermediate coil. As the loop repeats, the head generated by the intermediate coil will descend from being physically impossibly high, to one which can be supported within the dimensions of the

helix (Equation 5.18). The validity of the profile is found by examining the variable labelled as the current intermediate coil. If this variable has become negative, then as it is impossible to have a negative number of bubbling only coils, this indicates the coil cannot sustain the required head in the current environment. Control is finally passed back to the control procedure to allow the profile to be displayed in a graphical or tabular fashion.

Coil Number	Head Generated (metres)
1	0.009
2	0.012
3	0.019
4	0.032
5	0.055
6	0.096
7	0.167
8	0.287
9	0.477
10	0.738

Values of Parameters Used to Generate the above Table

Coil Parameters	Associated Values
Coil Diameter	1.000 metres
Pipe Diameter	0.050 metres
Number of Coils	10
Depth of Immersion	30 percent
Rotational Speed	1 RPM
Head Required	1.500 metres

FIGURE 6.8, Non-Bubbling, Non-Spilling Tabular Output

Coil Number	Head Generated (metres)
1	0.086
2	0.113
3	0.173
4	0.281
5	0.455
6	0.694
7	0.840
8	0.840
9	0.840
10	0.840

Values of Parameters Used to Generate the above Table

Coil Parameters	Associated Values
Coil Diameter	1.000 metres
Pipe Diameter	0.050 metres
Number of Coils	10
Depth of Immersion	30 percent
Rotational Speed	1 RPM
Head Required	5.000 metres

FIGURE 6.9, Bubbling, Non-Spilling Tabular Output

Coil	Head
	(metres)
1	0.098
2	0.124
3	0.181
4	0.280
5	0.851
6	0.791
7	0.736
8	0.688
9	0.645
10	0.606

Values of Parameters Used to Generate the above Table

Coil Parameters	Associated Values
Coil Diameter	1.000 metres
Pipe Diameter	0.050 metres
Number of Coils	10
Depth of Immersion	55 percent
Rotational Speed	1 RPM
Head Required	5.000 metres

FIGURE 6.10, Non-Bubbling, Spilling Tabular Output

Coil Number	Head Generated (metres)
1	0.100
2	0.100
3	0.100
4	0.100
5	0.100
6	0.500
7	1.000
8	1.000
9	1.000
10	1.000

Values of Parameters Used to Generate the above Table

Coil Parameters	Associated Values
Coil Diameter	1.000 metres
Pipe Diameter	0.050 metres
Number of Coils	10
Depth of Immersion	10 percent
Rotational Speed	1 RPM
Head Required	5.000 metres

FIGURE 6.11, Bubbling, Spilling Tabular Output

6.4 DISPLAYING OUTPUTS OF PROGRAMS

6.4.1 Tabular Output

The tabular output of the simulation needs to have sufficient information for it to be compared to information collected visually for validation purposes. The information can also be used to investigate the effects certain parameters have on the helix. Examples of useful parameters are:

1. Coil number,
2. Water plug length,
3. Air plug length,
4. Mean water plug velocity through the coil,
5. Head generated by the right hand side of the coil,
6. Head generated by the left hand side of the coil,
7. Resistive pressure head,
8. Gross pressure head generated by the coil
(water level difference across the water plug),
9. Net pressure head generated by the coil
(gross minus the resistive pressure head),
10. The cumulative pressure head generated by this
and all the previous coils in the pump.

N.B. A number of examples of tabular outputs of simulations can be seen in figures 6.8 to 6.11.

6.4.2 Graphical Outputs

The graphical data consists of displaying the head difference profile in the two dimensions, along the horizontal axis for the coils and along the vertical for the head difference for each of the coils in relation to the diameter of the drum.

The graphical output is useful for the following reasons:

1. It gives the user of the simulation an appreciation of the internal actions of the helix that is not readily apparent when looking at the tabular output.
2. The type of the profile can be immediately identified when the data is in a graphical form.
3. When demonstrating how the pump works, it is easier to do so when the explanation is accompanied by a diagram.

The internal logic of this procedure will not be described here as this will be dependant upon the computer, its language and its graphics capabilities.

FIGURE 6.12, First Validating Experiment Output

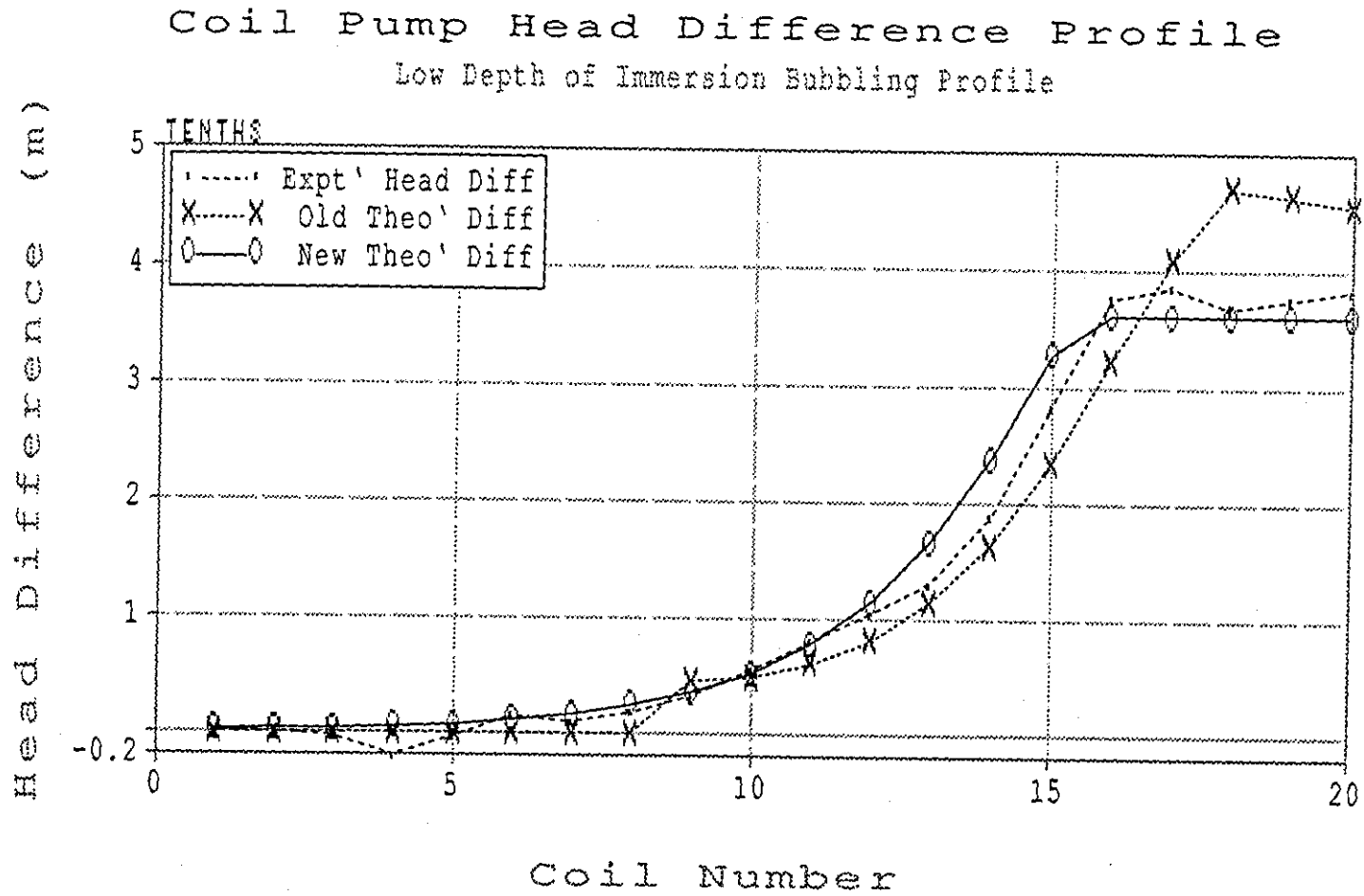
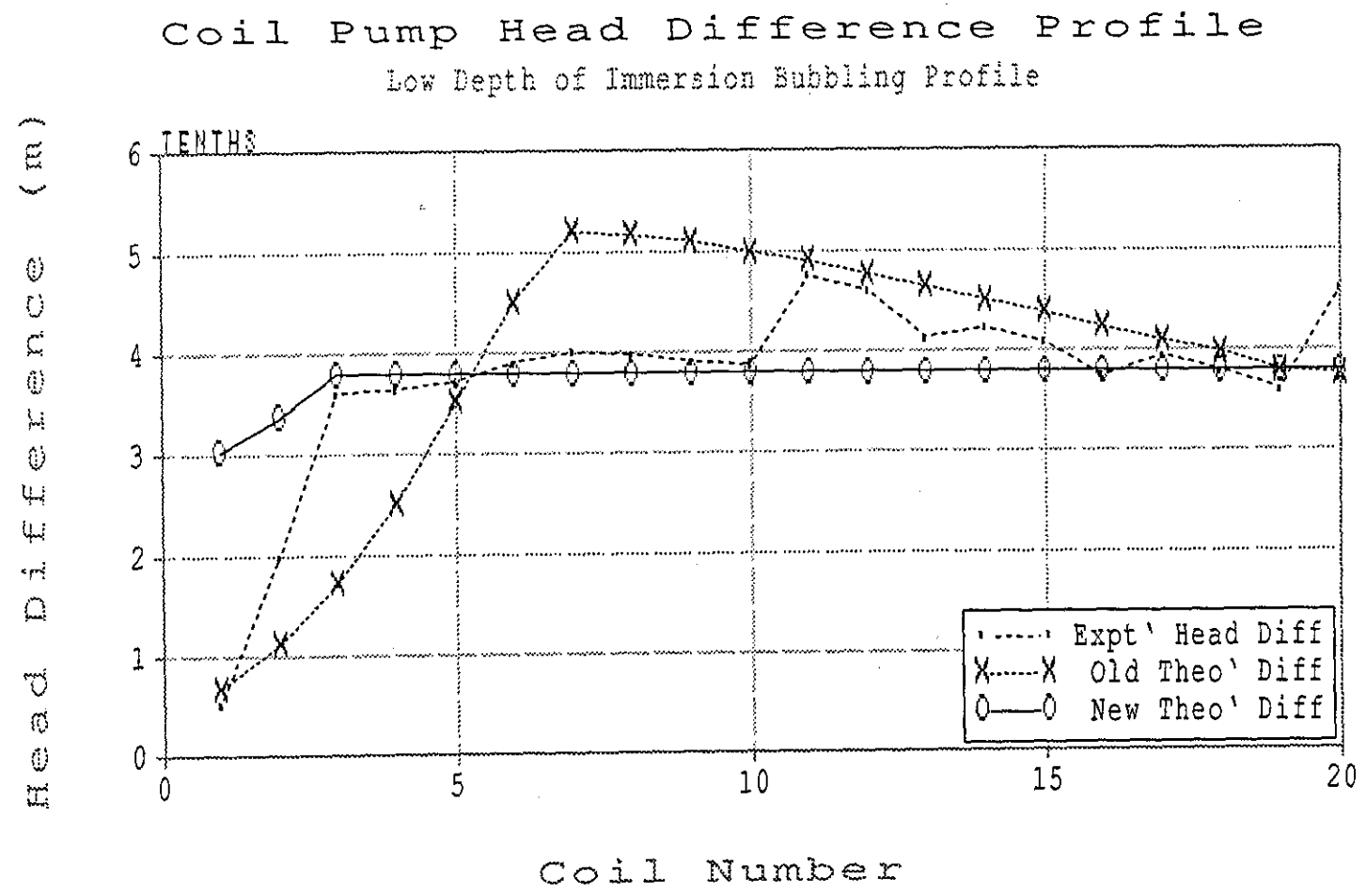


FIGURE 6.13, Second Validating Experiment Output



6.5 VALIDATING THE THEORETICAL PROFILES GENERATED

The bubbleback theories described in Chapter 5 have been observed and developed by the research connected with this thesis. Until quantitatively proven these theories will remain hypotheses. The objective of this section is to demonstrate the theory's ability to produce theoretical head difference profiles that reflect ones experimentally measured.

Annable (Ref. 7, page 84) realised the experiments he performed on the coil pump at low depths of immersion exhibited 'mechanisms of operations' previously unexplained. He actually observed (Ref. 7, page 79) air bubbling through the water plugs but did not expand the observations of this phenomenon into the theories described in this thesis. It is a selection of these experiments that have been chosen to compare the experimental head difference profiles to the theoretical, as predicted by the simulation.

6.5.1 The First Validating Experiment

Figure 6.12 shows a graph of the head difference generated by one of the experiments performed by Annable (Ref.7, page 42). There are three profile exhibited the experimental profile as recorded on the apparatus, the theoretical profile as generated by Annable simulation, and the theoretical profile as generated by this simulation.

The experiment has been performed upon a 0.487 metre diameter coil pump with a bore of the coils equal to 25

millimetres, lifting water to a height of 4 metres. the depth of immersion the pump is under is at 30 percent and it is rotating at 12 revolutions per minute. The complication of applying this simulation to the experiment is that a delivery pipe has been attached to the outlet of the helix. This simulation ignores the phenomena of allowing the air plugs to remain intact as they rise through the delivery pipe, thus increasing the height to which the pump can lift its discharge. To overcome this difficulty, the actual head differences exhibited by the water plugs inside the apparatus have been added together to produce the experimental pressure experienced at the outlet of the helix. It is this pressure head which has been used in the simulation to produce the profile shown in figure 6.12.

It can be seen from the graph that the simulation described in this thesis produces a profile significantly closer to the experimental compared to Annable simulation. The description of this profile is one which is just starting to bubbleback without spillback.

6.5.2 The Second Validating Experiment

Figure 6.13 shows the graph of another experiment performed by Annable (Ref.7, page 44) upon the same apparatus under the same conditions except that the helix is now lifting water to 10 metres. The same approach has been made to compensate for the delivery pipe in the experiment.

It can be seen from the graph that simulation described in this thesis produces a profile which is dramatically closer to the experiment compared to Annable. This profile can be described as one where most of the air plugs are bubbling back while none of the water plugs is spilling back.

6.5.3 CONCLUSION

The above two comparisons show that the phenomena of bubbleback can be understood and predicted by the theories discussed in this thesis.

CHAPTER 7

THESIS REVIEW

This chapter contains the abbreviated details of the research that has been completed on the subject of coil pumps, and the conclusions drawn. There is also a survey of avenues of research which could be useful in understanding further the internal mechanisms of the coil pump.

7.1 PREVIOUS RESEARCH

The earliest reference to a coil pump has been found in the 'Cyclopedia of Arts & Science' (Ref. 1, Figure 1.1). It shows two versions of a coil pump, one in the shape of a spiral and another a helix. The former was investigated by Rudolf Ohlemutz (Ref. 2) who argued that the spiral version had a number of advantages over the helix in terms of space and discharge.

At Loughborough University, Bamforth (Ref. 3) resolved a number of relationships to relate the speed of rotation with the pressure generated for different depths of immersion and rates of flows. Winstanley (Ref. 4) on the other hand used a video to make comparisons between water level differences whilst the pump was in motion and at rest. Robinson (Ref. 5) concluded, in his research, that water plugs always adopt the same levels for a given pumping height, but it

was Annable (Ref. 6 & 16) who developed the relationships used to predict the head level difference profile. His research consisted of experiments (Figure 1.2) varying the parameters of the pump to measure the internal water levels. From the relationships he derived a computer simulation and a set of design charts, to predict the behaviour of a pump under any given situation. He also tested a water driven coil pump in a nearby stream.

At Salford University, A.T. Stuckey and E.M. Wilson (Ref.8) measured flow rate at different speeds of rotation and depths of immersion. By developing a lift ratio, they found it possible to predict the number of coils required for a particular pumping height. They also looked into alternative means of powering the pump by developing turbine blades to be powered by the flowing stream. Wilson (Ref.9) continued by establishing relationships for the above measurements and from these, developed a computer simulation. He concluded by recommending more research be done on verifying the theories and investigating the different properties of the pump.

Meanwhile, at Loughborough University, G.H. Mortimer made the fundamental discovery that the coil pump can be used to lift water from a lower level to the level of the pump (Figure 1.2). This mode of operation might be considered, when the installation of a coil pump is, at best, difficult at the lower level.

Following this, he turned his attention to the use of a coil pump to treat waste water as it is being pumped (Ref.17). The surface area can be dramatically increased by increasing the width of the coils and incorporating flow media (described in Section 2.1) inside. The inherently large surface area is used to grow bacteria which feeds on the waste water that passes through and around the helix during the pumping. The development of this application is the dominant reason for this thesis.

This outline of the work done by previous researchers has been included in order to:

1. Provide future researchers in this field with a basic starting point from which their work can commence.
2. Avoid duplication of effort.
3. Gain knowledge and experience in this field.
4. Determine a direction and purpose for research.

7.2 THE FLOW MEDIA RESISTANCE EXPERIMENT

One of the most important properties of the flow media when used to treat water (Ref.17) is its hydraulic resistance. It was therefore felt to be advantageous to investigate this.

A number of control experiments were completed to determine the accuracy of the apparatus. It also led to the experiment being fully understood, and ensured the consistency of results.

The main experiment (section 2.5) commenced with partially filling the pipe with its first increment of flow media. It was realised that the first increment, in contract with the downstream manometer tappings, could distort the results for this increment. The decision was therefore taken to subtract the resistance of this increment from the total resistance before the regression analysis commenced. After processing the results in this manner, it was shown that the resistance to flow of the remaining increments was approximately double the resistance of the first.

It was the realisation of the difficulties and therefore the approach to take which led to the success of the experiment in terms of accounting for the behaviour of apparatus had a major influence in determining the hydraulic resistance of the flow media.

7.3 INCREASING THE DISCHARGE EXPERIMENT

A problem found with coil pumps is that at depths of immersion approaching 50 percent the shaft, drive shaft and bearings are exposed to the corrosive properties of the liquid in which it sits. As this is a handicap to the operation of the pump, it was felt to be advantageous to investigate ways of increasing the pump's discharge without lowering the coil pump into the liquid any more than necessary. The resulting experiment is discussed in Chapter 3.

A standard helix was modified to include a "bucket-like" device on the inlet to scoop up excess water. A hole was also punched into the skin of the helix three quarters of a revolution from the inlet to allow excess air to escape. Data was collected with the coil pump rotating at different speeds and depths of immersion. On completion of processing the data, it was evident that the discharge did increase relative to an unmodified helix, although the accuracy of the calculations could not fully justify supporting the quantitative relationships obtained. The lesson gained from this experiment is that there should be more time given to the preparation of the experiment in terms of the quantity and spread of the measurements taken, to ensure the calculations are performed on a realistic and meaningful set of data.

7.4 THE MAIN POWER EXPERIMENT

The objective of this experiment (discussed in Chapter 4) is to relate the environment of the pump to its performance in terms of power absorbed.

The nature of the data collection is important when discussing this experiment. With the use of a BBC Micro-Computer, it is possible to measure and store various parameters of the pump very accurately throughout a revolution. It is this data which would have been used to develop precise relationships. Constraints in storing and accessing the immense amount of data for 168 experiments on a small microcomputer, meant that only a small subset of the data could be used (discussed in section 4.3). The consequence of this is that there is reduced accuracy of the relationships developed compared to what was originally envisaged.

The results processing rationale initially consists of determining the order of the parameters to be regressed against the absorbed power of the pump. The multi-stage stepwise regression leads to a relationship (4.12) which, when compared to the initial data, is found to reasonably predict the absorbed power of the coil pump. This equation is empirical in nature and therefore does not represent the relationship in a dimensional sense (Ref.15). More research needs to be completed on this equation to assess it's validity across a range of pumps. Once successful, it can be

used to confidently predict the performance of many pumps, over a wide range of situations.

A large bucket was built to increase the size of the inlet but never formally experimented upon. It was noticed that it caused the coil pump to become out of balance while rotating it in the tank empty of water. The addition of appropriate counter balance weights was addressed on a trial and error basis, aided by the micro-computer.

Program 3 in Appendix E is used to graphically display the power used to rotate the drum in relation to the orientation of the drum in polar co-ordinates. The closer the resulting shape is to a circle, the more balanced the drum, as this corresponds to a steady power input throughout a revolution. It is envisaged that the coil pump will have to be balanced during its actual use as effect of the water in the bucket cannot be realised until it is actually pumping.

7.5 THE THEORY

The theories relating to the coil pump have been developed and modified over an extensive period of time, as discussed in Chapter 1. Chapter 5 combines the theories found by previous research with those discussed in this thesis.

The theories revolve around the helix as the equivalent of a series of manometer loops, each holding an air plug and a water plug, rotated to produce a head difference. It is the summation of head differences that counteracts the back pressure imposed on the outlet to the helix. Complications arise when water plugs rotate to such an extent that they spill back into the following water plugs, or they are prevented from rotating further by air plugs bubbling through them. A final restriction is that when all the water plugs are being bubbled through, the only way a higher head can be sustained is for the coils to start spilling and bubbling. These restrictions are related to the helix environment in terms of whether the helix is above or below 50 percent depth of immersion. Bubbling is primarily a quality of a helix below 50 percent, and spilling is a quality of a helix above 50 percent.

The different profiles arising from these combinations of restrictions have associated ranges of achievable headlifts. When determining the relevant profile, the one with the lowest range of headlifts is

investigated first. If this fails to produce a suitable profile, then another type of profile, with the ability to sustain a higher range of headlifts is investigated. This continues until either a suitable profile is found, or it is determined that the helix cannot sustain the required headlift in the envisaged environment.

When the pump is used to treat waste water the hydraulic resistance of the flow media will reduce the helix's maximum achievable headlift. This is due to a portion of the total internal headlift having to be utilised to overcome the combined resistance of all the water plugs flowing through the flow media.

7.6 THE SIMULATION

The simulation as described in Chapter 6 fully embodies the theories discussed in Chapter 5, as well as discussing how to use them.

The simulation initially defines the variables to be used in the program and then the parameters describing the coil pump and its environment are entered. The parameters are processed into variables useful to the rest of the program. The process to find a profile suitable to sustain the required headlift is then started. Each profile is investigated in turn, starting with the non-bubbling, non-spilling profile. If this does not provide a suitable headlift then either the bubbling non-spilling, or a non-bubbling spilling profile is explored depending upon whether the depth of immersion is below or above 50 percent depth of immersion respectively. As before, if either of these two profiles cannot provide a suitable profile then the bubbling spilling profile is investigated to attempt to provide a profile. The successful profile is then displayed in a tabular and/or graphical manner.

7.7 SUGGESTED FUTURE DIRECTIONS OF RESEARCH

There is a significant amount of research remaining before the coil pump can be considered to be fully understood. The following sections discuss avenues of research that would be helpful in further understanding the internal actions of the pump.

7.7.1 Flow Media Properties

Understanding the properties of flow media is important for the coil pump to be successful in treating waste water. Below, is a list of areas which could be investigated to further the understanding of the flow media:

1. The investigation of different type flow media will be useful in determining optimum shapes and surface areas in relation to their resistive properties.
2. It may be found that when experimenting to find how efficiently flow media treats waste water, that (say) the bubbling-only coils are the only ones to efficiently treat wastes in comparison to the resistance to flow the coil generates. It would therefore be profitable to investigate the situation where only some of the coils are filled with media.

3. The partial fillment of flow media inside the coils may pose advantages offsetting the reduction in the surface area for treating waste water. This needs to be further investigated for the following reasons:
 - (i) The movement of flow media inside the coils may assist in self cleansing the pump, preventing blockages due to the excessive increases of growths.
 - (ii) The hydraulic resistance of the media may be significantly lower if the media is not packed as densely as a fully filled helix.
4. Filling the vertical outlet pipe with flow media would be of benefit to the treatment unit by increasing the surface area for waste water to be treated. As it would induce excessive resistances to flow, this situation needs to be investigated.
5. There may be limiting factors which need to be investigated which restrict the various parameters of the pump when treating waste water. This is because the waste water might have to be in contact with the biological surfaces for a certain amount of surface area and time before it is considered to be treated.
6. The inclusion of flow media in a coil pump will elongate the air and water plugs as the media

itself has a volume. This problem has not been investigated, nor has it been included in the simulation discussed in this thesis. It would further enhance the accuracy of the theory if the impact of the flow media on the problem is studied.

7.7.2 Sediment Deposit -----

When a coil pump is used to treat waste water, deposits build up on the flow media, generated by the bacteria. These eventually become detached and travel towards the outlet of the helix. Once in the splash chamber, it is possible that the sediment could completely block up the pump. This hypothesis has to be investigated, as it could potentially effect the performance of the unit.

7.7.3 The "Blow-Back" Phenomena -----

The phenomenon of "blow-back" is very important in the theory of small bore coil pumps when lifting to high heads. The experiment described in Chapter 4 has been performed on a wide bore coil pump where the phenomena of "bubble-back" was discovered. It is believed that these two phenomena are related, the difference lies in the ability of an air plug to bubble through a wide water plug, as apposed to pushing the whole of a thin water plug towards the inlet.

Developing a relationship to predict the transition between these two phenomena, in the same manner as Reynolds Number (Ref. 15), would be useful in understanding the theories of the helix. Experimentation on different sizes of pipe near their theoretical maximum headlift would therefore be profitable.

7.7.4 Increasing the Discharge of a Coil Pump -----

The continuation of research into increasing the discharge of a coil pump, as described in Chapter 3, is important to increase the understanding of the coil pump.

Different shaped, enlarged inlets could be investigated together with different numbers, sizes and positions of air escape holes. The subject of what, if any, head differences can be supported across the first coil needs attention. The resulting relationships and observations could be included in a more realistic simulation.

It has been noted that an enlarged inlet could induce the first water plug to elongate. This hypothesis needs to be investigated to quantify its effects upon the performance of the pump in general, and its discharge in particular.

When utilising the coil pump to treat waste water in conjunction with an enlarged inlet. The combined effects could become important. This needs to be

investigated, together with the concept of attaching thin bore pipes to the holes in the helix to extend the outlets towards the centreline of the pump. This modification could have the effect of reducing the amount of water escaping from these.

The balancing of a coil pump by the investigation of the application of counterweights with the use of the program described in section 7.4 could be useful in predicting the weight and positioning of the counterweights. This could be incorporated in the simulation as part of the design process.

7.7.5 Different Types of Spirals

Ohlemitz (Ref.2) argued that the spiral pump is more efficient than the helix version in terms of space. As this type of pump has not been studied as intensively as the helix, there could be gaps in the useful areas of knowledge to be explored.

7.7.6 High Head Lift Coil Pumping

The helix has to bubble as well as spill to maximise the head lift capacity of the helix while keeping the helix over 50 percent depth of immersion. This is unnatural for a helix in this situation because as the water plugs are longer than the air plugs, spilling will occur initially.

A way to force the water plugs near the outlet to

bubble, is to modify the splash chamber so that air is restricted or prevented from escaping out of the chamber. This could be achieved by lowering the holes in the vertical pipe inside the splash chamber. This allows the splash chamber to hold an air plug by lowering the water level in the chamber. By lowering the water level, the output pressure exerted on the outlet of the helix will increase. Increasing the outlet pressure will force the air plug in the chamber to bubble back into the helix, fundamentally altering the head difference profile. This modification will allow the helix to pump to higher heads than would otherwise be achievable.

The theories surrounding the hypothesis will have to be investigated to assess their validity. It could yield valuable information to increase the performance of the pump further than is currently possible.

7.7.7 The First and Last Water Plugs

It is realised that the first and last water plugs cannot achieve their theoretical headlift as assumed in the current simulation. This is because these two plugs do not contain their full volume over their entire first or last revolutions respectively. This has been discussed in section 6.1.3 as to the limitations of the validity of the current simulation, and the suggested ways of adjusting the simulation to give it a

conservative bias.

The full implications of how seriously the reduction of the head differences achievable by these two plugs has still to be realised. More experimentation in this area would be advantageous.

7.7.8 Investigate the Interface Between Different Coils -----

There is a general lack of understanding of what actually happens between the interfaces of the different sections of the profiles. It would be profitable to know the head difference achievable throughout a revolution for any coil, with the change in profile from the non-bubbling to bubbling coils, the bubbling to bubbling and spilling coils, and the non-spilling to spilling coils.

Close observations and measurements would be very helpful in determining relationships, although it is very difficult to do so, due to the nature of the apparatus. This is one of the areas that finite element analysis (discussed in section 7.8.2) could help by simulating the situation on a computer.

7.7.9 Investigating Power Efficiencies -----

By investigating the power consumption in terms of efficiencies instead of by power absorption, it might be possible to compare the different properties of many pumps in a more comprehensive manner, relative to this

thesis. The following efficiencies could be investigated to prove their value:

1. Hydraulic Efficiency. This is the efficiency of the pump without the mechanical losses taken into account.
2. Mechanical Efficiency. This is the losses due to the belt, drive-chain, gearbox, motor, etc.
3. Overall Efficiency. This is the product of the previous two efficiencies.

7.7.10 Investigating Air Plug Power Loss

Power is wasted in compressing the air plugs under pressure. This is converted into heat energy and by measuring the input and output temperature of two phase flow. It might be able to quantify this effect.

7.7.11 Investigating the Compressibility of Air Plugs

Equation (5.2) describes the degree to which the air plugs will compress under a given pressure. The factor '1.15' is one which might need to be validated, to check that this is realistic over a range of environments envisaged.

7.8 SUGGESTED FUTURE DIRECTIONS OF THE SIMULATION

The areas of research that remain outstanding reflect the area that the simulation could be improved. The following sections describe the areas that need to be addressed to improve the quality of the simulation and therefore the understanding of the pump.

7.8.1 Multi-Snapshot Programs

A simulation which would help to address the problems associated with the differing lengths of the first and last water plugs (discussed in section 7.7.7) is one which calculates the profile at certain points throughout the revolution. This has the advantage of allowing different lengths of water plugs, thus ensuring that the pump sustain the required headlift over an entire revolution. This approach needs to be investigated to determine its usefulness relative to the simulation described in this thesis, and the one described in the following section.

7.8.2 Finite Element Analysis

The theories of finite element analysis (Ref. 12) could be applied to the coil pump simulation. The main complications are that the helix is itself moving, and potentially the helix could be filled with flow media and, the fact that two-phase flow is passing through the

helix. The shape and size of the elements, and the size of the rotational increments of the helix are critical in determining the accuracy of the simulation. These factors also influence the amount and complexity of the computations involved, and could determine the applicability of this method to real time simulations.

The advantages of this method is that it is suitable for generating suitable data for graphical outputs. This method might be the only way to process and generate meaningful data for real-time applications.

7.8.3 Use as a Designers Tool

The use of a simulation as a design tool could be investigated to determine its potential. The facility to graphically output data would provide the designer with the relevant information to determine the internal actions of the pump. An approach which could be useful to a designer is the development of a three dimensional surface, discussed in section 7.8.3.2. This approach enables the designer to examine a number of situations by varying one of the parameters of the pump. Consequently, the influence that the parameters have over the pump can be investigated.

7.8.4 Graphics Capabilities

The importance of displaying the outputs to the simulation cannot be over-emphasised, if it is to be of

any value to a user, whether an instructor, a student, researcher or a designer. These different types of users might need different outputs and so the description of different types of output and their usefulness are discussed below.

7.8.4.1 Two Dimensional Profile Output

Typical two dimensional head difference profiles can be seen in Chapter 5. These display the coils along the horizontal axis and their associated head difference along the vertical axis. They give a lot of visual information, such as showing the type of profile the helix has taken in response to the head lift required.

For research, other profiles could be utilised to investigate (say) the water velocities, the resistive heads, or the cumulative head throughout the helix.

Designers could use this as a simple check to ascertain whether the helix is capable of pumping to the required head in the current environment. It might also be of use by indicating how each of the coils are performing, so that flow media might be selectively included (as discussed in section 7.7.1).

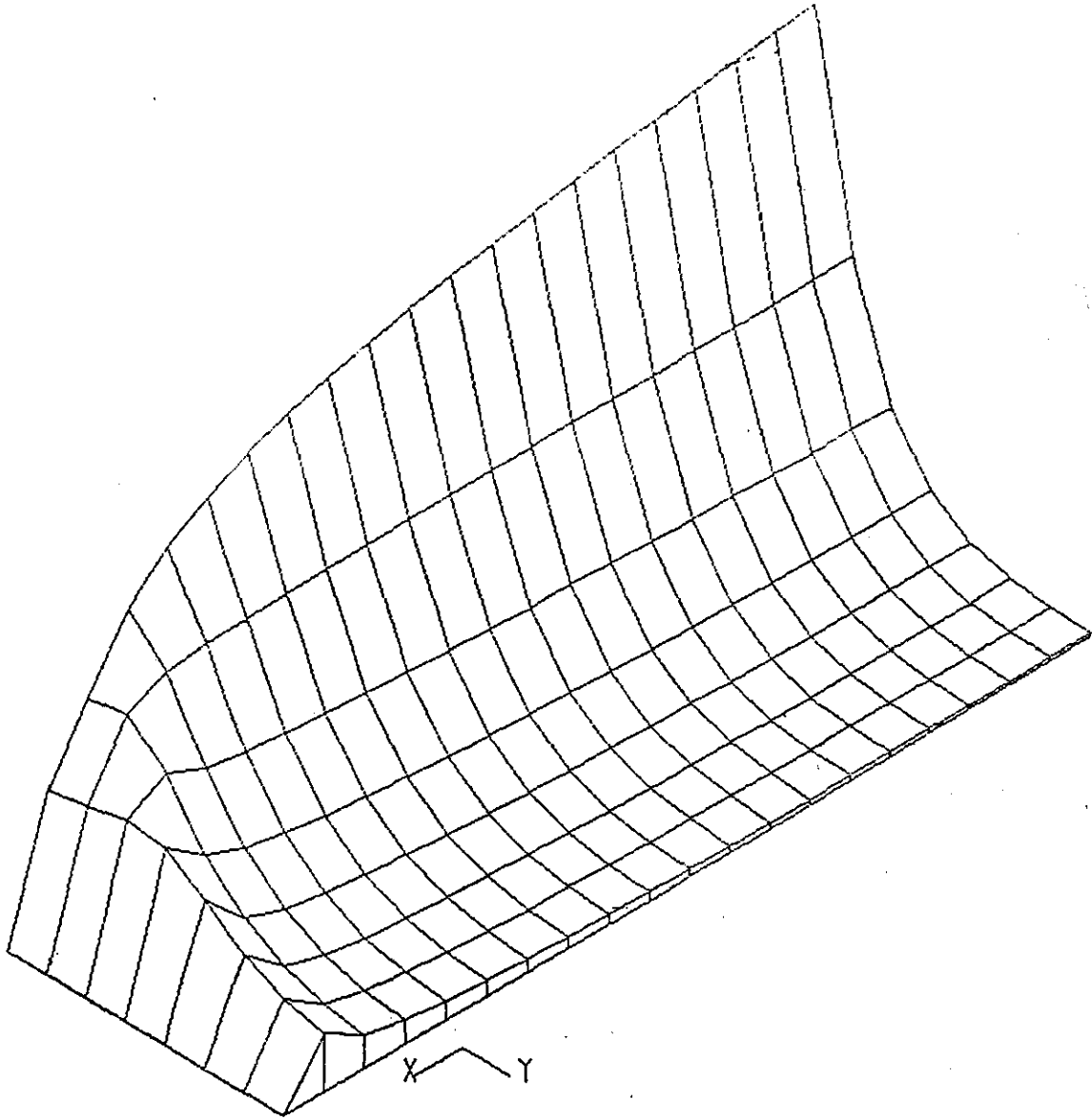


FIGURE 7.1, Example of an Isometric Surface Profile

(not drawn to scale)

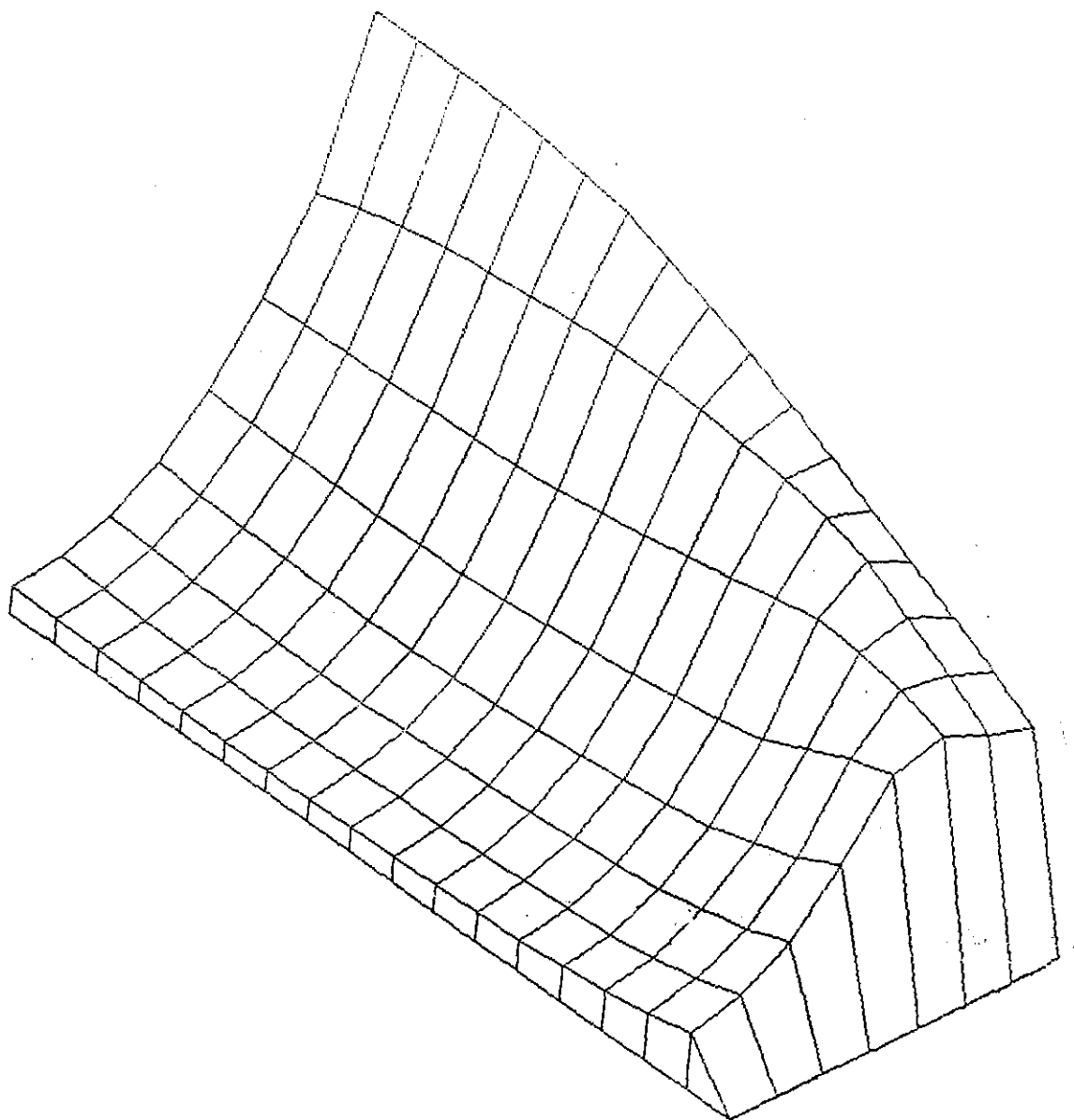


FIGURE 7.2, Example of an Isometric Surface Profile

(not drawn to scale)

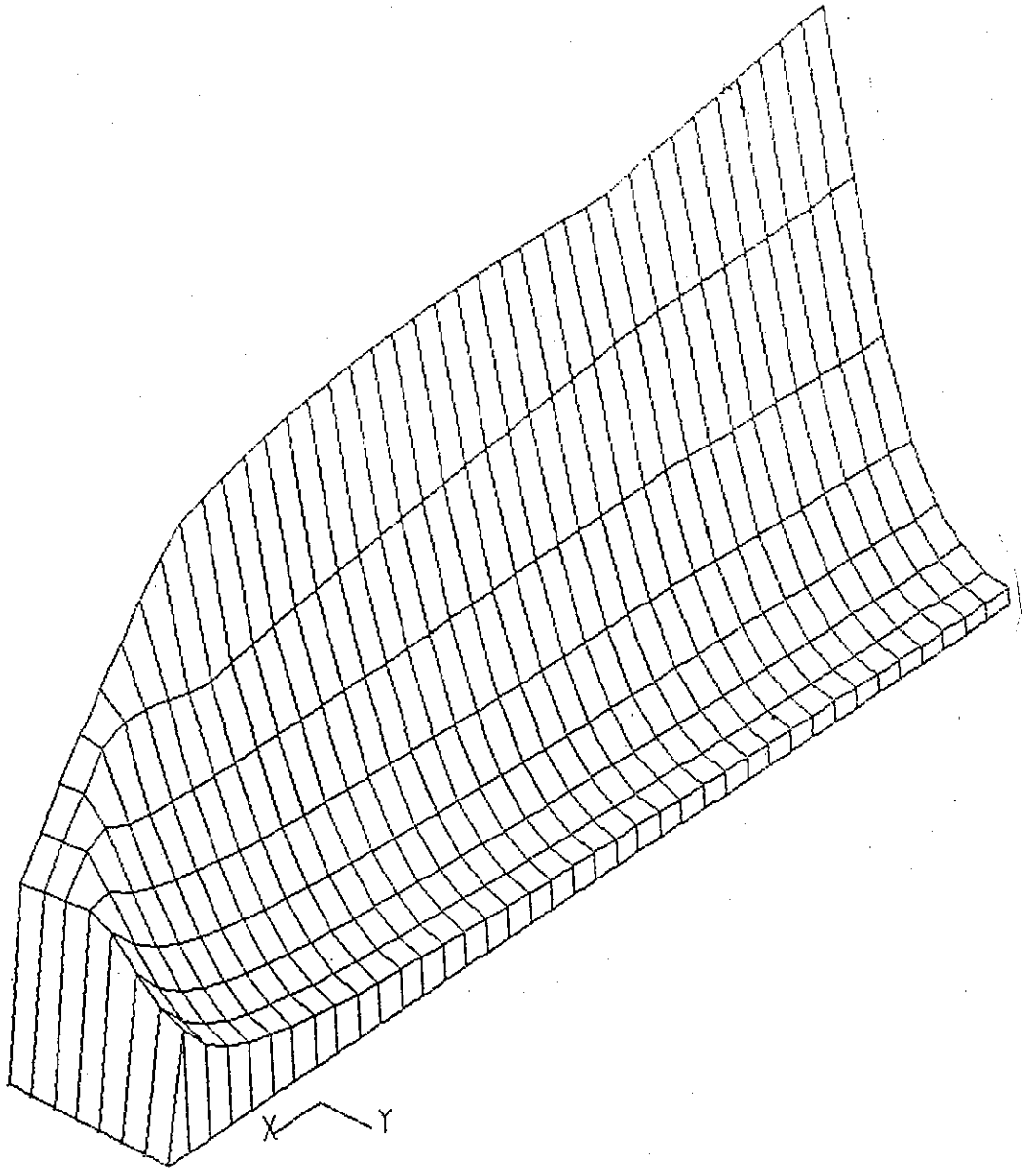


FIGURE 7.3, Example of an Isometric Surface Profile

(not drawn to scale)

To display the head difference profile of a helix could be advantageous in the instruction of the theories of the coil pump. This would help the visualisation of the internal actions of the helix, which is hard to appreciate when looking at the apparatus alone.

All the uses described above need to be investigated to assess the value of two dimensional profiles to describe the actions of the pump.

7.8.4.2 Three Dimensional Profile Outputs

The development of the three dimensional surface from two dimensional profiles is a natural progression. By allowing the user to enter a range of values and a step length, for one of the input parameters, a three dimensional surface can be generated in isometric projection from repeated simulations. A useful surface that can be generated is by varying the required headlift. This would produce a surface with the coil number, the varied parameter value and the head difference in the x, y and z directions drawn in isometric projection. Example surface profiles can be seen in Figures 7.1 to 7.3.

Three dimensional profiles have to be investigated for their value to different types of users in the same manner as the two dimensional profiles discussed in the previous section.

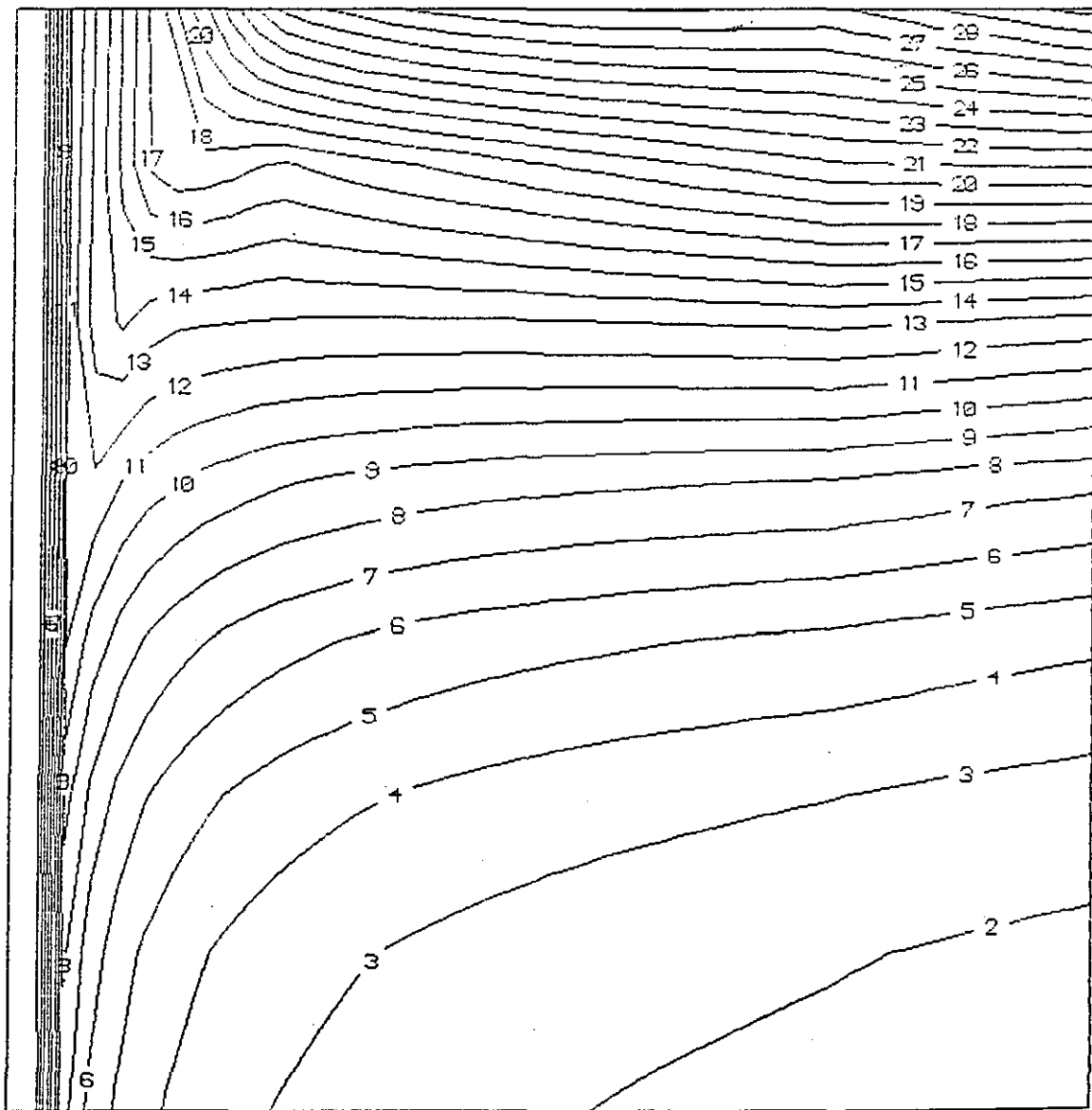


FIGURE 7.4, Example of a Contour Map Profile

(not drawn to scale)

7.8.4.3 Contour Map Output

The contour map profile (seen in figure 7.4) is very similar to the three dimensional profile described in the previous section in terms of the required input parameters. The difference is that it is drawn in plan view so that the user needs to appreciate that it is being looked at from a *plan* view.

The views of the three dimensional surface in isometric projection and plan view have to be investigated to provide a set of tools for the different types of users to understand and appreciate the knowledge on display.

7.8.4.4 Finite Element Analysis Output

To display the individual elements of the three dimensional finite element analysis is very difficult. It is complicated, not only by the realistic portrayal of a three dimensional situation by two dimensional means, but also by the fact that the helix itself is rotating. That is to say, it contains two phase flow, potentially travelling through mobile flow media, in maybe only some of the coils. Investigations on how this would be achieved will have to be addressed before finite element analysis can be considered to be the preferred simulation for analysing the coil pump.

7.9 EPILOGUE

The following factors have led to the success of the research connected with this Thesis:

1. It has been proved in Chapter 2 that there is a clear relationship between the headloss across, and the velocity of a liquid through, flow media.
2. By enlarging the inlet, it has been shown in Chapter 3, that the pump discharge is increased.
3. The power consumption for this pump can be quantitatively predicted by the equation derived from the experiment described in Chapter 4. When applying the relationship derived in Chapter 2 to this experiment, it successfully predicts the power lost due to the inclusion of the flow media inside the helix. This substantiates the theories described on Chapter 5, and therefore the experiment can be deemed successful.
4. The theories associated with the phenomena of bubble-back have been successfully integrated into the established coil pump theories, as described in Chapter 5.
5. The simulation described in Chapter 6, successfully embodies the theories described in Chapter 5.
6. A large number of suggestions have been included in Chapter 7 to highlight areas of concern for future researchers to investigate.

APPENDIX A

----- FLOW MEDIA RESISTANCE EXPERIMENTAL RESULTS -----

The six tables on the following pages contain the results from the experiment discussed in section 2.5. This experiment examines the flow resistance of flow media by passing a discharge through a pipe containing the media and examining the headloss across it. Each of the rows in the tables represent a single experiment. Each column is described thus:

1. Discharge (litres / second), Orifice Meter.
2. Mean Fluid Velocity (metres / second), calculated by dividing the discharge by the cross-sectional area of the pipe.
3. Logarithmic Fluid Velocity.
4. Total Headloss across Tappings. (metres), measured across both the flow media and the empty part of the pipe between the tapping points.
5. Empty Pipe Headloss. (metres), calculated from the Darcy Pipe Friction equation (equation 2.1).
6. Logarithmic Headloss across the Flow Media, calculated by taking of the total headloss against the headloss from the empty part of the pipe.

Column 3 is regressed against 6 to find the exponential relationship between the headloss and the velocity of the fluid passing through the flow media.

(1)	(2)	(3)	(4)	(5)	(6)
Disc- charge (l/s)	Veloci- ty, V (m/s)	Loge(V)	Total Head- loss (m)	Empty Pipe Headloss (m)	Loge (Total - Empty)
3.80	0.2083	-1.5687	0.163	0.00069	-1.8177
5.10	0.2796	-1.2745	0.272	0.00125	-1.3078
6.15	0.3371	-1.0872	0.367	0.00181	-1.0086
7.00	0.3837	-0.9578	0.489	0.00235	-0.7213
8.05	0.4413	-0.8180	0.666	0.00311	-0.4137
9.05	0.4961	-0.7009	0.829	0.00393	-0.1955
10.00	0.5482	-0.6011	1.047	0.00480	0.0367
11.25	0.6167	-0.4833	1.319	0.00607	0.2663
12.60	0.6907	-0.3700	1.673	0.00762	0.5023
14.70	0.8059	-0.2159	2.258	0.01037	0.7993
15.10	0.8278	-0.1890	2.394	0.01094	0.8573
15.75	0.8634	-0.1469	2.611	0.01190	0.9433
16.50	0.9045	-0.1003	2.747	0.01306	0.9928
10.65	0.5838	-0.5381	1.170	0.00544	0.1466
11.75	0.6441	-0.4398	1.414	0.00662	0.3354
13.90	0.7620	-0.2718	2.040	0.00927	0.6991

TABLE A.1, Flow Media Plug Length = 0.66 m Results

(1)	(2)	(3)	(4)	(5)	(6)
Discharge (l/s)	Velocity, V (m/s)	Loge(V)	Total Head-loss (m)	Empty Pipe Headloss (m)	Loge (Total -Empty)
4.80	0.2631	-1.3351	0.598	0.00092	-0.5160
5.75	0.3152	-1.1545	0.870	0.00132	-0.1416
7.20	0.3947	-0.9296	1.333	0.00207	0.2837
8.20	0.4495	-0.7996	1.850	0.00269	0.6108
9.50	0.5208	-0.6524	2.516	0.00361	0.9176
11.10	0.6085	-0.4968	3.631	0.00492	1.2831
12.05	0.6606	-0.4146	4.460	0.00580	1.4882

TABLE A.2, Flow Media Plug Length = 1.385 m Results

(1)	(2)	(3)	(4)	(5)	(6)
Disc- harge (l/s)	Veloci- ty, V (m/s)	Loge(V)	Total Head- loss (m)	Empty Pipe Headloss (m)	Loge (Total -Empty)
2.35	0.1288	-2.0493	0.258	0.00018	-1.3541
2.90	0.1590	-1.8390	0.408	0.00028	-0.8975
4.15	0.2275	-1.4806	0.829	0.00028	-0.1881
6.00	0.3289	-1.1119	1.591	0.00120	0.4625
6.90	0.3783	-0.9722	2.135	0.00159	0.7562
7.90	0.4331	-0.8368	2.802	0.00209	1.0274
8.75	0.4797	-0.7346	3.536	0.00256	1.2597
9.50	0.5208	-0.6524	4.420	0.00302	1.4824
10.20	0.5592	-0.5813	5.304	0.00348	1.6643

TABLE A.3, Flow Media Plug Length = 1.975 m Results

(1)	(2)	(3)	(4)	(5)	(6)
Disc-charge (l/s)	Velocity, V (m/s)	Loge(V)	Total Head-loss (m)	Empty Pipe Headloss (m)	Loge (Total - Empty)
2.05	0.1124	-2.186	0.353	0.00009	-1.0400
3.05	0.1672	-1.789	0.721	0.00021	-0.3279
3.85	0.2111	-1.556	1.047	0.00033	0.0455
4.50	0.2466	-1.400	1.387	0.00046	0.3265
5.15	0.2823	-1.265	1.877	0.00060	0.6286
6.00	0.3289	-1.112	2.516	0.00081	0.9215
6.80	0.3728	-0.987	3.155	0.00104	1.1480
7.65	0.4194	-0.869	4.066	0.00132	1.4010
8.60	0.4715	-0.752	5.358	0.00167	1.6770

TABLE A.4, Flow Media Plug Length = 2.955 m Results

(1)	(2)	(3)	(4)	(5)	(6)
Disc- harge (l/s)	Veloci- ty, V (m/s)	Loge(V)	Total Head- loss (m)	Empty Pipe Headloss (m)	Loge (Total -Empty)
1.70	0.0932	-2.373	0.353	0.00006	-1.0400
2.05	0.1124	-2.186	0.516	0.00009	-0.6604
2.65	0.1453	-1.929	0.761	0.00016	-0.2727
3.40	0.1864	-1.680	1.074	0.00026	0.0712
4.20	0.2302	-1.469	1.455	0.00040	0.3745
4.50	0.2467	-1.400	1.836	0.00046	0.6069
5.10	0.0796	-1.275	2.380	0.00059	0.8663
5.80	0.3180	-1.146	2.938	0.00076	1.0770
6.45	0.3536	-1.040	3.699	0.00094	1.3070
7.10	0.3892	-0.943	4.379	0.00114	1.4760
7.75	0.4249	-0.856	5.331	0.00136	1.6720

TABLE A.5, Flow Media Plug Length = 3.880 m Results

(1)	(2)	(3)	(4)	(5)	(6)
Disc-charge (l/s)	Velocity, V (m/s)	Loge(V)	Total Head-loss (m)	Empty Pipe Headloss (m)	Loge (Total - Empty)
1.25	0.0685	-2.681	0.217	0.0000	-1.5250
1.50	0.0822	-2.498	0.340	0.0000	-1.0790
1.70	0.0932	-2.373	0.530	0.0000	-0.6341
2.35	0.1288	-2.049	0.884	0.0000	-0.1233
3.20	0.1754	-1.741	1.306	0.0000	0.2667
3.50	0.1919	-1.651	1.632	0.0000	0.4898
4.00	0.2190	-1.517	2.054	0.0000	0.7196
4.50	0.2467	-1.400	2.448	0.0000	0.8953
5.10	0.2796	-1.275	3.060	0.0000	1.1180
5.65	0.3097	-1.172	3.713	0.0000	1.3120
6.00	0.3289	-1.112	4.257	0.0000	1.4490
6.70	0.3673	-1.002	5.304	0.0000	1.6690

TABLE A.6, Flow Media Plug Length = 5.000 m Results

APPENDIX B

RATIONALE TO REGRESSING EXPERIMENTAL RESULTS

- THE TWO-VARIABLE STATISTICAL LINEAR REGRESSION METHOD

In the theory of Linear Regression, there are three important values; r , a and b . The Correlation Coefficient r shows the quality of the relationship between the two variables for a particular sample of results. The value of r is always at or between -1 and $+1$. If r equals -1 or $+1$, all points on a graph depicting the two variables are on one straight line drawn through the results. The further the value is from -1 and $+1$, the less points are massed about the line and the less reliable is the correlation. If r is greater than zero, it shows a positive correlation (Y is proportional to X), and if r is less than zero, there is a negative correlation (Y is inversely proportional to X).

The equation for a straight line is given by:

$$Y = a + bX$$

Where a = The point at which the line crosses the Y axis

$$= Y - bX$$

b = Slope of the Regression line representing the relationship

$$= \frac{S_{xy}}{S_{xx}}$$

$$r = \frac{S_{xy}}{\sqrt{S_{xx} * S_{yy}}} \quad (B.1)$$

where X = The mean of the X results

Y = The mean of the Y results

S_{xx} = The standard Deviation of the X results

$$= \frac{\sum X^2 - (\sum X)^2}{n}$$

S_{yy} = The standard deviation of the Y results

$$= \frac{\sum Y^2 - (\sum Y)^2}{n}$$

S_{xy} = The standard deviation of the X results with respect to the Y results

$$= \frac{\sum XY - (\sum X * \sum Y)}{n}$$

n = Number of pairs of results.

To simplify the calculations equation B.1 representing the correlation coefficient can be reduced to

the following:

$$r = \frac{\Sigma (X * Y)}{\sqrt{(\Sigma X^2 + \Sigma Y^2)}} \quad (B.2)$$

This equation has been used to regress all the results taken from this thesis as it has been proved to be of great value to be able to mathematically comment upon the quality of the results taken in a consistent and direct method.

APPENDIX C

 INCREASED DISCHARGE EXPERIMENT RESULTS

The following four tables contain data obtained or derived from the increased discharge experiment described in chapter 3. Each column is described in more detail between the tables.

Col	1	2	3	4
Expt No.	RPM	EXT DOI (m)	DISCHARGE Q (l/m)	Plug Vol (l)
1	1.22	0.05	0.171	0.140
2	3.53	0.05	0.509	0.144
3	6.00	0.05	0.875	0.145
4	2.00	0.09	0.246	0.123
5	4.28	0.09	0.552	0.129
6	5.45	0.09	0.718	0.132
7	1.71	0.13	0.187	0.109
8	3.33	0.13	0.380	0.114
9	5.45	0.13	0.630	0.116

FIGURE C.1a, Increased Discharge Experiment Results

1. Experimental rotational velocity (r.p.m) of the drum.
2. Experimental depth of immersion (metres below the

centreline of the drum).

3. Experimental discharge (litres/minute) of the pump.
4. Experimental mean volume (litres) of the liquid plugs.

Col	5	6	7	8
Expt No.	Plug Angle	Max Plug DOI (m)	Min Plug DOI (m)	Mean Head Diff
1	3.794	-0.1250	-0.0801	0.1526
2	3.916	-0.1250	-0.0944	0.1597
3	3.946	-0.1250	-0.0979	0.1615
4	3.341	-0.0563	-0.0249	0.1306
5	3.499	-0.0563	-0.0444	0.1404
6	3.575	-0.0563	-0.0537	0.1450
7	2.965	-0.0047	+0.0439	0.1104
8	3.098	-0.0047	+0.0054	0.1297
9	3.139	+0.0047	+0.0004	0.1322

FIGURE C.1b, Increased Discharge Experiment Results

5. Experimental angle (radians) the liquid plug subtends at the centre of the drum.
6. Theoretical maximum internal depth of immersion of the water plug as it enters the inlet and before it

has a chance to escape through the hole.

Col	9	10	11	12
Expt No.	D.O.I Angle	Extra Water Vol	Theo Bucket Vol	Water escape time
1	2.755	0.0383	0.0457	25.65
2	2.755	0.0428	0.0457	9.02
3	2.755	0.0439	0.0457	5.33
4	2.435	0.0334	0.0428	13.79
5	2.435	0.0392	0.0428	6.62
6	2.435	0.0420	0.0428	5.27
7	2.094	0.0321	0.0400	14.13
8	2.094	0.0370	0.0400	7.44
9	2.094	0.0385	0.0400	4.58

FIGURE C.1c, Increased Discharge Experiment Results

-
7. Experimental internal depth of immersion of the liquid plug inside the helix (metres below the centreline of the drum). A negative number indicates the liquid level is above the centreline. This can be thought of in terms of the external depth of immersion required to form a liquid plug inside the helix without the aid of a bucket
 8. Mean head difference (metres) between the external &

internal depths of immersion found by comparing columns 2 and 6. It is an indication of the success of the experiment, in terms of the increased depth of immersion.

Col	13	14	15	16
Expt No.	Vol. (Theo - Actual)	Mean Velocity	$\sqrt{2*g*H}$	cd
1	0.0074	0.0918	1.7300	0.05308
2	0.0029	0.1023	1.7701	0.05781
3	0.0018	0.1075	1.7798	0.06040
4	0.0094	0.2170	1.6007	0.13554
5	0.0036	0.1731	1.6594	0.10431
6	0.0008	0.0483	1.6867	0.02865
7	0.0079	0.1780	1.4718	0.12092
8	0.0030	0.1284	1.5949	0.08047
9	0.0015	0.1043	1.6102	0.06474

FIGURE C.1d, Increased Discharge Experiment Results

9. Experimental angle (radians) of the external depth of immersion subtending the centre of the drum.
10. Experimental volume of liquid (litres) picked up by the bucket. Found by comparing column (5) with column (9) to find the total arc of the liquid plug above the external liquid level. This is

multiplied by the effective radius (i.e. the drum radius plus the pipe radius) and the cross-sectional area of the pump.

11. Theoretical volume (litres) the bucket can hold taking into account the orientation of the bucket to the surface of the liquid. This volume does not take into account the phenomenon of the liquid leaking through holes further around the helix.
12. Experimental mean time (seconds) that the hole in the helix is exposed to the liquid plug inside the helix. This gives an indication of the time available for the liquid to escape from the hole, and so reduce the increased depth of immersion.
13. Difference between the theoretical and actual volume (litres) of liquid picked by the bucket. It shows that significant amounts of liquid escape out of the hole.
14. The mean velocity of the liquid through the hole, found by dividing the volume lost by the cross-sectional area of the hole and the time the liquid has to escape (metres / second),
15. Part of equation (5.33), Torricelli's Equation. Used to find the Coefficient of Discharge for the hole in the pipe.
16. Coefficient of Discharge, found from equation (5.33), Torricelli's equation.

APPENDIX D

MAIN POWER EXPERIMENT RESULTS

Figure D.1a. Results for Experiments 1 - 12
of the Main Power Experiment.

	(1)	(2)	(3)	(4)
Expt No.	Drum Speed (rpm)	Power Input (watts)	Helix Pressure Head (metres)	DOI (mm)
1	.7728	25.50	2.762	382.0
2	1.897	43.10	2.758	382.0
3	3.013	59.65	2.727	382.0
4	2.963	59.60	2.740	361.0
5	1.900	33.81	2.740	361.0
6	1.010	33.28	2.795	361.0
7	.8894	33.69	2.819	160.0
8	1.903	49.33	2.780	165.0
9	3.188	66.64	2.716	175.0
10	2.850	51.19	2.538	140.0
11	1.785	37.24	2.635	130.0
12	1.039	28.65	2.720	111.0

Figure D.1b. Results for Experiments 13 - 24
of the Main Power Experiment.

	(1)	(2)	(3)	(4)
Expt No.	Drum Speed (rpm)	Power Input (watts)	Helix Pressure Head (metres)	DOI (mm)
13	1.072	18.33	1.913	369.0
14	1.903	27.04	1.881	377.0
15	2.975	38.29	1.873	390.0
16	3.030	38.83	1.888	320.0
17	1.959	27.70	1.906	310.0
18	1.047	18.95	1.923	305.0
19	1.011	18.69	1.805	185.0
20	1.878	27.66	1.772	193.0
21	2.963	39.19	1.693	234.0
22	2.992	35.77	1.749	77.00
23	1.957	24.74	1.795	52.00
24	1.107	17.37	1.843	44.00

Figure D.1c. Results for Experiments 25 - 36
of the Main Power Experiment.

	(1)	(2)	(3)	(4)
Expt No.	Drum Speed	Power Input	Helix Pressure Head	DOI
	(rpm)	(watts)	(metres)	(mm)
25	3.004	19.43	.9364	82.00
26	1.943	12.82	.9462	70.00
27	1.079	8.054	.9582	45.00
28	1.039	7.905	.9503	160.0
29	2.131	14.21	.9252	190.0
30	2.992	19.64	.9093	205.0
31	3.085	20.69	.8697	305.0
32	2.037	13.85	.8943	295.0
33	.9797	7.486	.9206	280.0
34	.9017	7.543	.9081	369.0
35	2.076	14.34	.8749	380.0
36	3.000	19.91	.8488	385.0

Figure D.1d. Results for Experiments 37 - 48
of the Main Power Experiment.

	(1)	(2)	(3)	(4)
Expt No.	Drum Speed	Power Input	Helix Pressure Head	DOI
	(rpm)	(watts)	(metres)	(mm)
37	2.670	7.817	.0430	420.0
38	1.998	5.921	.0403	400.0
39	1.122	3.232	.0156	380.0
40	1.175	3.311	.0233	300.0
41	2.025	5.951	.0544	315.0
42	2.853	9.199	.0934	320.0
43	2.850	8.730	.1316	188.0
44	1.917	4.929	.0660	169.0
45	1.074	2.522	.0272	145.0
46	1.117	2.336	.0324	48.00
47	2.128	5.502	.0968	62.00
48	2.996	9.476	.1846	80.00

Figure D.1e. Results for Experiments 49 - 60
of the Main Power Experiment.

	(1)	(2)	(3)	(4)
Expt No.	Drum Speed	Power Input	Helix Pressure Head	DOI
	(rpm)	(watts)	(metres)	(mm)
49	.0000	.0000	.0000	379.0
50	.0000	.0000	.0000	387.0
51	.0000	.0000	.0000	389.0
52	.0000	.0000	.0000	300.0
53	.0000	.0000	.0000	292.0
54	.0000	.0000	.0000	285.0
55	.9471	16.05	1.802	155.0
56	1.858	24.64	1.743	180.0
57	2.951	35.31	1.683	197.0
58	3.000	36.00	1.719	130.0
59	1.946	25.01	1.788	105.0
60	1.089	16.32	1.832	80.00

Figure D.1f. Results for Experiments 61 - 72
of the Main Power Experiment.

	(1)	(2)	(3)	(4)
Expt No.	Drum Speed	Power Input	Helix Pressure Head	DOI
	(rpm)	(watts)	(metres)	(mm)
61	1.071	12.08	1.393	50.00
62	1.954	18.59	1.368	73.00
63	3.004	27.40	1.344	92.00
64	2.951	27.73	1.303	215.0
65	1.871	18.65	1.332	209.0
66	.9924	11.85	1.359	205.0
67	.9400	11.90	1.341	280.0
68	2.037	20.27	1.359	292.0
69	3.129	27.20	1.430	297.0
70	3.051	27.30	1.429	391.0
71	2.020	18.67	1.449	388.0
72	1.054	11.56	1.431	381.0

Figure D.1g. Results for Experiments 73 - 84
of the Main Power Experiment.

	(1)	(2)	(3)	(4)
Expt No.	Drum Speed	Power Input	Helix Pressure Head	DOI
	(rpm)	(watts)	(metres)	(mm)
73	1.011	7.811	.9561	320.0
74	2.207	15.53	.9678	337.0
75	3.141	21.63	.9718	347.0
76	3.046	22.31	.9283	307.0
77	2.114	15.67	.8947	297.0
78	1.067	9.214	.9015	281.0
79	1.141	9.061	.9420	121.0
80	2.183	15.97	.9225	143.0
81	3.158	22.88	.9114	155.0
82	3.222	22.58	.9299	80.00
83	2.139	15.16	.9416	55.00
84	1.186	9.285	.9554	52.00

Figure D.1h. Results for Experiments 85 - 96
of the Main Power Experiment.

	(1)	(2)	(3)	(4)
Expt No.	Drum Speed	Power Input	Helix Pressure Head	DOI
	(rpm)	(watts)	(metres)	(mm)
85	1.084	3.536	.0159	368.0
86	2.939	11.08	.0813	380.0
87	2.939	.0000	.0000	383.0
88	2.967	11.37	.1155	275.0
89	1.962	6.429	.0597	254.0
90	.9369	2.918	.0198	227.0
91	.9639	2.892	.0241	146.0
92	1.957	6.293	.0752	168.0
93	3.095	12.01	.1634	193.0
94	3.109	11.80	.1905	133.0
95	2.008	6.169	.0819	112.0
96	1.007	2.836	.0293	80.00

Figure D.1i. Results for Experiments 97 - 108
of the Main Power Experiment.

	(1)	(2)	(3)	(4)
Expt No.	Drum Speed	Power Input	Helix Pressure Head	DOI
	(rpm)	(watts)	(metres)	(mm)
97	1.053	11.80	1.442	366.0
98	2.012	18.22	1.412	373.0
99	2.955	24.89	1.418	380.0
100	2.992	24.92	1.420	310.0
101	1.860	16.92	1.426	302.0
102	.9304	10.52	1.437	291.0
103	.9077	10.82	1.366	215.0
104	2.031	18.96	1.331	232.0
105	2.939	26.27	1.310	243.0
106	3.017	25.82	1.337	115.0
107	2.103	18.57	1.347	100.0
108	.9957	10.66	1.379	73.00

Figure D.1j. Results for Experiments 109 - 120
of the Main Power Experiment.

	(1)	(2)	(3)	(4)
Expt No.	Drum Speed	Power Input	Helix Pressure Head	DOI
	(rpm)	(watts)	(metres)	(mm)
109	1.081	2.511	.0151	342.0
110	1.918	4.794	.0422	359.0
111	2.963	8.550	.0819	369.0
112	2.959	8.567	.1070	294.0
113	1.913	4.797	.0526	281.0
114	1.046	2.532	.0204	264.0
115	1.102	2.464	.0279	150.0
116	2.092	5.186	.0779	172.0
117	2.984	8.670	.1428	189.0
118	3.000	8.583	.1785	88.00
119	2.000	4.494	.0854	53.00
120	.9437	1.918	.0270	90.00

Figure D.1k. Results for Experiments 121 - 132
of the Main Power Experiment.

	(1)	(2)	(3)	(4)
Expt No.	Drum Speed	Power Input	Helix Pressure Head	DOI
	(rpm)	(watts)	(metres)	(mm)
121	1.014	4.610	.5080	92.00
122	2.108	8.862	.5058	94.00
123	2.846	12.01	.5098	90.00
124	2.809	11.96	.4798	205.0
125	1.930	7.969	.4886	197.0
126	1.051	4.615	.4924	184.0
127	.9402	4.583	.4721	316.0
128	1.871	7.950	.4672	322.0
129	3.034	12.80	.4532	333.0
130	3.261	11.38	.5066	387.0
131	2.136	7.411	.4931	382.0
132	1.081	4.471	.4947	377.0

Figure D.1l. Results for Experiments 133 - 144
of the Main Power Experiment.

	(1)	(2)	(3)	(4)
Expt No.	Drum Speed	Power Input	Helix Pressure Head	DOI
	(rpm)	(watts)	(metres)	(mm)
133	1.049	6.690	.9628	358.0
134	1.978	11.23	.9450	366.0
135	2.895	16.06	.9339	373.0
136	2.816	15.83	.9485	282.0
137	1.891	11.23	.9731	276.0
138	.9795	6.653	.9835	260.0
139	.9600	6.734	.9162	153.0
140	1.850	11.46	.9148	160.0
141	2.903	17.50	.9019	182.0
142	2.963	17.43	.9237	84.00
143	2.036	12.16	.9342	56.00
144	.9862	6.718	.9405	78.00

Figure D.1m. Results for Experiments 145 - 156
of the Main Power Experiment.

	(1)	(2)	(3)	(4)
Expt No.	Drum Speed	Power Input	Helix Pressure Head	DOI
	(rpm)	(watts)	(metres)	(mm)
145	1.096	3.596	.0120	373.0
146	2.192	10.96	.0418	382.0
147	3.008	20.56	.0710	387.0
148	2.775	21.18	.0876	258.0
149	2.043	11.33	.0567	243.0
150	1.047	3.562	.0186	212.0
151	1.039	3.547	.0217	144.0
152	2.054	12.63	.0667	172.0
153	2.988	28.79	.1243	193.0
154	2.907	28.66	.1421	90.00
155	2.070	13.37	.0753	70.00
156	1.089	3.711	.0270	45.00

Figure D.1n. Results for Experiments 157 - 168
of the Main Power Experiment.

	(1)	(2)	(3)	(4)
Expt No.	Drum Speed	Power Input	Helix Pressure Head	DOI
	(rpm)	(watts)	(metres)	(mm)
157	1.093	6.684	.5090	82.00
158	1.981	16.20	.5023	67.00
159	2.923	34.90	.4983	86.00
160	3.093	37.18	.4889	200.0
161	2.043	16.21	.4830	190.0
162	1.102	6.715	.4857	180.0
163	1.100	6.623	.4695	297.0
164	1.973	14.17	.4693	306.0
165	3.117	32.44	.4594	315.0
166	3.270	32.02	.4450	388.0
167	1.936	12.75	.4506	380.0
168	1.111	6.741	.4531	373.0

Figure D.2a. Results for Experiments 1 - 12
of the Main Power Experiment.

	(5)	(6)	(7)	(8)
Expt No.	Discharge (litres/ /min)	Number of coils	Headlift (metres)	Power output (watts)
1	8.800	8.000	3.000	4.316
2	21.00	8.000	3.000	10.30
3	30.75	8.000	3.000	15.08
4	37.25	8.000	3.000	18.27
5	23.67	8.000	3.000	11.61
6	13.61	8.000	3.000	6.676
7	13.82	8.000	3.000	6.779
8	29.60	8.000	3.000	14.52
9	46.00	8.000	3.000	22.56
10	71.43	8.000	3.000	35.04
11	63.20	8.000	3.000	31.00
12	13.75	8.000	3.000	6.744

Figure D.2b. Results for Experiments 13 - 24
of the Main Power Experiment.

	(5)	(6)	(7)	(8)
Expt No.	Discharge (litres/ /min)	Number of coils	Headlift (metres)	Power output (watts)
13	12.00	8.000	2.000	3.924
14	23.00	8.000	2.000	7.521
15	31.28	8.000	2.000	10.23
16	35.83	8.000	2.000	11.72
17	24.25	8.000	2.000	7.930
18	13.39	8.000	2.000	4.379
19	22.80	8.000	2.000	7.456
20	42.20	8.000	2.000	13.80
21	63.75	8.000	2.000	20.85
22	77.75	8.000	2.000	25.42
23	52.73	8.000	2.000	17.24
24	29.10	8.000	2.000	9.516

Figure D.2c. Results for Experiments 25 - 36
of the Main Power Experiment.

	(5)	(6)	(7)	(8)
Expt No.	Discharge (litres/min)	Number of coils	Headlift (metres)	Power output (watts)
25	78.50	8.000	1.000	12.83
26	51.14	8.000	1.000	8.361
27	29.45	8.000	1.000	4.815
28	26.78	8.000	1.000	4.379
29	50.80	8.000	1.000	8.306
30	65.50	8.000	1.000	10.71
31	53.00	8.000	1.000	8.666
32	65.26	8.000	1.000	10.67
33	19.00	8.000	1.000	3.107
34	13.60	8.000	1.000	2.224
35	29.14	8.000	1.000	4.764
36	39.43	8.000	1.000	6.447

Figure D.2d. Results for Experiments 37 - 48
of the Main Power Experiment.

	(5)	(6)	(7)	(8)
Expt No.	Discharge (litres/min)	Number of coils	Headlift (metres)	Power output (watts)
37	28.00	8.000	.0000	.0000
38	27.75	8.000	.0000	.0000
39	16.08	8.000	.0000	.0000
40	21.18	8.000	.0000	.0000
41	35.71	8.000	.0000	.0000
42	49.80	8.000	.0000	.0000
43	63.50	8.000	.0000	.0000
44	43.75	8.000	.0000	.0000
45	25.45	8.000	.0000	.0000
46	29.50	8.000	.0000	.0000
47	57.80	8.000	.0000	.0000
48	78.50	8.000	.0000	.0000

Figure D.2e. Results for Experiments 49 - 60
of the Main Power Experiment.

	(5)	(6)	(7)	(8)
Expt No.	Discharge (litres/ min)	Number of coils	Headlift (metres)	Power output (watts)
49	9.780	6.000	2.000	3.198
50	22.67	6.000	2.000	7.413
51	30.57	6.000	2.000	9.996
52	40.67	6.000	2.000	13.30
53	26.67	6.000	2.000	8.721
54	17.27	6.000	2.000	5.647
55	20.67	6.000	2.000	6.759
56	39.29	6.000	2.000	12.85
57	60.50	6.000	2.000	19.78
58	72.00	6.000	2.000	23.54
59	48.80	6.000	2.000	15.96
60	28.40	6.000	2.000	9.287

Figure D.2f. Results for Experiments 61 - 72
of the Main Power Experiment.

	(5)	(6)	(7)	(8)
Expt No.	Discharge (litres/ min)	Number of coils	Headlift (metres)	Power output (watts)
61	27.56	6.000	1.500	6.759
62	53.20	6.000	1.500	13.05
63	76.25	6.000	1.500	18.70
64	60.80	6.000	1.500	14.91
65	39.29	6.000	1.500	9.636
66	20.73	6.000	1.500	5.084
67	17.00	6.000	1.500	4.169
68	29.76	6.000	1.500	7.299
69	40.80	6.000	1.500	10.01
70	32.67	6.000	1.500	8.012
71	22.00	6.000	1.500	5.396
72	12.31	6.000	1.500	3.019

Figure D.2g. Results for Experiments 73 - 84
of the Main Power Experiment.

	(5)	(6)	(7)	(8)
Expt No.	Discharge (litres/min)	Number of coils	Headlift (metres)	Power output (watts)
73	13.47	6.000	1.000	2.202
74	26.75	6.000	1.000	4.374
75	36.00	6.000	1.000	5.886
76	39.30	6.000	1.000	6.426
77	29.38	6.000	1.000	4.804
78	17.38	6.000	1.000	2.842
79	21.11	6.000	1.000	3.451
80	49.44	6.000	1.000	8.083
81	73.50	6.000	1.000	12.02
82	86.86	6.000	1.000	14.20
83	58.67	6.000	1.000	9.593
84	32.78	6.000	1.000	5.360

Figure D.2h. Results for Experiments 85 - 96
of the Main Power Experiment.

	(5)	(6)	(7)	(8)
Expt No.	Discharge (litres/min)	Number of coils	Headlift (metres)	Power output (watts)
85	15.12	6.000	.0000	.0000
86	28.50	6.000	.0000	.0000
87	39.14	6.000	.0000	.0000
88	54.40	6.000	.0000	.0000
89	37.60	6.000	.0000	.0000
90	18.90	6.000	.0000	.0000
91	22.08	6.000	.0000	.0000
92	45.33	6.000	.0000	.0000
93	66.50	6.000	.0000	.0000
94	75.50	6.000	.0000	.0000
95	47.17	6.000	.0000	.0000
96	25.91	6.000	.0000	.0000

Figure D.2i. Results for Experiments 97 - 108
of the Main Power Experiment.

	(5)	(6)	(7)	(8)
Expt No.	Discharge (litres/min)	Number of coils	Headlift (metres)	Power output (watts)
97	11.89	4.000	1.500	2.916
98	21.00	4.000	1.500	5.150
99	31.50	4.000	1.500	7.725
100	35.00	4.000	1.500	8.584
101	23.17	4.000	1.500	5.682
102	11.61	4.000	1.500	2.847
103	19.73	4.000	1.500	4.839
104	39.67	4.000	1.500	9.729
105	57.25	4.000	1.500	14.04
106	73.00	4.000	1.500	17.90
107	51.00	4.000	1.500	12.51
108	25.36	4.000	1.500	6.220

Figure D.2j. Results for Experiments 109 - 120
of the Main Power Experiments

	(5)	(6)	(7)	(8)
Expt No.	Discharge (litres/min)	Number of coils	Headlift (metres)	Power output (watts)
109	16.36	4.000	.0000	.0000
110	27.37	4.000	.0000	.0000
111	40.43	4.000	.0000	.0000
112	51.60	4.000	.0000	.0000
113	34.57	4.000	.0000	.0000
114	19.29	4.000	.0000	.0000
115	25.33	4.000	.0000	.0000
116	47.54	4.000	.0000	.0000
117	65.00	4.000	.0000	.0000
118	77.14	4.000	.0000	.0000
119	52.60	4.000	.0000	.0000
120	24.10	4.000	.0000	.0000

Figure D.2k. Results for Experiments 121 - 132
of the Main Power Experiment.

	(5)	(6)	(7)	(8)
Expt No.	Discharge (litres/min)	Number of coils	Headlift (metres)	Power output (watts)
121	25.50	4.000	.5000	2.085
122	54.00	4.000	.5000	4.415
123	70.00	4.000	.5000	5.723
124	59.33	4.000	.5000	4.850
125	40.67	4.000	.5000	3.325
126	22.55	4.000	.5000	1.843
127	14.73	4.000	.5000	1.204
128	29.50	4.000	.5000	2.412
129	48.00	4.000	.5000	3.924
130	32.40	4.000	.5000	2.649
131	21.29	4.000	.5000	1.740
132	11.50	4.000	.5000	.9401

Figure D.2l. Results for Experiments 133 - 144
of the Main Power Experiment.

	(5)	(6)	(7)	(8)
Expt No.	Discharge (litres/min)	Number of coils	Headlift (metres)	Power output (watts)
133	11.70	4.000	1.000	1.913
134	20.23	4.000	1.000	3.308
135	30.75	4.000	1.000	5.028
135	30.75	4.000	1.000	5.028
136	33.20	4.000	1.000	5.428
137	24.67	4.000	1.000	4.034
138	13.30	4.000	1.000	2.175
139	18.00	4.000	1.000	2.943
140	43.60	4.000	1.000	7.129
141	66.25	4.000	1.000	10.83
142	75.00	4.000	1.000	12.26
143	53.00	4.000	1.000	8.666
144	25.70	4.000	1.000	4.202

Figure D.2m. Results for Experiments 145 - 156
of the Main Power Experiment.

	(5)	(6)	(7)	(8)
Expt No.	Discharge (litres/min)	Number of coils	Headlift (metres)	Power output (watts)
145	15.40	8.000	.0000	.0000
146	29.13	8.000	.0000	.0000
147	38.00	8.000	.0000	.0000
148	48.60	8.000	.0000	.0000
149	33.22	8.000	.0000	.0000
150	20.30	8.000	.0000	.0000
151	22.92	8.000	.0000	.0000
152	44.62	8.000	.0000	.0000
153	62.25	8.000	.0000	.0000
154	70.00	8.000	.0000	.0000
155	49.83	8.000	.0000	.0000
156	27.65	8.000	.0000	.0000

Figure D.2n. Results for Experiments 157 - 168
of the Main Power Experiment.

	(5)	(6)	(7)	(8)
Expt No.	Discharge (litres/min)	Number of coils	Headlift (metres)	Power output (watts)
157	27.08	8.000	.5000	2.214
158	48.00	8.000	.5000	3.924
159	71.20	8.000	.5000	5.821
160	69.75	8.000	.5000	5.702
161	42.00	8.000	.5000	3.434
162	23.08	8.000	.5000	1.887
163	18.90	8.000	.5000	1.545
164	31.17	8.000	.5000	2.548
165	50.33	8.000	.5000	4.114
166	41.75	8.000	.5000	3.413
167	25.00	8.000	.5000	2.044
168	14.93	8.000	.5000	1.221

APPENDIX E

PROGRAMS USED ON THE BBC MICROCOMPUTER

Program (1)

```
10 REM *****
20 REM *          DATA LOGGING PROGRAM          *
30 REM *          WRITTEN BY S.GALVIN           *
40 REM *          IN BBC BASIC                 *
50 REM *****
60 MODE 7
70 I = 0
80 OLDT = 0
90 DIM ARRAY (3999)
100 INPUT "APPROX RPM=", DELAY
110 DELAY = 74 / (100 * DELAY)
120 TIME = 0
125 :
130 ARRAY(I) = ADVAL (1)
140 ARRAY(I+1) = ADVAL (2)
150 ARRAY(I+2) = ADVAL (3)
160 ARRAY(I+3) = ADVAL (4)
170 NEWT = TIME / 100
180 ARRAY(I+4) = NEWT
190 I = I + 5
195 :
200 IF I > 3996 THEN 220
205 :
210 IF OLDT <= NEWT-DELAY
    THEN OLDT = NEWT:GOTO 130
    ELSE NEWT = TIME / 100:GOTO 210
215 :
220 SOUND1,-15,53,10
230 *SPOOL TEST10
235 :
240 FOR I = 0 TO 3999
250 PRINT STR$(ARRAY(I))
260 NEXT I
265 :
270 *SPOOL
280 SOUND1,-15,53,20
290 END
```

Program (2)

```
10 REM *****
20 REM *   PROGRAM TO DOWNLOAD DATA TO   *
30 REM *   THE MAINFRAME COMPUTER       *
40 REM *   WRITTEN BY S.GALVIN          *
50 REM *   IN BBC BASIC                 *
60 REM *****
70 DIM ARRAY(4000)
80 I = 0
90 INPUT"FILE",NAME$
100 X = OPENIN(NAME$)
105 :
110 REPEAT
120 INPUTEX,R
130 ARRAY(I) = R
140 I = I + 1
150 UNTIL EOFEX
155 :
160 CLOSEEX
170 I = 0
180 SOUND 1,-15,53,20
190 INPUT A$
205 :
200 *SPOOL TESTT3
210 REPEAT
220 PRINT STR$(ARRAY(I))
230 I = I + 1
240 UNTIL I = 4000
245 :
250 *SPOOL
260 SOUND 1,-15,53,20
```

Program (3)

```

10 REM *****
20 REM *   PROGRAM TO GRAPHICALLY DISPLAY   *
30 REM *   DATA CURRENTLY BEING LOGGED    *
40 REM *   WRITTEN BY S.GALVIN             *
50 REM *   IN BBC BASIC                    *
60 REM *****
70 DMAX  = 2.415
80 DMIN  = 1.664
90 TIME  = 0
100 FLAG = 0
110 T    = 0
120 D    = 0
130 FLAG2 = 0
140 MAX  = 0
150 MIN  = 0
160 @%   = &20309
170 MODE 0
180 PRINT "GRAPHICS, TEXT, OR EXIT? (G/T/E)?"
190 A$ = GET$
200 MODE 0
205 :
210 IF A$ = "T" THEN 260
    ELSE IF A$ = "G" THEN 230
    ELSE IF A$ = "E" THEN END
220 GOTO 170
230 :
240 PRINT "WHAT GRAPH? (1,2,3,4,5 OR 6)?"
250 PRINT
260 PRINT "      X-AXIS,      Y-AXIS"
270 PRINT
280 PRINT "(1) = TIME      VS  ROTATION"
290 PRINT "(2) = TIME      VS  POWER"
300 PRINT "(3) = ROTATION VS  POWER"
310 PRINT "(4) = PRESSURE VS  POWER"
320 PRINT "(5) = ROTATION VS  PRESSURE"
330 PRINT "(6) = TIME      VS  PRESSURE"
335 :
340 FLAG = VAL(GET$)
345 :
350 IF FLAG = 0 OR FLAG > 6 THEN 170
355 :
360 MODE 5
370 DRAW 0,1023
380 DRAW 1279,1023
390 DRAW 1279,0
400 DRAW 0,0
405 :
410 IF FLAG = 1 OR FLAG = 2 OR FLAG = 6 THEN SCALE = 20
    ELSE SCALE = 5
415 :
420 A   = ADVAL(1) / 26208
430 B   = ADVAL(2) / 26208
440 C   = ADVAL(3) / 26208

```

```

450 OLDD = D
460 OLD T = T
470 D = ADVAL(4) / 26208
480 T = TIME / 100
485 :
490 IF T >= 1279/SCALE AND A$="G"
    THEN TIME = 0:FLAG2 = 0:GOTO 360
495 :
500 PROCAXB
510 IF FLAG = 0 THEN PROCREVS:PRINT
    VOLTS,AMPS,POWER,PRESSURE,T
520 IF FLAG = 1 AND FLAG2 = 0
    THEN MOVE T * SCALE,D * 800:FLAG2 = 1
530 IF FLAG = 1
    THEN DRAW T * SCALE,D * 800
540 IF FLAG = 2 AND FLAG2 = 0
    THEN MOVE T * SCALE,POWER * 4:FLAG2 = 1
550 IF FLAG = 2
    THEN DRAW T * SCALE,POWER * 4
560 IF FLAG = 3 AND FLAG2 = 0
    THEN MOVE D * 1000,POWER * 4:FLAG2 = 1
570 IF FLAG = 3
    THEN DRAW D * 1000,POWER * 4
580 IF FLAG = 4 AND FLAG2 = 0
    THEN MOVE PRESSURE * 300,POWER * 4:FLAG2 = 1
590 IF FLAG = 4
    THEN DRAW PRESSURE * 300,POWER * 4
600 IF FLAG = 5 AND FLAG2 = 0
    THEN MOVE D * 1000,PRESSURE * 300:FLAG2 = 1
610 IF FLAG = 5
    THEN DRAW D * 1000,PRESSURE * 300
620 IF FLAG = 6 AND FLAG2 = 0
    THEN MOVE T * SCALE,PRESSURE * 300:FLAG2 = 1
630 IF FLAG = 6
    THEN DRAW T * SCALE,PRESSURE * 300
640 IF INKEY$(0) = "E"
    THEN RUN
    ELSE 420
660 :
670 DEF PROCAXB
680 VOLTS = 100 * A
690 AMPS = 3 * B
700 POWER = VOLTS * AMPS
710 PRESSURE = 10.194 * C * 0.77 / 3.03
720 ENDPROC
730 :
740 DEF PROCREVS
750 IF D < DMIN THEN DMIN = D
760 IF D > DMAX THEN DMAX = D
770 L = (20 * (D - DMIN)/(DMAX - DMIN)) + 150
780 ANGLE = (L^2 + 10^2 - 160^2) / (20 * L)
790 ROTATION = (PI - ACS(ANGLE)) * 180 / PI
800 ENDPROC

```

APPENDIX F

 COMPUTER SIMULATION PROGRAM LISTING

```

1010 ' *****
1020 ' *
1020 ' * PROGRAM TO DETERMINE THE THEORETICAL WATER *
1022 ' * PROFILE OF THE COIL PUMP *
1024 ' * WRITTEN BY S. GALVIN *
1026 ' * IN APPLE MICROSOFT BASIC *
1030 ' *
1040 ' *****
1050 '
1060 ' *****
1070 ' * VARIABLE DEFINITION *
1080 ' *****
1090 '
1110 DEFINT B, I, N ' INTEGER VARIABLES
1120 DEFSNG A, C, D, G, H, L, P, R ' REAL VARIABLES
1030 '
1040 ' *****
1050 ' * ARRAY DEFINITIONS *
1060 ' *****
1180 DIM HARR (50) ' HEADS EACH COIL GENERATES
1190 DIM HSUM (50) ' SUMMATION OF HEADS
1200 DIM ADEL (50) ' WATER PLUG ROTATIONS
1210 DIM ATHE (50) ' ANGLES WATER PLUGS MAKES
' AT SHAFT
1230 DIM LOME (50) ' LENGTHS OF AIR PLUG
' COMPRESSIONS
1240 DIM LAIR (50) ' LENGTHS OF AIR PLUGS
1250 DIM LWAT (50) ' LENGTHS OF WATER PLUGS
1260 DIM HFLC (50) ' FLOW MEDIA HEAD
1265 '
1270 ' *****
1280 ' * MAIN CONTROL PROCEDURE *
1290 ' *****
1310 GOSUB 2000 ' INPUT PROCESS
1320 GOSUB 3000 ' INITIALISATION PROC
1330 GOSUB 4000 ' NO BUBBLING +SPILLING
1340 '
1350 IF (HCAL < HREQ) AND (DOIM =< .5)
' THEN GOSUB 5000 ' BUBBLING PROCESS
1360 IF (HCAL < HREQ) AND (DOIM > .5)
' THEN GOSUB 6000 ' SPILLING PROCESS
1370 IF (HCAL < HREQ) AND (DOIM =< .5)
' THEN GOSUB 7000 ' BUBBLING & SPILLING
1380 '
1390 GOSUB 8000 ' DISPLAY PROCESS
1400 '
1410 END ' END OF PROGRAM
  
```

```

2000 ' *****
2010 ' * INPUT PROCEDURE *
2020 ' *****
2060 INPUT "DIAMETER COIL      = "; DIAC
2070 INPUT "DIAMETER PIPE      = "; DIAP
2080 INPUT "NUMBER OF COILS    = "; NCOL
2090 INPUT "DEPTH OF IMMERSION = "; DOIM
2110 INPUT "HEAD LIFT          = "; HREQ
2120 INPUT "FLOCUR? (0/1)      = "; FLCR
2190 '
2200 RETURN
2220 '
3000 ' *****
3010 ' * INITIALISATION PROCEDURE *
3020 ' *****
3040 APIE      = 3.14159           ' 1 RADIAN
3050 HATM      = 10.182           ' ABS' ATMOS' HEAD
3060 LCOM      = .869565         ' COMPRESSION INDEX
3070 '
3080 RADC      = DIAC / 2!       ' RADIUS OF HELIX
3090 RADP      = DIAP / 2!       ' RADIUS OF PIPE
3100 DOIM      = DOIM / 100!     ' DOI AS A FRACTION
3110 AFST      = APIE / 200!     ' ROT'N INCREASE INDEX
3115 RADH      = RADC + RADP     ' RADIUS OF HELIX
3116 DIAH      = DIAC + DIAP     ' DIAMETER OF HELIX
3120 DIMM      = DIAC * DOIM     ' DEPTH OF HELIX
3130 HREQ      = HREQ + HATM     ' ABS' HEAD REQUIRED
3135 PMTR      = DIAH * APIE     ' PERIMETER OF HELIX
3140 PIN       = ( RADC - DIMM ) / RADH ' INPUT PARAMETER TO..
3150 '
3160 POUT = 1.5708 - ATN ( PIN / SQR ( 1! - PIN * PIN ))
                                     ' ..GET ARC COS FOR..
3170 '
3180 ATHE (0) = POUT * 2!         ' ..WATER PLUG ANGLE
3190 LAIR (0) = RADH * ( 2! * APIE - ATHE (0))
                                     ' 1ST AIR PLUG LEN'
3200 LWAT (0) = RADH * ATHE (0)   ' 1ST WATER PLUG LEN'
3210 HSUM (0) = HATM              ' INPUT PRESSURE HEAD
3220 PIN       = RADC / RADH     ' INPUT PARAMETER TO..
3230 :
3240 POUT = 1.5708 - ATN ( PIN / SQR ( 1! - PIN * PIN ))
                                     ' ..GET ARC COS FOR..
3250 '
3260 AGAM      = POUT            ' ..GAMMA ANGLE
3270 ASPL      = APIE - ( ATHE (0) / 2! ) - AGAM
                                     ' SPILLING ANGLE
3280 ABUB      = ( ATHE (0) / 2! ) - AGAM ' BUBBLING ANGLE
3290 '
3291 IF ASPL < ABUB
    THEN ARES = ASPL
    ELSE ARES = ABUB
3300 RETURN

```

```

4000 ' *****
4010 ' * NO BUBBLING NO SPILLING PROCEDURE *
4020 ' *****
4040 HCAL          = 0!           ' INIT FOR WHILE LOOP
4050 ADEL (1)      = AFST         ' INIT FOR WHILE LOOP
4060 ADEL (NCOL + 1) = 0!       ' INIT FOR WHILE LOOP
4070 '
4090 WHILE (HREQ > HCAL) AND (ADEL (NCOL + 1) < ARES)
4090 '
4100   FOR ICNT = 1 TO NCOL
4110     HRHS = RADH * COS (ATHE (0)/2! + ADEL (ICNT))
4120     HLHS = RADH * COS (ATHE (0)/2! - ADEL (ICNT))
4122     LVEL = RADH * (2! * APIE - LOME (ICNT -1)) * RPM / 60!
4124     HFLC (ICNT) = RADH * ATHE (0) * FLCR *
                    7.385 * (LVEL ^ 1.86)
4130     HARR (ICNT) = HRHS - HLHS
4140     HSUM (ICNT) = HARR (ICNT) + HSUM (ICNT-1) - HFLC (ICNT)
4150     LAIR (ICNT) = LAIR (0) *
                    ((ABS (HSUM(0) / HSUM (ICNT))) ^ LCOM)
4160     LOME (ICNT) = LAIR (0) - LAIR (ICNT)
4170     ADEL (ICNT+1) = ADEL (ICNT) + (LOME (ICNT) / RADH)
4180   NEXT ICNT
4190 '
4200   ADEL (1) = ADEL (1) + AFST
4210   HCAL = HSUM (NCOL)
4220 WEND
4230 '
4240 RETURN
4250 '
5000 ' *****
5010 ' * BUBBLING NO SPILLING PROCEDURE *
5020 ' *****
5060 WHILE ( HREQ > HCAL ) AND ( ADEL (1) < ABUB )
5070 '
5080   FOR ICNT = 1 TO NCOL
5100     IF ADEL (ICNT) > ABUB THEN ADEL (ICNT) = ABUB
5110     '
5120     HRHS = RADH * COS (ATHE (0)/2! + ADEL (ICNT))
5130     HLHS = RADH * COS (ATHE (0)/2! - ADEL (ICNT))
5132     LVEL = RADH * (2! * APIE - LOME (ICNT -1)) * RPM / 60!
5134     HFLC (ICNT) = RADH * ATHE (0) * FLCR *
                    7.385 * (LVEL ^ 1.86)
5140     HARR (ICNT) = HRHS - HLHS
5150     HSUM (ICNT) = HARR (ICNT) + HSUM (ICNT-1) - HFLC (ICNT)
5160     LAIR (ICNT) = LAIR (0) *
                    ((ABS (HSUM(0) / HSUM (ICNT))) ^ LCOM)
5170     LOME (ICNT) = LAIR (0) - LAIR (ICNT)
5180     ADEL (ICNT+1) = ADEL (ICNT) + (LOME (ICNT) / RADH)
5190   NEXT ICNT
5200 '
5210   ADEL (1) = ADEL (1) + AFST
5220   HCAL = HSUM (NCOL)
5230 WEND
5240 '
5250 RETURN

```

```

6000 ' *****
6010 ' *  SPILLING NO BUBBLING PROCEDURE  *
6020 ' *****
6030 '
6060 HSUM (NCOL) = HREQ
6070 ICNT      = NCOL
6090 LPER      = 0!           'INIT SO THAT PMTR > LPER
6100 '
6120 WHILE (ICNT <> 0) AND (PMTR > LPER)
6130 '
6140     LAIR (ICNT) = LAIR (0) *
        ((ABS (HSUM (0) /HSUM (ICNT))) ^ LCOM )
6150     LWAT (ICNT) = PMTR - LAIR (ICNT)
6160     ATHE (ICNT) = LWAT (ICNT) / RADH
6170     LPER      = LAIR (ICNT) + LWAT (0)
6190     HLHS      = RADH * COS (APIE - AGAM)
6200     HHS      = RADH * COS (AGAM - APIE + ATHE (ICNT))
6205     LEVEL     = RADH * (APIE + ATHE (0)) * RPM / 60!
6207     HFLC (ICNT) = RADH * ATHE (0) * FLCR *
        7.385 * (LEVEL ^ 1.86)
6210     HARR (ICNT) = HRHS + HLHS
6220     HSUM (ICNT-1) = HSUM (ICNT) - HARR (ICNT) + HFLC (ICNT)
6230     ICNT      = ICNT - 1
6240 WEND
6270 IF ICNT = 0
    THEN HCAL = 0! : RETURN
6280 '
6290 ICOL = NCOL
6300 NCOL = ICNT + 2
6310 HNED = HREQ
6320 HREQ = HSUM (ICNT+2)
6330 '
6340 GOSUB 4000
6350 '
6360 HREQ = HNED
6370 HCAL = HREQ
6380 NCOL = ICOL
6390 '
6400 RETURN

```

```

7000 ' *****
7010 ' * BUBBLING SPILLING PROCEDURE *
7020 ' *****
7030 '
7070 HPAT = 0
7090 NMIN = NCOL
7100 NMAX = -1
7110 HCAL = 0!
7112 '
7114 LVMA = RADH * 2 * APIE * RPM / 60!
7116 LVMI = RADH * (APIE + ATHE(0)) * RPM / 60!
7120 '
7122 HFMA = FLCR * RADH * APIE * 7.385 * (LVMA ^ 1.86)
7124 HFMI = FLCR * RADH * ATHE (0) * 7.385 * (LVMI ^ 1.86)
7126 HFPA = FLCR * RADH * ((APIE + ATHE (0)) / 2!) *
          7.385 * (LVMI ^ 1.86)
7128 '
7130 WHILE ( HPAT < (HMIN - HFMI)) OR (HPAT < (HMAX - HFMA)
7140     NMAX = NMAX + 1
7145     NMIN = NMIN - 1
7150     HPAT = HREQ - HATM - (NMIN * (HMIN - HFMI))
          - (NMAX * (HMAX - HFMA))
7160     IF (NMIN < 0) OR ((NMIN = 0) AND (HPAT) > (HMIN - HFMI))
          THEN RETURN
7170 WEND
7180 '
7190 IF ( NMIN < 0 ) OR (( NMIN = 0 ) AND ( HPAT > HMIN ))
          THEN RETURN
7200 '
7210 HCAL = HREQ
7220 '
7230 FOR ICNT = 1 TO NCOL
7240     IF ICNT < NMIN + 1
          THEN HARR (ICNT) = HMIN
7245     IF ICNT < NMIN + 1
          THEN HSUM (ICNT) = HSUM (ICNT - 1) + HARR (ICNT) - HFMI
7250     IF ICNT = NMIN + 1
          THEN HARR (ICNT) = HPAT
7255     IF ICNT = NMIN + 1
          THEN HSUM (ICNT) = HSUM (ICNT - 1) + HARR (ICNT) - HFPA
7260     IF ICNT > NMIN + 1
          THEN HARR (ICNT) = HMAX
7265     IF ICNT > NMIN +1
          THEN HSUM (ICNT) = HSUM (ICNT - 1) + HARR (ICNT) - HFMA
7270 NEXT ICNT
7290 RETURN

```

```
8000 ' *****
8010 ' * DISPLAY PROCEDURE *
8020 ' *****
8030 '
8040 ' IF HREQ > HCAL
      THEN PRINT "NO SOLUTION":RETURN
8050 '
8060 FOR ILIN = 1 TO 20
8070   PRINT "|";
8080   HDIS = DIAC * ( 20 - ILIN ) / 20
8090 '
8100   FOR ICOL = 1 TO NCOL
8110     IF HARR (ICOL) > HDIS
      THEN PRINT " **";
      ELSE PRINT "  ";
8120   NEXT ICOL
8130 '
8140   PRINT "|          ";
8150   IF ILIN <= NCOL
      THEN PRINT "COIL ";ILIN;" = "; HARR (ILIN)
      ELSE PRINT
8160 NEXT ILIN
8170 '
8180 PRINT "+";
8190 '
8200 FOR ICOL = 1 TO NCOL
8210   PRINT "----";
8220 NEXT ICOL
8230 '
8240 PRINT "+"
8250 '
8260 HINC = 0! : FOR ICOL = 1 TO NCOL : HINC = HINC + HARR (ICOL) :
      NEXT ICOL
8270 PRINT "HEAD GENERATED = ", HINC
8280
```

